MINIMAL NON-SIMPLE SETS ON 3D AND 4D GEOMETRIC GRIDS

by

CHYI-JOU GAU

A dissertation submitted to the Graduate Faculty in Computer Science in partial fulfillment of the requirements for the degree of Doctor of Philosophy, The City University of New York

2005

INFORMATION TO USERS

The quality of this reproduction is dependent upon the quality of the copy submitted. Broken or indistinct print, colored or poor quality illustrations and photographs, print bleed-through, substandard margins, and improper alignment can adversely affect reproduction.

In the unlikely event that the author did not send a complete manuscript and there are missing pages, these will be noted. Also, if unauthorized copyright material had to be removed, a note will indicate the deletion.

ProQuest Information and Learning Company
300 North Zeeb Road
P.O. Box 1346
Ann Arbor, MI 48106-1346

This manuscript has been read and accepted for the Graduate Faculty in Computer Science in satisfaction of the dissertation requirements for the degree of Doctor of Philosophy.

12/16/04
Date

Tat Yung Kong
Chair of Examining Committee

1/10/05
Date

Executive Officer

Sébastien Fourey / External Examiner

Gabor Herman

Ralph Kopperman

Bojana Obrenic

Supervisory Committee

THE CITY UNIVERSITY OF NEW YORK

Abstract

MINIMAL NON-SIMPLE SETS
ON 3D AND 4D GEOMETRIC GRIDS

by

Chyi-jou Gau

Advisor: Professor Yung Kong

Ronse introduced the concept of a minimal non-simple ("MNS") set of 1s of a binary image; if no iteration of a proposed parallel thinning algorithm can ever delete an MNS set, then it follows that the proposed algorithm "preserves topology". Ronse, Ma, Kong, Hall, and other authors have solved the problem of finding all those sets of grid points that can be MNS sets of binary images on the 2D and 3D Cartesian grids and the 2D hexagonal grid. This thesis solves the same problem for the 3D face-centered cubic grid (with (18,12)-, (12,18)-, or (12,12)-adjacency) and the 4D Cartesian grid (with (80,8)- or (8,80)-adjacency). Kong's concept of the attachment set of a point in a binary image is used to study of the effect of deleting non-simple 1s and MNS sets. In the attachment set approach, the definition of a simple point (which involves continuous deformation) is independent of the dimensionality and form of the grid and is therefore a convenient basis for our work. At the end of the thesis a staggered tiling system for n-dimensional Euclidean space is proposed. The author believes that thinning algorithms for images on the corresponding n-dimensional grids will be easier to analyze than similar algorithms on n-dimensional Cartesian grids.

Acknowledgements

I would like to thank Tat Yung Kong, my advisor, for his constant support and patient guidance during this research. As proud as I am of being his second disciple, and although I have collected abundant superb works on digital topology written and published by him, I have been able to specialize only a narrow branch of his knowledge, i.e., the study of the attachment set. It is my wish to carry his lineage[1] forward, at least insofar as this tiny branch is concerned.

Over these ten years, my interest in minimal non-simple sets has also greatly benefited from Ralph Kopperman, Gabor Herman, Bojana Obrenic and Paul Meyer. I am thankful to Dr. Kopperman for his kindness in inviting me to participate in the New York Seminars on General Topology and Topological Algebra through the early years of my research. Dr. Obrenic and Dr. Meyer shared their knowledge and friendly encouragement. While they shared their 'enlightenment' [2] in digital topology with me, I felt like a mere practitioner in the company of gurus.

Professor Gabor Herman gave me a clear perspective on the Face-Centered Cubic Grid, and I am indeed very encouraged by the application of digital processing in medical imagery. In addition, I have been fortunate enough to have worked with him on the algorithms for fuzzy segmentation.

I should also thank Dr. Ted Brown and mention that my participating at the 10th International Conference on Discrete Geometry for Computer Imagery in France, and at Dagstuhl Seminar - Mathematical Structures for Computable Topology and Geometry in

---

[1] The term is used in Buddhism tradition for the oral instructions of the guru.

[2] The term is refer to the full realization, borrowed from Vajrayana Buddhism.

Germany were both supported in part by the Graduate Center of the City University of New York.

Of course, I am grateful to my parents for their patience and *love*.

I wish to thank my wife, Jan, my faithful Dakini[3] for her ten years of support (and for telling people that her old husband is still in a Doctorial program); and my sons, Gene, Vincent and John for all the good times we had together making 3D dodecahedron models and for letting me show off my 4D tesseract animation.

Finally, I should thank Dr. Barbara Astone, my Sarasvati[4], for correcting my painful English.

Forest Hills New York
February 24, 2004

[3] My protector (female sky-goer in Sanskrit).
[4] Goddess of poetry and eloquence in Hinduism and Buddhism.

Table of Contents

Table of Contents vii

Introduction 1

1 Basic Concepts and Introduction to Digital Image 3
1.1 Digital Image 5
1.1.1 Basic Notations 6
1.1.2 Bricks and Mortar 8
1.1.3 Graphical Representations 9
1.1.4 Natural tiles — Voronoi Neighborhoods 12
1.2 Nearest-neighbor Adjacency
and Tile Adjacency 17
1.2.1 Truncated Tiles and The Adjacency Schema 18
1.2.2 Xels and The Tile Assemblies 22
1.3 Good Pair of Connectedness 26
1.4 The Foreground of An Image 30
1.5 Xel's Boundary and The Schlegel Diagram 31
1.5.1 3D Schlegel Diagram 32
1.5.2 The Tesseract (or 4-Hypercube) 33
1.5.3 4D Schlegel Diagram 34
1.6 Conclusion of Part I 36

2 Topology Preservation 37
2.1 Attachment Set of *d*-Xel 38
2.2 Simple Xels and Simple Sets 39
2.2.1 Simple Xel's Characterizations 40
2.2.2 Simple Sets 42

2.3 Minimal Non-simple Set 44
2.4 Useful Theorems for Minimal Non-simple Set 45
2.5 Conclusion of Part II 46

3 MNS set on Face-Centered-Cubic-Grid 48
3.1 FCC grids. Complementary FCC grids. Voxels in FCC grids. 49
3.2 Core cubes and void cubes of an FCC grid. Shape of a voxel. Boundary of a voxel. 12- and 18-adjacency. 50
3.3 FCC-binary images. Attachment Set Revisited. *Fm;n(I)* and *Am;n(v; I)*. 53
3.4 Topology-preserving deletion of 1's: (*m; n*)-simple 1's revisited. 56
3.5 Minimal nonsimple sets and Small sets revisted. 59
3.6 (18,12)-MNS sets. Use of a Schlegel diagram of an FCC-voxel. 63
3.7 (12,12)-MNS sets. 69
3.8 (12,18)-MNS sets. 71
3.9 Conclusion of Part III 75

4 MNS set with (80,8)-connectedness 77
4.1 Preamble 77
4.2 Main Theorem with (80,8)-connectedness 80
4.3 Proof of the Main Theorem with (80,8)-connectedness 81
4.3.1 Useful results 81
4.3.2 The "if" parts of the Main Theorem 83
4.3.3 The "only if" parts of the Main Theorem 85
4.4 Conclusion of Part IV 90

5 MNS set with (8,80)-connectedness 92
5.1 Preamble 92
5.2 *n*-Xels, 4D Images, Xel-Complexes and Attachment Sets 93
5.3 Simple 4-Xels with (8,80)-connectedness 95
5.3.1 (8,80)-simple Xels and Coattachment Sets 97
5.3.2 Schlegel Diagram 98
5.4 Simple sets and MNS sets with (8,80)-connectedness 99
5.5 Main Theorem with (8,80)-connectedness 101
5.6 Proof of the Main Theorem with (8,80)-connectedness 102
5.6.1 The "if" parts of the Main Theorem 102
5.6.2 The "only if" parts of the Main Theorem 106
5.7 Concluding Remarks 113

6 A Good Tiling System for Studying Thinning **114**
6.1 Bricks and Mortar revisited 114
6.2 The Staggering Procedure 114
6.3 Simple Features 115
6.4 No Digital Paradox 116

Appendix **118**
.1 Some Application Considerations for Staggered Tiling 118

Bibliography **120**

Introduction

In a binary image (or black and white image), grid points are labelled 1 or 0 according to some segmentation process. The 1's and 0's are usually stored in computer memory as an n-dimensional array (for nD images).

Thinning is an important low-level operation that is often performed on binary images. It is a useful method of pre-processing in image processing. Various image analysis algorithms have been proposed to produce the skeleton of a digital binary pattern by thinning. [5] [21] [23]

In this thesis we provide a means to verify the topological soundness of proposed thinning algorithms on the 4D Cartesian grid and the Face-Centered Cubic grid (FCCgrid).

Ideally, the sampled binary image according to some segmentation process should retain all the basic topological properties of the original image such as connectedness and simply connectedness. In reality, these properties very often become too ambiguous for high level image analysis, or cause digital paradox if the same adjacency is used for both the foreground and background (as seen in figure 1.1(A) of Chapter 1). Figure 1.1(B) shows the ambiguity and the related diffculty for analyzing the image due to this ambiguity. A simple solution to resolve this is obtained by differentiating the adjacency relationship between the foreground, and the background, elements of the sampled images. It results in many reasonable ways of defining connectedness and we call them "good pairs" of connectedness, for sets of 1's and 0's in a binary image.

These relationships complicate the computation to verify the topological soundness of proposed image processing algorithms on non-Cartesian and/or high dimensional grids, in particular, with regard to computations used in developing optical character recognition (OCR) or 4D video data analysis, which increase the practical interest of topology preservation, and make heavy use of the thinning algorithms.

One can prove that a specified parallel thinning algorithm always preserves the topology of the input binary image by verifying that no iteration of that algorithm can ever delete a minimal non-simple ("MNS") set of 1's in an image. The problems for binary images on Cartesian grids were first solved by Ronse [27] (in the 2D case) and Ma [22] (in the 3D case).

In this thesis, we solve the same problem on the following grids:

Non-Cartesian grid — the 3D face-centered cubic ("FCC") grid, which is one of the most frequently used non-Cartesian grids, with (18,12)-, (12,18)- and (12,12)-connectedness in Chapter 3.

High dimensional Cartesian grid — the 4D Cartesian grid with (80,8)- and (8,80)-connectedness in Chapter 4.

Our method is based on the *attachment sets* of 1's in binary images. This concept was introduced by Dr. Kong in [13], and we use the same general approach to MNS sets as was used there.

Chapter 1

Basic Concepts and Introduction to Digital Image

As Dr. Kong once stated in [19], "Arguably, the starting point of research on digital topology was the simple but important idea of using different adjacency relations for black and white points, a device which as far as we know was first recommanded by Duda, Hart, and Munson [3]. The reason for this at first sight rather bizarre decision was to avoid paradoxes such as those pointed out in [28]". Here, a simple example of the digital paradox [19] is reproduced in figure 1.1(A). If 4-adjacency is used for all pairs of points on figure 1.1(A), then the central white point is separated from the other white points by four "totally disconnected" black points. If 8-adjacency is used then the black points form a loop and yet the white points are not separated. (For 4- and 8-adjacencies see figure 1.2.) Also, without any rule to follow, can you tell if the diagonal array of blacks is a continuous line?

Figure 1.1(B) shows that two different kinds of segmentations have the same

scanning result of a binary image (see figure 1.1(C) for the scanned image). So, figure 1.1 illustrates that it is necessary to impose a well-defined relationship on the binary image. The well-defined relationships for various grid systems are often derived from using the good pairs of adjacencies. For example, in the figure 1.1(A), if 8-adjacency is used for the blacks and 4-adjacency for the whites we have a good pair, 4- and 8-adjacencies in this 2D Cartesian grid.

In this thesis we are not to verify which pair of adjacencies can be good pair, but given the commonly used good pairs in the 4D Cartesian and 3D FCC grids, we are to determine which set of grid points can be minimal non-simple.

We take the route of showing some pictures, which are rather informal, and postpone the mathematical definition; this is just one of the possible approaches to provide all the intuition we need in this thesis. This is also our general slant towards geometry rather than topology, when dealing with certain specified grids.

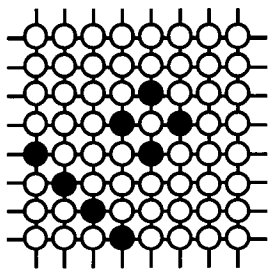

(A)

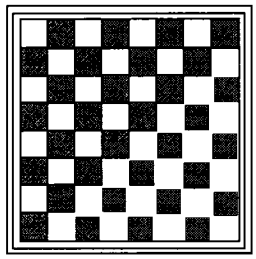

(B)

0 1 0 1 0 1 0 1
1 0 1 0 1 0 1 0
0 1 0 1 0 1 0 1
1 0 1 0 1 0 1 0
0 1 0 1 0 1 0 1
1 0 1 0 1 0 1 0

(C)

Figure 1.1: (A) shows a board of the game GO — a 2D grid, which has a simple "digital paradox" by black and white grid points. Figure (B) is a poorly printed checker board. It has the black squares on the white board at the lower right quater, but the white squares on the black board on the upper left. However, the difference between these two quarters can not be detected by studying the scanned binary image shown on figure (C).

1.1 Digital Image

2D binary images are obtained by regular sampling at grid points labelling them by 0 and 1, and then storing them in the 2D memory array. This is certainly a highly simplified solution to differentiating objects. Nevertheless, enough data for computer manipulation is captured provided that the adjacency relationship of each grid point is well defined.

This simple scanning process has great similarity to the system of vision in certain animals and its related brain process, which can faithfully map light values to each of the cells in the retina. Researchers have surmised that even the octopus, with its limited vision, is able to detect patterns among cells in the retina without processing a complete image of the object before it. Their vision cells are interwoven sort of horizontally and vertically in the retina as the pixels are connected.

The result of this research, studied independently from computer image analysis, reveals that checking merely some local conditions might be sufficient to verify a thinning process. That is, on a geometry grid having well defined adjacency, we would be able to determine the correctness of parallel thinning software, whose outputs — skeletons[1]– preserve the topology of the original images without processing the entire image. Also, at each step of deleting a pixel, it is sufficient to check the pixel's local condition at the moment of the parallel processing.

[1]the word 'skeleton' represents the result of thinning in many researches. The 'skeletons' resulting from thinning require additional constraints besides topology preservation as defined here.

Indeed, Ronse has pointed out in [27] that a specified parallel thinning algorithm always preserves the topology of the input binary image by verifying that no iteration of that algorithm can ever delete a minimal non-simple ("MNS") set of 1's of an image. The problems for binary images on Cartesian grids were first solved by Ronse (in the 2D case) and Ma (in the 3D case).

Our aim in this thesis is to solve the same problems on 3D FCC grid and 4D Cartesian grid.

1.1.1 Basic Notations

In this subsection, we are to introduce some notations, but skip many very commonly used definitions and notations such as $\in, \cup, \cap, \subset, \subseteq, \not\subseteq, \subsetneq, \emptyset$, binary relation (reflective, anti-reflective, symmetric, transitive and equivalence relations), partial order, and so forth.

We use the notation $\mathbb{Z}^d$ for the set of d-tuples $(z_1, z_2, \ldots, z_d)$ of the real Euclidean d-space having integer coordinates and use the notation $\mathbb{R}^d$ for the set of d-tuples $(x_1, x_2, \ldots, x_d)$ of the real Euclidean d-space having real number coordinates.

A polytope $\subset \mathbb{R}^d$ is a bounded set $\{\mathbf{x} \in \mathbb{R}^d : A\mathbf{x} \leq b\}$ where $A \in \mathbb{R}^{m \times d}$ and $b \in \mathbb{R}^m$. [32] [2]

For any polytope p, a face f of p is any set of the form: $\{\mathbf{x} \in p : \mathbf{cx} = c_0\}$ where $\mathbf{cx} \leq c_0$ is satisfied for all $\mathbf{x} \in p$. Since $\mathbf{0x} \leq 0$, p is always a face of p. All other

[2] By this computational definition, the polytope is called an $\mathcal{H}$-polytope.

faces of p are called *proper faces* of p, and denoted by $f < p$. A face of dimension $d-1$ is called a *facet* of the polytope of dimension d. (Here, we intend to adopt the terminology of the cell complex or polyhedral complex. Please refer to Lecture 5 in [32] for definition of polyhedral complex.)

Sticking to the convention, a *tiling* is a collection of disjoint open sets, the closures of which cover the plane. A regular tiling of polygons (in two dimensions), polyhedra (three dimensions), or polytopes (d dimensions) is called a *tessellation.* In this thesis the disjoint open sets are interiors of the polytopes, which cover Euclidean d-space. We call the polytopes *tiles* or *d-tiles*, if this set of polytopes tessellates Euclidean d-space.

A *digital space* is generally defined [3] as a pair (V, π); since the work in this thesis is studying the MNS sets in the 4D Cartesian grid (or 3D Face-Centered Cubic grid), we restrict V to be $\mathbb{Z}^4$ (or subset of $\mathbb{Z}^3$ such that the sum of the coordinates is even). A point with integer coordinates in V is called a *grid point.*

Quite naturally, the binary relation π will be some good pair of adjacencies (see section 1.3) but we shall postpone stating the precise meaning of π until we define the term *xel*, then this binary relation will be given in section 1.3 in a WYSIWYG[4] manner. For now, let us ask the following questions in sequence:

1. Given a grid system, how does one tessellate an Euclidean space?

[3] Dr. Herman and many authors define V as an arbitrary nonempty set and π as a symmetric binary relation on V such that V is π-connected (see sections 1.4 and 3.1 in [10])

[4] WYSIWYG, what you see is what you get.

2. What is the shape of the tile of this tessellation?

3. How does one "modify" these tiles so that a good pair of adjacencies can be properly built by them?

1.1.2 Bricks and Mortar

— Pixels and Adjacency

Most of the images in computer graphics and computer vision are represented in $\mathbb{Z}^2$ or $\mathbb{Z}^3$. Some of them are in $\mathbb{Z}^4$, which come quickly into view involving research on computer digital video, medical imagery or GIS spatial analysis.

Let us have an easy start with 2D Cartesian grid, compare the cells in the retina with the pixels in a 2D image on a computer screen (or the smallest unit stored in computer memory). As vision cells — rods and cones — are the smallest sensing units tessellating the retina surface, pixels are also tiny elements: the tiny points of data that make up a digital image, from the ink dots in newspaper photos to the grains of silver or particles of color dye in film photography. Rely on our vision intuition: a "thin" diagonal array of pixels, as shown in figure 1.1(A), is considered to be a *continuous* line. (By a "thin diagonal array" of pixels we mean: each consecutive pair of pixels share exactly one vertex.) This notion is also true in computer vision. But digital topology has more varieties of connectedness, which are mathematically defined. (A rigorous definition will be made precise in Chapter 2).

In digital topology, we cautiously examine how the pixels are adjacent to each

other in the ambient image. One shall always ask:

What is the adjacency relationship?

By what granularity can the relationships be properly presented?

It would be nice if these relationships are compatible with that of traditional media (visually) by the grains of silver, by the ink dots, or by some sort of tiling system.

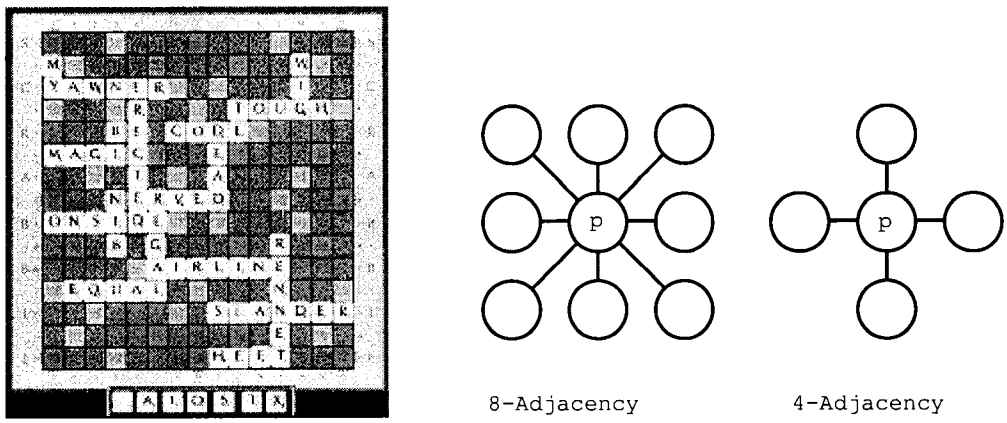

Figure 1.2: The rule of game Scrabble uses 4-adjacency for letter blocks so that the diagonal array of letter blocks are not continuous. In digital topology two pixels are 4-adjacent if the intersection of their Voronoi neighborhoods is an edge, and they are 8-adjacent if their intersection is at least a vertex. (See definition 1.1.1 for Voronoi neighborhood.)

1.1.3 Graphical Representations

"It's not about pixels alone. It's about pictures." — Olympus Camera

Image process computation does not deal with stand-alone pixels; that is why spatial relation or connectedness is such an important feature in computer image analysis. There are two prominent approaches toward graphical representation of image (or object) connectedness :

1. Graph approach

2. Topological approach

The first approach is using the edges to indicate the adjacency relationships. Therefore, a dD image is very often defined as a graph structure capturing the adjacency relations among grid points. We call this approach the *graph approach*[5]. For example, the molecular structure or chemical compound in figure 1.3(A) presents the adjacency relationships — the chemical bounds — as edges. But the adjacency of the same structure can also be presented by the attachment of balls, as shown in figure (B). This approach uses the "cells" to show the adjacency relation; if two cells intersect then they are adjacent. The second approach is called the *topological approach.* Note: cells show clear adjacencies among them but they do not tessellate this everyday Euclidean space (not even part of it in this molecular structure).

Both methods shown on figure 1.3 have their pros and cons. The first one is clear and straightforward in lower dimensions; the grid points are the nodes and the adjacency relationships are the edges. A serious drawback: it is too complicated to read the graph representation in higher dimension (e.g., 4-dimensional images).

Also, the proof methods based on this approach are complicated by the fact that one may have to consider "deformations" of paths to show that doughnut-type "holes" in images are always preserved by the algorithm (referring to [9] [12] [17]), and such

[5]Graph approach is also called "pathalogical" or path-based approach by some authors.

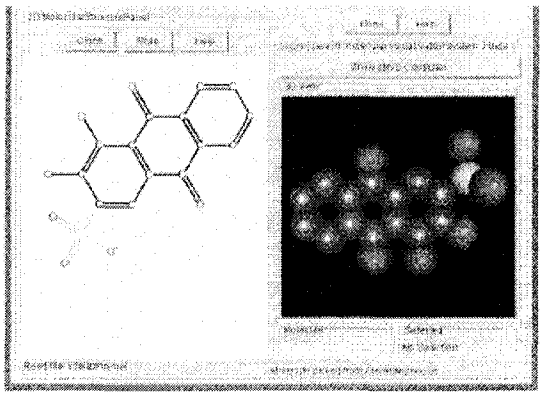

Figure (A) Figure (B)

Figure 1.3: (A) The graph approach versus (B) the topological approach.

proof methods have not yet been fully investigated, especially in higher dimension.

Yet another drawback: one often studies 3D or 4D topological properties based on 3D observation; these observations quite often lead one astray when reading 4D graphs (e.g., many 4D images, whose 3D projections have tunnel look-alikes by observation, have no 4D tunnels at all.) Thus, we are not going to use this approach.

The second method — the *topological approach* — "begins" with tiling the Euclidean space by Voronoi neighborhoods (see definition 1.1.1). The advantage of this approach is that all the adjacency relationships are coded on the "surface" of balls — Voronoi neighborhoods.

Here is an elementary description of Voronoi neighborhoods: tessellate the 3D space by blowing one balloon at each grid point at the same speed until all the voids are filled up. The closed sets bounded by the totally expanded balloons (which are unit cubes in this case) are called Voronoi neighborhoods. Voronoi neighborhoods are

also called the Direchlet cells. [25]

Although this approach gives us intuitive visualization, it also has drawbacks. One is that without expanding the Voronoi neighborhood its front face blocks most part of the surface. As a remedy, wire diagrams are used to exhibit the polyhedra and their expanded perspective views are displayed (see Schlegel diagram in section 1.5) in the ensuing sections so we can "see" better. Another drawback of this approach is that without "modification" Voronoi neighborhoods can not properly present good pair of adjacencies other than the pair $(3^d - 1, 2d)$, even some of the commonly used pair such as (18,6). (Good pairs are to be detailed in section 1.3.)

In the following subsections we will present some tiling system mathematically by using the topological approach.

For readers who are interested in the comparison of the graph-based and the topological approaches, please read [15] and Chapter 11 in [26]

1.1.4 Natural tiles — Voronoi Neighborhoods

Samples of Voronoi neighborhoods tiling the Euclidean space can be easily discovered in our surrounding nature environment. Regardless which 3D grid system we are working with, cells grow into Voronoi neighborhoods. We define it mathematically for our geometric grid systems as follows:

Definition 1.1.1. A *Voronoi neighborhood* in 4D Cartesian grid (or 3D FCC-grid) system is the convex polytope consisting of all points in Euclidean d-space that are

at least as close to p as to any other grid point.

The Voronoi neighborhood of a grid point is in the form of a polytope $\{\mathbf{x} \in \mathbb{R}^d : A\mathbf{x} \leq z\}$ where $A \in \mathbb{R}^{m \times d}$ and $z \in \mathbb{R}^m$ define its m facets meeting with the grid point's neighbors. It is readily confirmed that these naturally grown tiles are bounded and the interiors of them do not overlap. The intersection of any pair of tiles is a set of their shared proper faces. Voronoi neighborhoods provide a natural way to create a tessellation.

Different grid systems generate different shapes of tiles. In general, tiles do not have to be convex, but the convex ones — natural tiles can be easily computed. (See examples in figure 1.4)

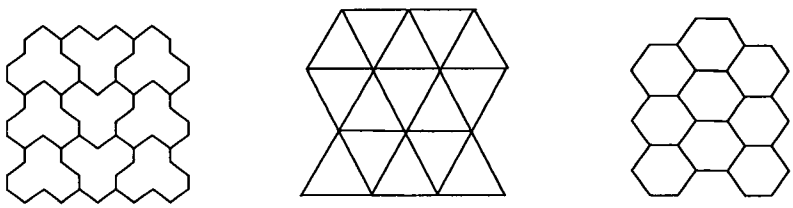

Figure 1.4: The left figure shows the tessellation on many color CRT monitors. This tiling does not consist of Voronoi neighborhoods. Each of them is a cluster of three hexagons — tiny red, green and blue each. In general, tiles are congruent polyhedra (not necessarily convex) tessellating the d-dimensional Euclidean space. Can you see that the left tessellation can be continuously deformed into the right one? The figure in the middle shows the triangles on a hexgonal grid. The right figure shows the hexagons on a trigonal grid. Both triangle and hexagon tiles are Voronoi neighborhoods for the related grids.

On Cartesian grids, the natural tiles are: a 0-*tile* is a singleton set $\{i\}$, where i is an integer; a 1-*tile* is a closed unit interval $[i, i+1]$ of the real line, where i is an integer. For $0 \leq d \leq 4$ a *d-tile*, on a 4D Cartesian grid, is a Cartesian product of d 1-tiles and $4 - d$ 0-tiles, in some order. Therefore, a *d-tile* is a d-dimensional

hypercube (or a cube for $d = 3$).

If q is a d-tile for some d, then we say q is a *tile*. A 0-tile will also be called a *vertex*, a 1-tile is called an *edge*, a 2-tile in 2-space is called a *pixel* and a 3-tile in 3-space is called a *voxel*. It is clear that pixels and voxels tessellate 2- and 3-space respectively.

Figure 1.5 illustrates d-tiles as the trajectories of $(d-1)$-tiles. The reader may sometimes find it helpful to think of a 4-tile as the trajectory of a 3-tile as it moves one unit in the positive or negative direction of the (virtual) coordinate axis that is perpendicular to the 3-tile.

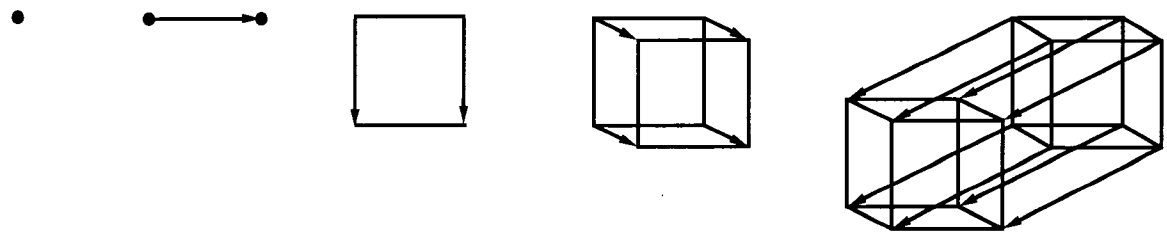

Figure 1.5: A d-tile can be viewed as the trajectory of a $(d-1)$-tile as it moves one unit of time.

On non-Cartesian grids, triangles and hexagons give two examples of 2D tiles (see figure 1.4).

A 3D non-Cartesian example is given in figure 1.6. It shows that the natural tile in a Face-Centered-Cubic grid is a rhombic dodecahedron. (FCC grid[6]). Digital images on FCC grids have been considered by a number of authors [10][6]. We focus on this

[6]FCC grid is one of the non-cubic grids preferred by many authors; see Geometry of Digital Space, Chapter 2. [10]

particular grid for the following reasons:

Three advantages of an FCC grid over a 3D Cartesian grid are:

1. An FCC grid is more evenly spaced than a 3D Cartesian grid: For grids containing k^3 grid points per unit volume, every point in Euclidean 3-space is within a distance of $0.794/k$ from an FCC grid point, but some points are further than $0.866/k$ from a Cartesian grid point.

2. The natural neighborhood of a 3D grid point consists of 27 grid points for images based on a 3D Cartesian grid, but consists only of 19 grid points for images based on an FCC grid. As a result, some local image processing operations on FCC images involve less computational effort than the analogous operations on 3D Cartesian images.

3. The nearest-neighbor adjacency relation can be used to define connectedness for both 1's and 0's of binary images on an FCC grid, without producing the kinds of connectivity "paradoxes" that are associated with the use of a single adjacency relation to define connectedness for both 1's and 0's in Cartesian binary images.

As shown in figure 1.6, the grid points of an FCC grid are the centers of the tiles — rhombic dodecahedra. A further discussion of rhombic dodecahedron tessellation will be given in the third chapter.

FCC grids can be one of the following sets:

1. $\{(x, y, z) \mid x, y$ and z are integers such that $x + y + z$ is even$\}$, and

2. $\{(x, y, z) \mid x, y$ and z are integers such that $x + y + z$ is odd$\}$.

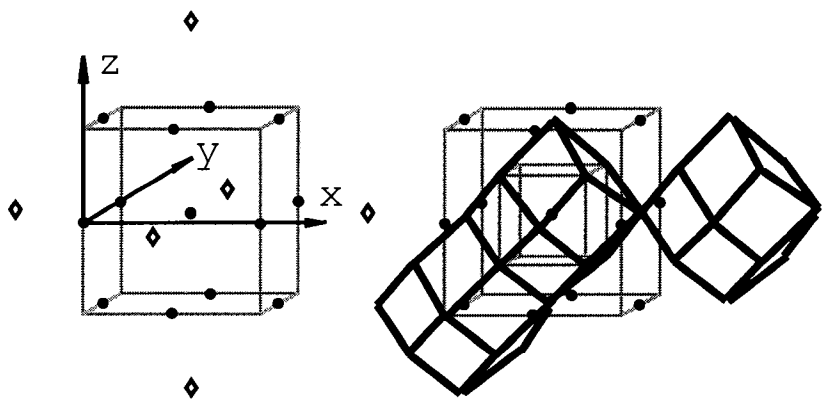

Figure 1.6: The left figure shows a grid point in FCC-grid at (1,1,0) with 12 nearest neighbors indicated by dots and 6 second nearest ones indicated by diamonds. The right figure shows three FCC tiles, which are rhombic dodecahedra associated with three grid points. The grid point at (1,1,0) is at the center of two cubes. The big cube is part of the coordinate grid; the small cube, called *core cube* (see section 3.2), is an auxiliary one to help readers locate the obtuse vertices of this FCC tile; others are sharp vertices. A tile 18-adjacent to the center tile is shown to the right. To the lower left shows a tile 12-adjacent (18-adjacent as well) to the center one.

As well as the natural d-tiles tessellate the d-space (on Cartesian and non-Cartesian grids) based on definition 1.1.1, they are not good enough to build images. (It will be explained in section 1.2.1) Now, we are ready to discuss the nearest-neighbor adjacency, which leads to the topic of "truncated tiles".

1.2 Nearest-neighbor Adjacency and Tile Adjacency

Let us revisit the topological approach in 2D Cartesian grid, (see figure 1.2) where every circle — the 2D balloon — grows and touches the four nearest neighbor circles at the same time. If they keep growing, they will eventually turn into unit squares, each of which touch eight neighbor circles including the first four. In terms of the 4-, 8-adjacency of a grid point p, we say grid point p is 4-, 8-adjacent to the four, or eight grid points, which are the centers of these four, or the eight nearest neighbor circles respectively.[7] And they are called p's 4-, 8-adjacent neighbors.

Nearest-neighbor adjacency relation is based on the number of neighbors (Voronoi neighborhoods) that can be adjacent to a given tile (also a Voronoi neighborhood) on a 2D Cartesian grid during their process of "growing", one speaks of 4-, 8-neighborhoods, 4-, 8-adjacency relations[8]. Similarly, one speaks of m-adjacency where m = 6, 18, 26 for a 3D Cartesian grid and m = 8, 32, 64 and 80 for a 4D Cartesian grid.

Equivalently, we can define tile-adjacency without depending on its process of growing. For any grid point p in 3-space, m-adjacency of p where $m = 6$ means the

[7]Pure topologists may stay clear of the term "nearness" but this spatial relation is commonly used in the literature of digital topology in the Euclidean space, (rather the metric space).

[8]Many authors also specify 6-adjacency on 2-space. A pixel p with 6-adjacency associates 4-adjacency neighbors plus two extra neighbors, which share only one vertex with p in one particular diagonal direction. This kind of adjacency can be skewed to the nearest-adjacency in the triangular grid.

tile at p sharing a pixel, a 2d-face, with the tiles of six grid points; $m = 18$ means sharing either a vertex or an edge; and $m = 26$ means sharing either a pixel, an edge or a vertex. The same approach can be applied to the grid points in 4-space.

We also say two 4-tiles are *attached* (*diagonal, diametric or antipodean*) to each other if their intersection is a 3d-tile, (a pixel, an edge or a vertex respectively). Similarly, two 3-tiles are *attached, diagonal* or *diametric* if their intersection is a pixel, an edge or a vertex respectively.

With metric [31] specified on the Euclidean space, one very often assigns two "nearest-neighbor adjacency" relations for connectedness to avoid digital paradox: one for the foreground and the other for the background.

In the next subsection we are to define the truncated tiles, which show clear picture of tile adjacency relations without the ambiguous result by using nearest-neighbor adjacency relations.

1.2.1 Truncated Tiles and The Adjacency Schema

"Just cut the damn thing off." — Lee Iacocca

On an FCC-grid, two rhombic dodecahedra of 3D(12,12)-images (as well as two cubes of 3D(18,6)-images on a Cartesian grid) sharing only a vertex are not connected by the definition of 3D(12,12)-images (or 3D(18,6)-images on a Cartesian grid). So, the natural tiles fail to show this intricate adjacency relationship. Here, we are to introduce our WYSIWYG approach — a "modified" picture.

Let us explain it by using 3D(18,6)-images:

On Cartesian grids, look at 3D(18,6)-connectedness. Any two Voronoi nieghborhoods of 3D(18,6)-image, which "intersect" at only one vertex, are not considered to be connected. One could ask: "How about using a picture of half-grown balls/tiles?" Well, we tried them on figure 1.7, and that did not make a clear picture.

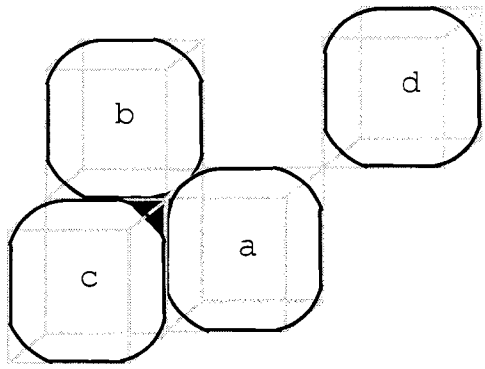

Figure 1.7: Two tiles "intersecting" at only one vertex are not considered to be connected in 3D(18,6)-image; this (visual) representation problem can be resolved by showing half grown tiles (see the tiles a and d). However, a new problem arises that the hole (shown in black) surrounded by the three half grown tiles a, b and c contradicts the 8-adjacency of the background.

It would be nice to hold more information at the intricate areas — the vertices and to encode precise connectedness data. One approach to encode the data is suggested in [8] to use an extended grid — hyperlattice so that more data entries can be encoded for the contour of segments. (This approach fails if a simple extended hyperlattice were used.)

Our approach is to encode them by chopping the predetermined vertices according to certain adjacency schema. This approach is visually easier to comprehend,

graphically easy to present and mathematically easy to compute (adopting polyhedral complex). Just chop a tiny piece off each of the *predetermined* corners of tiles so that this tiny piece would have a cutting section of an arbitrarily small standard d-simplex.

We say a tile is a *truncated* tile if it is derived from a natural tile modified or chopped by a particular schema. The truncated tiles following the predetermined rules reflect the *connectedness* defined mathematically.

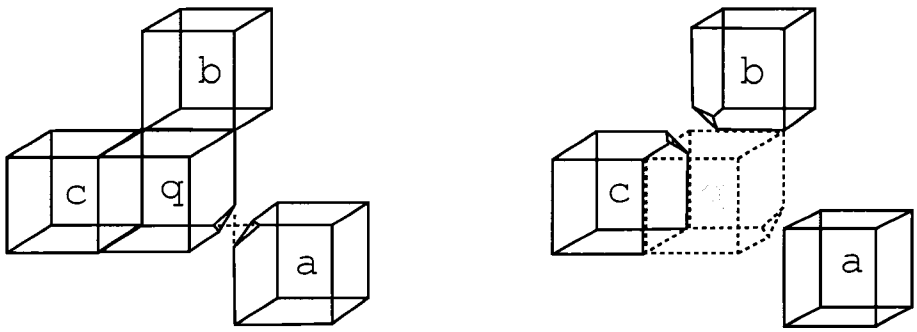

Figure 1.8: The left and right figures are the 3D image with (18,6)-connectedness before and after deleting the tile q, respectively. The truncated tiles are modified by Schema 1 at the moment of the deletion process. As accurately as they show the picture of adjacencies they are not consistent with the concept of strong deformation retract (to be detailed in the next chapter).

A clear picture of a 3D image with (18,6)-connectedness begins to merge (see figure 1.8) once we establish the chopping rules of Schema 1:

Let I be a set of 3D tiles — unit cubes and $V(I)$ be the set of vertices v of the cubes to be chopped off.

Schema 1. *Vertex v is a vertex of just two cubes of I, and these cubes share only vertex v.*

In view of this example we see that the chopped tiles fit into our visual intuition and rule out the ambiguity in this connectedness. (Hold on, they are not good enough. More chopping to come.)

Another topologically equivalent Schema is listed below. This schema cuts more corners (thus, needs more computational power).

Schema 2. *Let $V(I)$ be the set of cube vertices v to be chopped off, where v satisfies one of the following rules:*

1. *v is a vertex of just two cubes of I, which share only vertex v.*
2. *v is a vertex of just one cube of I*

At first glance Rule 2 in Schema 2 seems to have no effect on the (18,6)-connectedness since the results of both schema 1 and 2 are homotopic equivalent; however, when deletion of tiles is studied (see the right illustration in figure 1.9) schema 2 will be chosen because it satisfies topology preservation (to be detailed in the next chapter).

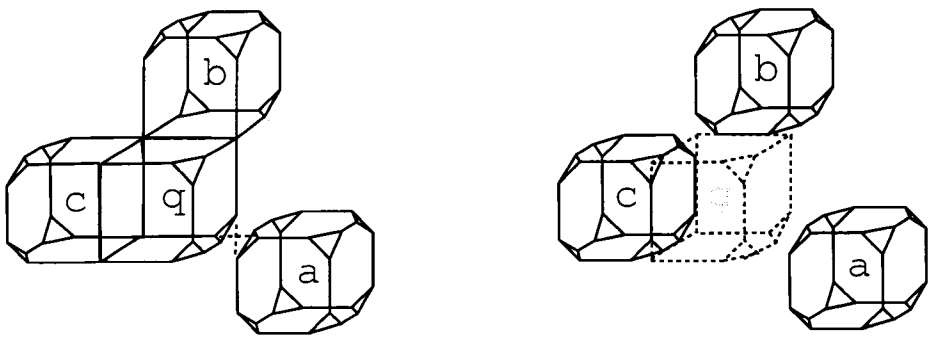

Figure 1.9: The left and right figures are truncated tile at grid points q,a,b and c in a 3D image with (18,6)-connectedness before and after deleting the tile q respectively. The truncated tiles are modified by Schema 2. Rule 2 is applied to the vertex shared by tiles q and a before the deletion of tile q, and applied to the vertex shared by tiles b and c after the deletion.

The rules dictate adjacency relationships for each image on the digital space, and decide which corners of tiles are to be chopped.

According to the allocation of its neighbors, a truncated tile can be computed by $\{\mathbf{x} \in \mathbb{R}^3 : A\mathbf{x} \leq b\}$ where $A \in \mathbb{R}^{m\times 3}$, $b \in \mathbb{R}^m$ and m is the sum of 6 plus the number of the chopped corners. 6 indicates the six inequalities corresponding to the 6 facets of the 3-tile. Note that since the truncated tiles are modified according to the relative locations of their neighbors, the truncated tiles are not always congruent.

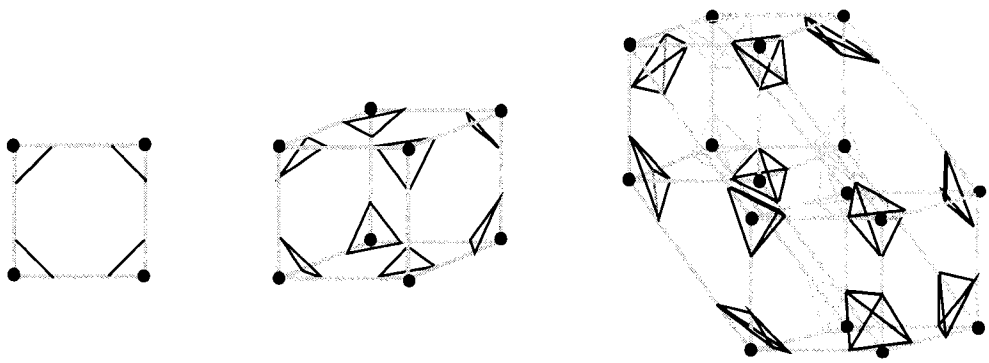

Figure 1.10: For d= 2, 3 and 4, on dD Cartesian grids, *tile assembly* consists of the truncated center polyhedron and all the broken corner pieces, which are standard d-simplexes (isometric to $\Delta^{d-1} = \{(t_0, ..., t_d) \in \mathbb{R}^d \mid \sum_i t_i = \alpha \text{ and } t_i \geq 0 \text{ for all } i\}$ where α is an arbitrarily small number; equals to 1/8 per se). The dots indicate the corners. Note that every cutting section is shown as a simplex Δ^{d-1} in black outline. Connecting all the vertices of the simplex to the corner dot makes a piece of corner simplex or corner polyhedron. (In order to be easily perceptible on paper, the connecting edges were not shown in black.) The middle figure is prepared for use in 3D(18,6)-connectedness, and the right for 4D(64,8)-connectedness.

1.2.2 Xels and The Tile Assemblies

"Xel, xel, axed cell complex." — ?

Since truncated tiles are not always congruent, it would be nice that they can be build like jig saw puzzles so that one can distinguish the different shapes of the

truncated tiles at different stages if any of its neighbors being deleted. (See the middle figure of Fig. 1.10 for 3D(18,6)-connectedness.)

How does one make the jig saw puzzle of a d-tile?

First we need the chopping schema. Pick up all the possible cutting corners, which are targeted by this schema. We break all the targeted corners off Voronoi neighborhood (at grid point q). The collection of these pieces is a polyhedral complex consisting of all the possible corner simplexes plus the truncated center piece of the tile. (The center piece is also a polyhedral complex itself.) We call this collection of pieces a *tile assembly* at the grid point q, and denote it by $x(q)$.

With this jig saw puzzle polyhedral complex, $x(q)$, we can build any truncated tile. The truncated tile complex being built at the grid point q in the image I is called "xel q in I", and denoted by $\delta(q, I)$. In this thesis, we very often use the term "xel q" for brevity, instead of xel q in I, should there be no ambiguity about the shape of its truncated tile-complex. [9]

In summary, Voronoi neighborhood is the polyhedron given by the union of all the elements of $x(q)$; the truncated tile is the polyhedron given by the union of all the elements of $\delta(q, I)$.

[9] In 4D or higher dimensions we need to chop off edges in order to make a jig saw puzzle, $x(q)$ in addition to chopping the corners (for example, taking 4D(32,8)-connectedness).

Name or notation	Description
q	grid point in d-space
Tiles	polytopes that tessellate d-space
Natural tile	Voronoi neighborhood
$x(q)$	tile assembly at q
	(it is a cracked Voronoi neighborhood)
$\delta(q, I)$ or xel q	the truncated tile complex built from $x(q)$
Voronoi neighborhood at q	is the same as $\bigcup x(q)$
Truncated tile	shows correct adjacencies and it is
	the same as $\bigcup \delta(q, I)$

Of course, one could ask whether it is really necessary to go through these details, since the result of using the truncated tiles is quite obvious anyway. There are several good reasons to go these extra nine yards. One is that by using the polyhedral complex $\delta(q, I)$ we can give a clear definition of attachment set in the image of adjacencies other than $(3^d - 1, 2d)$-connectedness. Thus, we will formulate the definition of simple point better. Readers may notice that we are using concepts of cell complex (polyhedral complex) and we are going to take advantage of the flexibility to allow many natural constructions to be performed on them. In addition, it also yields a basic algorithmic tool to deal with special connectedness other then Cartesian grid.

2D(8,4), 3D(26,6) or 4D(80,8)-images do not need chopping, therefore no cracks. Their xels always are the Voronoi neighborhoods!

Although 4D(64,8)-images are not to be studied in this thesis, the same approach can be applied by a similar chopping schema, and the xels of 4D(64,8)-image can be

obtained by removing corner simplexes from their 4-tile assemblies.

Here is an interesting question to ask: "Besides no chopping as a naive schema, is there a chopping schema that is targeted at some but not all of the vertices of a tile?" The answer is yes.

On non-Cartesian grids, let us look at (12,12)-connectedness on an FCC grid. We know that standard tile of a 3D(18,12)-image is a rhombic dodecahedron.

Similar to the chopping rule of 3D(18,6)-connectedness, the chopping schema is

(12,12)-FCC Schema

targeted at the six "sharp" corners v but not the obtuse ones of the rhombic dodecahedron, if this sharp corner v is a vertex of just two 1's of I, and those two FCC-tiles share only v (that is equivalent to the condition of v is a sharp corner for both 1's).

The xel on an FCC grid with (12,12)-connectedness is simply a truncated rhombic dodecahedron with a schema targeted at all the sharp corners so that unless through its nearest nearest neighbors it has no connection to its "second" nearest neighbors.

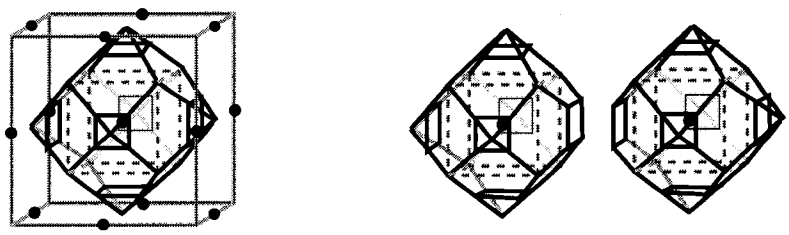

Figure 1.11: The left figure shows tile-assembly $x(q)$ of xel q on an FCC grid with (12,12)-connectedness. The right figure shows two FCC-xels, which are chopped based on Schema 1 for the (12,12)-connectedness. Again, this schema is not good enough.

The truncated FCC-tile in figure 1.11 can be formulated by $\{\mathbf{x} \in \mathbb{R}^3 : A\mathbf{x} \leq z\}$ where $A \in \mathbb{R}^{13\times 3}$, $z \in \mathbb{R}^{13}$ and 13 is the sum of 12 (facets) plus 1 (chopped corner piece). This truncated FCC-tile can be easily disassembled into FCC-xel. Again, we would reiterate that xels are not always congruent, but their standard tiles and tile-assemblies are.

It is easy to comprehend by studying the xels, or truncated tiles, so we can "see" the adjacency of the good pairs such as 3D(18,12), 3D(12,18) and 3D(12,12).

1.3 Good Pair of Connectedness

In general, if an image uses m-adjacency for the grid points of 1's and n-adjacency for 0's, we say the image is an (m, n)-image or an image with (m, n)-connectedness. If this (m, n)-connectedness avoids digital paradox for all the images, then (m, n) is called a *good pair* of connectedness[10].

We also use $d\mathrm{D}(m, n)$ to indicate that this (m, n)-connectedness is used in d-space, and $d\mathrm{D}(m, n)$-image I denotes the image I with $d\mathrm{D}(m, n)$-connectedness. The *complement* of image I, denoted by I^c, is the image whose 1's are the 0's of I and whose 0's are the 1's of I. Very often, in this thesis I^c is associated with $d\mathrm{D}(n, m)$-connectedness, if I is a $d\mathrm{D}(m, n)$-image.

[10]A good pair of connectedness ensures a valid digital Jordan curve/surface theorem or region contour by using two different types of connectedness for the image's foreground and background. Note that the digital paradox has no underlying actual contradiction, e.g., in graph theory neither (4,4)- nor (8,8)-connectedness are self-contradictory. The digital paradox is rather a pseudoparadox.

Here are commonly used good pairs on Cartesian and non-Cartesian grids as follows:

On Cartesian grids, 2D(8,4) and 2D(4,8) are good pairs.

3D(26,6), 3D(6,26), 3D(18,6) and 3D(6,18) are good pairs.

4D(80,8), 4D(8,80), 4D(64,8), 4D(8,64), 4D(32,8) and 4D(8,32) are good pairs.

To be mathematically simple, the same (m,n)-connectedness shall be applied to all the grid points monotonically for all the 1's and 0's. This does not oversimplify problems or discard the image details because as long as the digital image is scanned in high resolution, a monotone rule suffices to process and retain the details of the original image.

On non-Cartesian grids, we present good pairs 3D(18,12), 3D(12,18) and 3D(12,12) for the FCC-grid.

One would expect that (18,12)-connectedness on the FCC grid is deduced by 18-adjacency for the foreground and 12-adjacency for the background. Indeed, it is the case as shown in figure 1.6.

Our definition of 3D(12,18)-connectedness is based on the complement image, so we study the inverse image (to be detailed in the next section).

3D(12,12)-connectedness for an FCC grid is also a good pair because it avoids digital paradox as well, but the segmentation is quite different from that of 3D(18,12)-connectedness. A detailed explanation of 3D(12,12)-connectedness will be clear by

studying the xels. (The remaining case 3D(18,18)-connectedness is not a good pair because it generates connectivity "paradox". For example, there are unbounded "digital planes" which have no holes in the sense that every "disk" (refer to [31]) having the perimeter of closed digital 18-path on such a digital plane can be digitally deformed within the plane to a single FCC-xel, but which fail to separate their complements into two 18-components).

Note that all the good pairs mentioned in this thesis are of the dD(m, n)-connectedness such that if μ is the minimum of m and n then two μ-adjacent xels share a facet.

The followings are the connectedness to be studied in this thesis:

Connectedness	Schema	Shape of xel to build image
4D(80,8)	No chopping	4d hypercube
4D(8,80)	No chopping	4d hypercube on complement image
3D(18,12)	No chopping	Rhombic dodecahedron
3D(12,18)	No chopping	Rhombic dodecahedron on complement image
3D(12,12)	(12,12)-FCC Schema	Truncated rhombic dodecahedron

Note we are taking advantage of using xels on the d-space with (m, n)-connectedness, where $m \geq n$. First, pick a (m, n)-connectedness in the grid system that we are working. Second, decide the schema by the chart above. Third, build image by using xels.

The image built will be used for verifying image processing algorithms. Simply analyze the m-adjacency of xels; there is no need to check the n-adjacency for the background (by the intrinsic merit of the xels or truncated tiles, the n-adjacency for

the background will be satisfied).

Now, tailored for the particular use in this thesis, we define a *dD(m,n) digital space* where $m > n$ as a pair (V, π) where V is $\mathbb{Z}^4$ (or subset of $\mathbb{Z}^3$ such that the sum of the coordinates is even), and π is a symmetric binary relation on V such that $(p, q) \in \pi$ iff xel p and xel q intersect where xels are built according to the schema of $dD(m, n)$-connectedness.

A binary image is a two-valued function defined on the subgrid of a digital d-space:

Definition 1.3.1. A *dD(m,n) image I* is a set of grid points on the dD(m,n) digital space with its adjacency graph structure. Its grid points are labelled 1 and all others are labelled 0.

A grid point is called a 1 of I if it is assigned the value 1, and called a 0 of I if it is assigned the value 0.

Should there be no ambiguity, we also use the notation dD image and digital d-space relaxing us of the heavy symbols.

Our approach is in a reverse manner; schema first, then the shapes of truncated tiles, finally the adjacency relationships. Thus, schema determines the digital image. We build the image like masons did... a mural is created by applying tiles one by one on the wall, and by cutting corners of tiles if necessary. One could argue that this approach and the definition of adjacency is not aesthetic nevertheless it provides us with a good and clear picture to read.

1.4 The Foreground of An Image

Let $\delta(I)$ denote the set of all the xels in an image I, i.e., the truncated 1's modified by the schema of $d\mathrm{D}(m,n)$-connectedness. We are able to analyze the adjacency relationship among the components of I by simply studying the polyhedral set $\bigcup\delta(I)$.

Given a dD image I with (m,n)-connectedness, we denote the *foreground* of image I by $\mathcal{F}(I)$ (or, to be more specific, by $\mathcal{F}_{m,n}(I)$).

Definition 1.4.1. Let I be a $d\mathrm{D}(m,n)$-image. The *foreground* of image I, $\mathcal{F}_{m,n}(I)$, is defined in two cases as follows:

1. If $m \geq n$ then $\mathcal{F}_{m,n}(I)$ is the polyhedral set $\bigcup\delta(I)$.
2. If $m < n$ then $\mathcal{F}_{m,n}(I)$ is the set $\mathbb{R}^d - F_{n,m}(I^c)$ (i.e., the complement in Euclidean d-space of the polyhedron given by the union of all the xels at 0's of I).

$\mathcal{F}(I)$ is also used relaxing us of the symbol $\mathcal{F}_{m,n}(I)$ with the schema of $dD(m,n)$ connectedness.

As shown in figure 1.9 it is easy to see that two xels belong to the same m-component of I if and only if they lie in the same connected component of $\mathcal{F}(I)$.

We have paved to give the definition of the attachment set of a grid point q (it was introduced by Dr. Kong), but to display the adjacencies of each grid point p with $\mathcal{F}(I)$ by q's attachment set we postpone it till section 2.1 after we study the Schlegel diagrams.

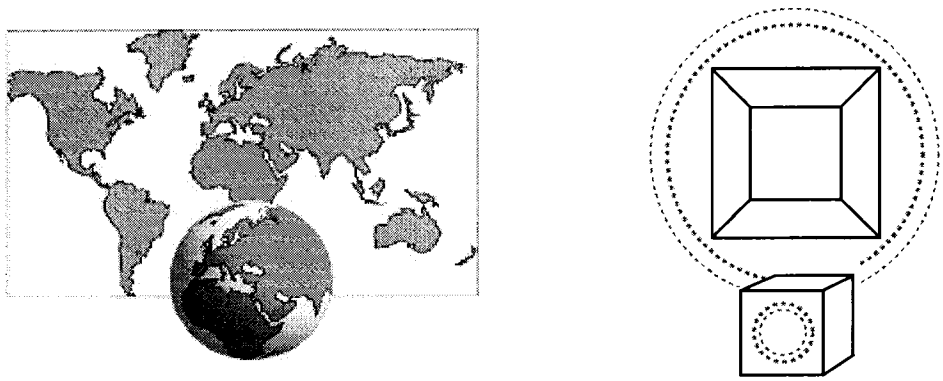

Figure 1.12: Just as the globe (to be exact, the surface of the globe) can be stretched to a 2D map, the boundary of a 3-xel can be stretched onto 2-space. (Obviously their deformations are different, where the 3-xel is stretched by the single point perspective. See figure 1.13 for details). Note that as the front face of the voxel is stretched open, its center is mapped to infinity.

1.5 Xel's Boundary and The Schlegel Diagram

Obviously, the connectedness relation between xels is implemented only on the faces and thus on the boundary of the xels.

Here is our definition of the boundary set of an elementary q, $Boundary(q)$ is defined to be the collection of all the proper faces of the polytope of dimension d in $\delta(q, I)$. Recall that $x(q)$ is a cracked Voronoi neighborhood, and $\delta(q, I)$ a cracked truncated tile. Now, the $Boundary(q)$ is a collection of cracked shell of the xel with the cracks shown as black lines in figure 1.10. All of them are polyhedral complexes.

The complex $Boundary(q)$ is called the boundary set of a xel q, and $\bigcup Boundary(q)$ denotes its polyhedral set. If dD(m, n)=2D(8,4), 3D(26,6) or 4D(80,8) this definition is equivalent to that previously defined in [7] because the tile-assembly in each schema is itself the natural tile — the hypercube without chopping.[11]

[11] Topologically, the attachment of the $x(q)$ is homopotic to that of the xel q.

For sparse images[12] with (m, n)-connectedness it is easy to analyze them by either the graph or topological approach, but for high dimensional dense or sponge images, we shall make strenuous efforts to get a comprehensive picture.

In this thesis we are interested in the d-space for $d \leq 4$, therefore the topological approach is still applicable because we are still "at home" in studying the 3D Schelegel diagram. The primary difficulty is that the front facet of a xel covers most parts of the xel, making it hard to study.

To uncover the full picture of the surface of the Voronoi neighborhood of a d-xel we introduce the *Schlegel diagram*, which completely encodes its adjacency relationships with its neighbors on a (d-1)-dimensional space. If $d = 4$ we further introduce the wire diagram for 4-xel and then expand it on 3-space. This reduction in dimension makes the Schlegel diagram especially useful in studying the adjacency relationship of 4-xels.

1.5.1 3D Schlegel Diagram

The technique of the linear perspective view can be traced back 300 years B.C. to Euclid's Optics. The simplest and most easily visualized one is called single point perspective (see figure 1.13 for a xel in a 3D(26,6)-image).[13] Zoom view is the single

[12]The term sparse (dense) is used to describe images whose components are far apart from (close to) others. Sponge images are dense and connected.

[13]For readers interested in step by step learning perspective drawing, please look at reference [2], which is easy to read.

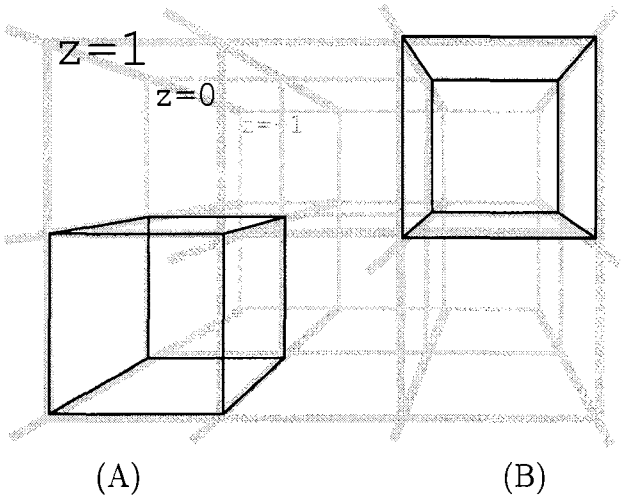

Figure 1.13: The boundary of an elementary 3-xel can be viewed by single point perspective. Both (A) and (B) show the same 3-xel where (A) is a wire frame side view, and (B) is a zoom view along the z-axis. The gray lines are the 3D coordinate axis reference lines.

point perspective having the vanishing view point at the center of the picture. By flattening the zoom view and mapping the center of the front facet to infinity, we obtain the Schlegel diagram of 3-xel on 2-space. Since perspective is to capture the projection image on a plane [1], loosely speaking, we may think of the Schlegel diagram as a projection image of the continuous perspective projection function — a close up view of a polyhedron on the projection screen intersecting the perimeter of a (large bulged) front facet of the polyhedron.

1.5.2 The Tesseract (or 4-Hypercube)

Recall that it is helpful to think of the 4-xel as a trajectory of 3-xel as it moves one unit of time. The boundary of a wire frame 4-xel can also be viewed by single point

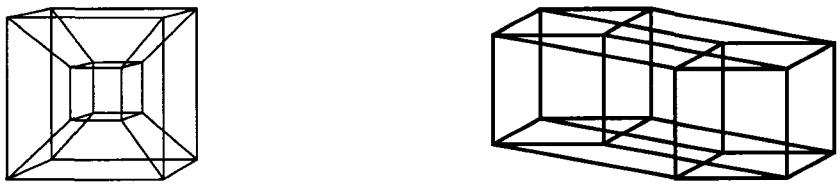

Figure 1.14: The tesseract — the wire diagram of a 4-xel; the zoom view is shown on the left and the oblique view on the right. The oblique view is a parallel side view (similar to the perspective side view), which is sometimes simple and clear to read.

perspective.[14] "Flatten" the zoom view by transforming (and shrinking) the cube at t = 0 to the center of cube at t=1 (by changing the x-, y-, z-coordinates and moving the cube to time slice t=1) and we obtain a wire diagram, nicknamed the tesseract (unfortunately, not a word in the dictionary as yet). The oblique view, as opposed to the zoom view of the 4-xel, is also used in much of the literature, especially when one would like to display a xel in the image, which has a thickness greater or equal to 3.

1.5.3 4D Schlegel Diagram

Please note that by now the solid cube at t=1 overlaps the transformed solid cube at t = 0, and both are facets. To avoid the overlapping, we stretch the cube at t =1 to the whole 3-space outside the flattened part by mapping the center of the cube (where t = 1) to infinity. Doing so will faithfully keep the adjacency relationships among all the faces of this xel's boundary. That is the merit of the Schlegel diagram of a 4-xel on 3-space.

[14]In the research of computer motion stereo, the side view is just a 3-xel's lateral motion model, and the zoom view is the 3-xel's longitudinal motion model.

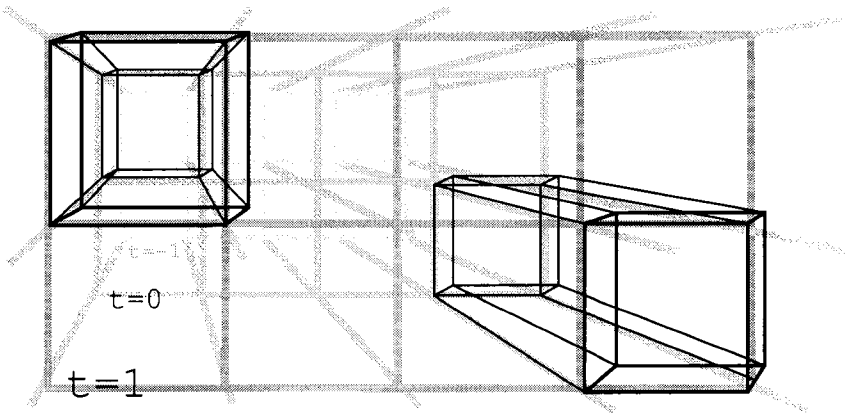

Figure 1.15: The boundary of an elementary 4-xel can also be "viewed" by single point perspective as in the 3-xel case; (A) is a 4-xel's wire frame zoom view along t-axis where the gray lines are x-, y- and t-coordinate reference lines of 4-space. The z-vanishing point is preset at some infinity point to the upper right direction (so to speak). In order to be easily perceptible on paper, the z-axis coordinate lines are omitted. They are (virtually) perpendicular lines to x-, y-, t- hyperplane in 4-space. (B) is a 4-xel's side view, which we will also use for illustrations in the ensuing sections.

The Schlegel diagrams illustrated above are for standard 3D cubes or 4D hypercubes. If a d-xel q is modified or chopped, then its associated Schlegel diagram must be modified accordingly in order to encode the adjacencies with its neighbors, as well as the adjacency relations among its neighbors. The modification can be easily made by a Y-to-$\triangle$ transformation[15] and X -to-tetrahedron transformation for 3D and 4D Schlegel Diagrams respectively. Loosely speaking, these transformations insert a small "standard" 2- or 3-simplex at the chopped vertex.

[15]We refer readers to Section 4.2 in [32] for details.

1.6 Conclusion of Part I

In this chapter we have defined the elementary building blocks of this thesis, i.e., the d-xel, the boundary set of the d-xels and the adjacency among the xels.

Besides terminology, we also introduced a method for viewing the adjacency relationships of a xel, i.e., the Schlegel diagram, which will be a very useful tool in the proofs. Here, instead of considering the Schlegel diagram as an projection image, we do encourage readers to read and study all the elements in the view (i.e., the Schlegel diagram) as if they were not flat but in the original 2D and 3D images. When we study the boundary of a grid point in 4D images using the attachment set (to be given in the next chapter) the existing tools developed for polyhedral complex can be adopted to the faces of boundary, not to the projection image on the Schlegel diagram.

Chapter 2

Topology Preservation

Human vision amazingly comes into correspondence when communicating ideas on the drawing board. Almost all young children learning to draw start by depicting a balloon head with a match-stick body, which artistically abstracts the image of the human figure and declares an awareness of the thinning concept.

Image processes imitate this same process of human intuition and obtain abstract forms through the erosion method. Binary images are thinned by deleting one pixel at a time; or a set of pixels, by parallel thinning algorithms. Loosely speaking, topology preservation is required here to ensure that the image process is not going to overdo its job, otherwise the match-stick human figure might end up with a broken leg, a hole in the head or a whole "component" missing.

The concept of a component is given to humankind and can be mathematically described as follows:

For any set S of d-xels, two xels $q_1, q_2 \in S$ are said to be *m-connected in* S if they

are related by the reflexive transitive closure of the m-adjacency relation on S. This is an equivalence relation on S, and its equivalence classes are called the *m-components* of S.

An equivalent way of defining the m-component is as follows:

Definition 2.0.1. A set S of xels of a grid is said to be m-disconnected if S can be partitioned into two (nonempty) subsets S_1 and S_2 which are such that no element of S_1 is m-adjacent to an element of S_2. S is said to be m-connected if S is not m-disconnected.

Definition 2.0.2. Let S be a nonempty set of xels of a grid. An m-component of S is a maximal m-connected subset of S.

2.1 Attachment Set of d-Xel

Skin deep, How Your House is Connected —Heritage Preservation Services, National Park Service

The partition walls to houses are the common faces to xels. To harness thinning algorithms we encode the xel's adjacency relations to its image using the concept, *attachment set* [13]:

$Attach(q, I) = \{f \mid f < \delta(q, I)$ *and* $f < y$ for some $y \in \delta(I \setminus \{q\})\}$ is called the *attachment complex* of a xel q in an image I. We caution readers that $\delta(q, I)$ is a xel, the polytope complex before the deletion, and y is a xel in the image I, and therefore $\delta(y, I)$ could be different from $\delta(y, I \setminus \{q\})$, i.e., before and after removing xel q. $\delta(y, I \setminus \{q\})$ is the xel y in the above definition. Its closed polyhedral set

$\bigcup Attach(q, I)$ is called the *attachment set* of q in I. This set can also be computed by $\bigcup Attach(q, I) = \bigcup \delta(q, I) \cap \mathcal{F}(I \setminus \{q\})$, which is homotopic to $\bigcup x(q) \cap \mathcal{F}(I \setminus \{q\})$. Note that in general $x(q) \neq \delta(q, I)$ and less computational effort is required for $\bigcup x(q) \cap \mathcal{F}(I \setminus \{q\})$.

Furthermore, in order to study the adjacency relations after deletion of this xel q, the Schlegel diagrams should be modified according to the foreground $\mathcal{F}(I \setminus \{q\})$. For example, the connectedness relation between xels b and c changes before and after the deletion of q as shown in figure 1.9.

2.2 Simple Xels and Simple Sets

Loosely speaking, a d-xel (of a grid point) in a dD binary image I is said to be *simple* in I if its deletion "preserves topology." Ideally, q is simple [1] if and only if the foreground of I can be continuously deformed onto the foreground of $I \setminus \{q\}$ in such a way that all points in $\mathcal{F}(I \setminus \{q\})$ (here we refer to the points of the Euclidean space in the polyhedra sets, not to the grid points) at the start remain fixed throughout the deformation process. More precisely, if I is a dD binary image, we say that a grid point $q \in I$ is *simple* if the polyhedron $\mathcal{F}(I \setminus \{q\})$ is a strong deformation retract of the polyhedron $\mathcal{F}(I)$ (see figure 1.9).

This definition of simpleness in terms of the polyhedra $\mathcal{F}(I)$ and $\mathcal{F}(I \setminus \{q\})$ is not

[1] The term "simple xel" is not related to simple polytope but to deformation.

consistent with figure 1.8 (Schema 1), therefore we have to use Schema 2.

2.2.1 Simple Xel's Characterizations

The definition involves continuous deformation, but Theorems 2.2.1 and 2.2.2 below give essentially discrete sets of necessary and sufficient conditions for d-xel q to be simple in I where $d \leq 4$ regardless of the grid type. [14]

These two theorems depend on the concept of the *attachment complex* of a xel q in I. Evidently, $\mathrm{A}ttach(q, I) \subseteq \mathrm{B}oundary(q)$. Also, note that the third condition is redundant in both theorems for $d = 3$.

Theorem 2.2.1. *Let q be a d-xel in a dD binary image I. Then q is simple in I if and only if the following all hold:*

1. $\bigcup \mathrm{A}ttach(q, I)$ *is connected and nonempty.*
2. $\bigcup \mathrm{B}oundary(q) - \bigcup \mathrm{A}ttach(q, I)$ *is connected and nonempty.*
3. $\bigcup \mathrm{A}ttach(q, I)$ *is simply connected.*

The following theorem applies to 3D(26,6) or 4D(80,8)-images on Cartesian grids only, although it can generally apply to many images with different connectedness. The notation $\chi(K)$ denotes the Euler characteristic for any xel-complex K.

Theorem 2.2.2. *Let q be a d-xel in a dD binary image I. Then q is simple in I if and only if the following all hold:*

1. $\bigcup \mathrm{A}ttach(q, I)$ *is connected.*

2. $\bigcup \mathrm{B}oundary(q) - \bigcup \mathrm{A}ttach(q, I)$ *is connected.*

3. $\chi(\mathrm{A}ttach(q, I)) = 1$.

For any xel-complex K, the *Euler characteristic* of K is the integer $\chi(K)$ defined by $\chi(K) = c_0(K) - c_1(K) + c_2(K) - c_3(K) + c_4(K)$, where $c_n(K)$ is the number of n-tiles in K. If $\mathcal{P}$ is the union of the xels of a xel-complex K, then we define $\chi(\mathcal{P})$ to be $\chi(K)$. It can be shown that if x is any truncated xel then $\chi(x) = 1$.

Theorems 2.2.1 and 2.2.2 are Theorems 7 and 9 in [14], except that the definition of a simple 4-xel used in that paper might seem to be more stringent than the definition given above: In [14], a 4-xel q is said to be simple in a 4D binary image I if $\bigcup \mathrm{A}ttach(q, I)$ is a strong deformation retract of q.

As is explained in [14], it follows from the main result of [16] that the three conditions of Theorem 2.2.1 are equivalent to the three conditions of Theorem 2.2.2 for 3D(26,6) or 4D(80,8)-images. So the two theorems are equivalent for 3D(26,6) or 4D(80,8)-images on Cartesian grids.

An elementary proof of the "if" parts of these theorems is given in [14]. A shorter proof can be given using the results of algebraic topology—notably Fact 3.4 in [29] (which follows from Corollaries 3.2.5, 1.3.11, and 1.4.10, and Theorem 1.4.11, in [30]) and Corollary 8.3.11 in [24].

Although the "only if" parts of Theorems 2.2.1 and 2.2.2 are easy to prove if simple 4-xels are defined as in [14], we have to work a little harder to give a proof

for the definition of simpleness used in this work. However, standard techniques of algebraic topology suffice. Indeed, assuming q is simple in I one can use the exact homology sequences of the pairs $(\bigcup \delta(q), \bigcup \mathrm{A}ttach(q, I))$ and $(\bigcup \delta(I), \bigcup(\delta(I \setminus \{q\})))$ together with the excision theorem to deduce that the reduced homology groups of $\bigcup \mathrm{A}ttach(q, I)$ are all trivial. The three conditions of Theorem 2.2.2 follow from this and the Alexander duality theorem. Readers may also be interested to read the characterization of 3D simple points in [4].

Our definition of simpleness has the advantage of being independent of dimensionality and of the shapes of xels. For example, the same definition of simpleness could be used for 3D, 4D binary images on a Cartesian grid and 3D binary images on an FCC grid. For FCC grids we would have dodecahedral rhomboids belonging to a tessellation of 3-space by congruent dodecahedral rhomboids. In fact, this definition can be used for non-congruent polyhedra tessellating d-space, and therefore it is applicable to the 3D tessellation of configuration of a tesseract.

2.2.2 Simple Sets

Now we are ready to consider parallel deletion of sets of d-xels. A set D of grid points in a dD binary image I is said to be *simple* in I if the d-xels of elements of D can be arranged in a sequence in which each element is simple after all of its predecessors in the sequence have been removed from the image.

Here is a more precise statement of this definition:

Definition 2.2.1. A sequence of d-xels in a dD binary image I is called a *simple sequence* of I if it is the empty sequence, or if it is a sequence $< q_1, q_2, ..., q_k >$ such that, for $1 < i \leq k$, q_i is a simple d-xel of $I - \{q_j | 1 \leq j < i\}$. A set D of d-xels in a dD binary image I is said to be *simple* in I if there is a simple sequence of I whose elements are exactly the elements of D.

In particular, the empty set is simple in I, and a singleton set $\{q\}$ is simple in I if and only if q is a simple d-xel of I.

Since the deletion of a single simple d-xel "preserves topology," so does the parallel deletion of a simple set of d-xels. More precisely, if D is a simple set of d-xels of a dD binary image I, then it follows from the definition of a simple d-xel (and the transitivity of the relation "is a strong deformation retract of") that $\mathcal{F}(I \setminus D)$ is a strong deformation retract of $\mathcal{F}(I)$.

A set D is called a hereditarily simple set in I if all subsets of D are simple in I. This type of sets was introduced by Dr. Kong in [13], and it provides the basis for useful methods of verifying that thinning algorithms preserve topology. Some authors called them p-simple sets. A related thinning algorithm is implemented by using hereditarily simple sets. [21]

2.3 Minimal Non-simple Set

We are interested in ways of proving that the set of d-xels deleted at each iteration of a given parallel thinning algorithm for dD binary images is always a simple set. (This would imply that the algorithm "preserves topology.") Since a non-simple set must evidently contain a *minimal* non-simple (MNS) set, one method of proof would be to show that at each iteration no set of d-xels that all satisfy the algorithm's deletion condition can be an MNS set of the image.

Definition 2.3.1. A set D of grid points is an MNS set in an (m, n)-image I if and only if D is a non-simple set of I but every proper subset of D is a simple set of I.

In fact, this would show that the subset of d-xels deleted at each iteration is not only simple but also *hereditarily* simple —i.e., all of its subsets are simple sets of the image.

The practicality of our approach depends on the fact that there are few types of possible MNS sets, and even fewer types of sets that can be MNS without being components of the 1's. (We say that a set of pixels/voxels *can be MNS* if there is a binary image in which that set is an MNS set of 1's.) Here we consider two sets of grid points to be of the same *type* if one set is a translate of the other. Some useful constraints will be given in the next section.

Here is a trivial example of an MNS set: If $q \in S$, an MNS set in image I and $\bigcup \mathrm{B}oundary(q) = \bigcup \mathrm{A}ttach(q, I)$ i.e., q is an interior xel of the image I and deleting

q forms a d-dimensional cavity (3D hole); this occurs if and only if the singleton $\{q\}$ is the MNS set S. Note that most of the binary images scanned in high resolution result in many such singleton MNS sets. Skipping the deletion of this kind of MNS set often speeds up the thinning process.

2.4 Useful Theorems for Minimal Non-simple Set

The next four theorems state algebraic properties of MNS sets. These results were established for 3D binary images in [13]—see Propositions 4.3, 4.5, 4.6, and 4.7 in that paper—and since they are proved by algebraic techniques using definitions and properties, which are not related to the dimensions and the shapes of tiles, they can be proved for dD images in the same way regardless of the grid type or dimensions.

Theorem 2.4.1. *Let D be a nonempty set of d-xels in a dD(m,n) binary image I. Then D is MNS in I if and only if the following conditions both hold:*

1. *Each element $q \in D$ is non-simple in $I \setminus (D \setminus \{q\})$.*
2. *Each element $q \in D$ is simple in $I \setminus D'$ whenever $D' \subsetneq D \setminus \{q\}$.*

We say that a set D of d-xels *can be MNS* if there is some $d\mathrm{D}(m,n)$ binary image I such that D is an MNS set of I. We say that a set D of d-xels *can be MNS without being a component* if there is some dD binary image I such that D is an MNS set of I and D is not an m-component of I.

Theorem 2.4.2. *Let D be an MNS set of a dD binary image I, and suppose D is not an m-component of I. Then every element of $\dot{D}$ is m-adjacent to a d-xel of I that is not in D.*

Theorem 2.4.3. *If a set D of d-xels can be MNS without being a component, then every subset D' of D can be MNS without being a component.*

The following is applied to d-dimensional Cartesian grid only.

Theorem 2.4.4. *A set of d-xels can be MNS only if it is a subset of some 2^d block of d-xels.*

The set satisfiing the above theorem is called a small set . A more general version of Theorem 2.4.4 is that every (m, n)-MNS set must be *small* in the sense of the following definition:

Definition 2.4.1. A set of xels of any grid is said to be small if no two xels in the set are disjoint (or, equivalently, if every pair of xels in the set are adjacent).

2.5 Conclusion of Part II

The attractiveness of the MNS proof method depends largely on the fact that if we regard two sets of pixels/voxels as being of the same type whenever one is a translate of the other, then only a few types of sets can be MNS. Indeed, it can be shown that no MNS set can contain two disjoint pixels or voxels: Every two pixels or voxels in an MNS set must share at least a vertex. Given a digital space, the key questions are:

1. Which types of sets can be MNS?

2. Which of those types of sets can be an MNS set of a binary image without being a component of the 1's?

We are ready to give the answers on an FCC-grid and a 4D Cartesian grid in the rest of this thesis.

Chapter 3

MNS set on Face-Centered-Cubic-Grid

In this chapter we determine which sets of voxels can be MNS on an FCC-grid, and also which of those sets can be MNS without being a component of the 1's. These two problems are complicated by the fact that there are (at least) three good pairs of connectedness in a binary image on an FCC grid, since one can:

Case 1: use 18-connectedness for sets of 1's and 12-connectedness for sets of 0's

Case 2: use 12-connectedness for sets of 1's and 18-connectedness for sets of 0's

Case 3: use 12-connectedness both for sets of 1's and for sets of 0's

We solve the two problems in all three cases, which wrap up the $d\mathrm{D}(m,n)$-images with $m \geq n$ (in Case 1) and $m \leq n$ (in Case 2), and the technique using Truncated xels (in Case 3). The xels of an FCC grid are rhombic dodecahedra, which are rather more difficult to visualize and draw than the cubical voxels of a 3D Cartesian grid.

3.1 FCC grids. Complementary FCC grids. Voxels in FCC grids.

A face-centered cubic ("FCC") grid is a 3D analog of a 2D hexagonal grid. An FCC grid is derived from a 3D Cartesian grid by picking every other grid point. More precisely, if G_C is the set of grid points of a 3D Cartesian grid, then we say that a subset G_F of G_C is an *FCC grid derived from* the Cartesian grid if, for each pair of 6-adjacent points p and p' of G_C, exactly one of the points p and p' is in G_F.

Two FCC grids can be derived from a 3D Cartesian grid: If G_F is an FCC grid derived from the Cartesian grid G_C, then the set $G_C - G_F$ of all Cartesian grid points that are *not* points of G_F will also be a derived FCC grid of G_C. We will say that these two FCC grids are *complementary*. If, for example, we start with the Cartesian grid given by the points with 3 integer coordinates, then the two complementary derived FCC grids are:

1. $\{(x, y, z) \mid x, y$ and z are integers such that $x + y + z$ is even$\}$, and

2. $\{(x, y, z) \mid x, y$ and z are integers such that $x + y + z$ is odd$\}$.

A few of the points of the first of these two FCC grids are shown in Figure 3.1.

Let G be an FCC grid. For each point p of G we define the *FCC-xel* associated with p in G to be the polytope consisting of all points in Euclidean 3-space that are at least as close to p as to any other point of G. This is the *Voronoi neighborhood* of

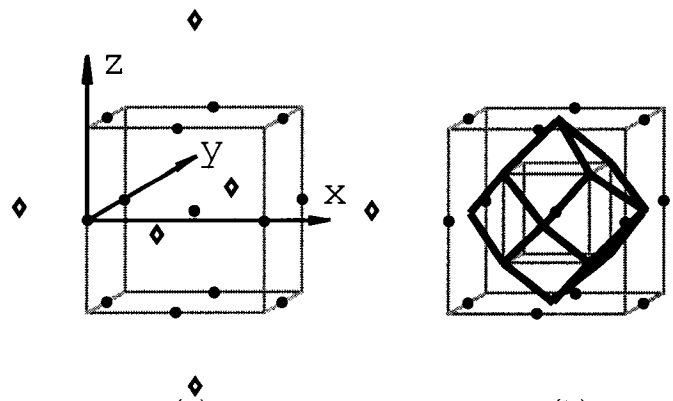

Figure 3.1: (a) The neighbors of an FCC-xel; (b) the FCC-xel and its core cube.

p in G. Every such polytope will also be called an *FCC-xel of* G. For brevity we will usually refer to an FCC-xel simply as a *voxel.* In the next section we determine the shape of a voxel, and consider how the FCC-xels tessellate 3-space.

3.2 Core cubes and void cubes of an FCC grid. Shape of a voxel. Boundary of a voxel. 12- and 18-adjacency.

In this section we point out an easy way to generate the Voronoi neighborhood on an FCC-grid.

Let G and G' be complementary FCC grids. Consider the "3D checkerboard" tessellation of Euclidean 3-space given by black cubes centered at the points of G and white cubes centered at the points of G'. The black cubes will be called the *core cubes* of the grid G, while the white cubes will be called the *void cubes* of G. Thus

each core cube of G is face-adjacent to 6 void cubes of G, and each void cube to 6 core cubes. (Note that the core cubes of G are the void cubes of G', and vice versa.) If v is a voxel associated with a point p in G, then the core cube centered at p will be referred to as *v's core cube.*

Let p be a point of G, and let C be the core cube of G that is centered at p. All points in C are at least as close to p as to any other point of G. Thus C is a subset of the voxel associated with p in G. Now let C' be any one of the 6 void cubes of G that are face adjacent to C. Which parts of C' lie in the voxel associated with p in G? C is just 1 of 6 core cubes of G that are face adjacent to C', so only 1/6 of C' will consist of points that are at least as close to p as to the points at the centers of the other 5 core cubes. We can subdivide C' into 6 congruent pyramids, where the base of each pyramid is a face of C' and the apex of each pyramid is the center of C'. The pyramid whose base is the common face of C and C' will be part of the voxel associated with p in G, but the rest of C' will not.

Thus the voxel associated with p in G is the union of the voxel's core cube C with 6 pyramids, where the base of each pyramid is a face of C and the apex of each pyramid is the center of one of the 6 void cubes of G that are face adjacent to C. Fig. 3.1(b) shows the voxel associated with p.

A voxel has 12 faces, each of which is a rhombus: It is a rhombic dodecahedron. The *boundary of* an FCC-xel v with respect to $(18, 12)$-connectedness, denoted by

Boundary(v), is the union of the 12 faces of v, including all the edges and vertices of v. Note that *Boundary*(q) was defined as the collection of all the proper faces of the polytope $\delta(q)$ where $\delta(q)$ is the Truncated xel. Thus, the boundary of an FCC-xel v with respect to $(12, 12)$-connectedness shall be modified accordingly.

Note that each of the 12 faces in *Boundary*(v) is bisected by one of the 12 edges of v's core cube. In fact, two core cubes of an FCC grid meet if and only if the voxels which contain them share the face that is bisected by the common edge of the cubes. Note also that a voxel has two types of vertices: (a) 6 vertices at the centers of the void cubes that are face-adjacent to the voxel's core cube, and (b) 8 vertices that are the vertices of the voxel's core cube. Each vertex of type (a) is also a vertex of 5 other voxels, as a void cube is face-adjacent to 6 core cubes. Each vertex of type (b) is also a vertex of 3 other voxels, as each vertex of a core cube is a vertex of 4 core cubes.

As we see from Fig. 1.6, each voxel meets 18 others. It shares just a vertex (of type (a)) with 6 of the 18, and shares a face with each of the other 12. Thus there are two natural concepts of adjacency and connectedness for FCC-voxels:

Definition 3.2.1. Two voxels v and w of an FCC grid are said to be 18-adjacent if $v \neq w$ but v meets w, and are said to be 12-adjacent if $v \neq w$ but v shares a face with w. If v and w are i-adjacent then we may also say that v is i-adjacent to w. (See Fig. 1.6)

3.3 FCC-binary images. Attachment Set Revisited. $F_{m,n}(I)$ and $A_{m,n}(v, I)$.

In this section we reiterate the definitions of foreground of 3D(m,n)-images on an FCC-grid and the attachment set of an FCC-xel.

If S is a subset of the 1's of an image I then $I - S$ denotes the image in which the voxels in S are 0's but all other voxels have the same values as they have in I. The process of changing I to $I - S$ is called *deletion* of S from I. (For example, each iteration of a parallel thinning algorithm deletes a set of 1's from the image.)

The deletion of certain sets of 1's is considered to "preserve topology". In order to be able to make precise statements about this, we associate each image with a subset of Euclidean 3-space. The way we do this depends on how we choose to define connectedness for sets of 1's and 0's. Specifically, if m-connectedness is used for sets of 1's and n-connectedness for sets of 0's, where $(m, n) = (18, 12)$, $(12, 18)$ or $(12, 12)$, then the image I is associated with its (m, n)-*foreground*, which we now define based on Definition 1.4.1:

Definition 3.3.1. For (m, n)=(18,12) or (12,12), let I be a 3D(m,n)-image on an FCC-grid. The (m, n)-foreground of I, denoted by $F_{m,n}(I)$, is the polyhedron given by the union of all the Truncated 1's of I.

Definition 3.3.2. Let I be a 3D(12,18)-image on an FCC-grid. The $(12, 18)$-foreground of I, denoted by $F_{12,18}(I)$, is the set $\mathbb{R}^3 - F_{18,12}(I^c)$ (i.e., the complement in Euclidean 3-space of the polyhedron given by the union of all the 0's of I).

If v is any 1 of I, then we may think of $F_{18,12}(I)$ as being obtained by gluing v onto $F_{18,12}(I - \{v\})$. The set of points on the boundary of v at which glue might

usefully be applied for this purpose is called the $(18, 12)$-*attachment set* of v in I and denoted by $A_{18,12}(v, I)$. Here is a precise definition:

Definition 3.3.3. Let v be a 1 of an FCC-binary image I. The (m, n)-attachment set of v in I where (m, n)=(18,12) or (12,12), denoted by $A_{m,n}(v, I)$, is the set $Boundary(v) \cap F_{m,n}(I - \{v\})$.

Thus $A_{18,12}(v, I)$ consists of all points on the boundary of v that also lie on the boundary of at least one other 1 of I (see the upper figure of Fig. 3.2). Also, $A_{12,12}(v, I)$ can be obtained by deleting the left vertex from $A_{18,12}(v, I)$ for the Truncated (12,12)-FCC-xel v (please refer to the lower figure of Fig. 3.2)

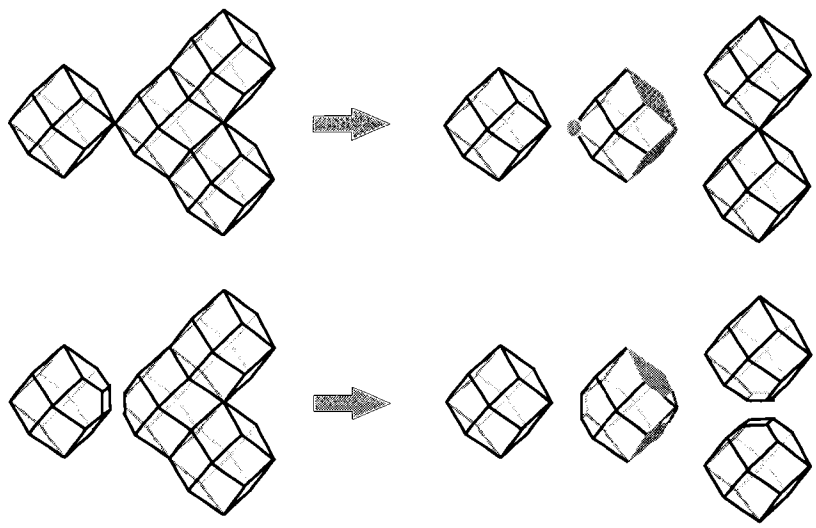

Figure 3.2: The upper figure shows the $(18, 12)$-attachment set of a non-simple FCC-xel v, sandwiched in an image, as the jointed gray faces and gray vertex; v's deletion splits the left FCC-xel from the image. For simplicity Schema 1 is used (informally) for the lower figure showing its $(12, 12)$-attachment set as two disjoint gray faces; v's deletion splits two right FCC-xels. In both cases the attachment set consists of two disjoint components.

The $(12, 18)$-attachment set is defined by using image complementation:

Definition 3.3.4. Let v be a 1 of an FCC-binary image I. The $(12,18)$-attachment set of v in I, denoted by $A_{12,18}(v,I)$, is the set $Boundary(v) - A_{18,12}(v,(I-\{v\})^c)$.

The interior of a face of v lies in $A_{12,18}(v,I)$ if and only if that face is also a face of another 1 of I. The interior of an edge of v lies in $A_{12,18}(v,I)$ if and only if both of the voxels of $I-\{v\}$ that are incident on that edge are 1's of I. A vertex of v lies in $A_{12,18}(v,I)$ if and only if all 3 or all 5 of the voxels of $I-\{v\}$ that are incident on that vertex are 1's of I.

The following proposition is a straightforward consequence of the above Definitions:

Proposition 3.3.1. *Let v be a 1 of an FCC-binary image I. Then, for $(m,n) = (18,12)$, $(12,12)$ or $(12,18)$:*

1. *$A_{m,n}(v,I)$ is empty if and only if v is not m-adjacent to any 1 of $I-\{v\}$.*
2. *$Boundary(v) - A_{m,n}(v,I)$ is empty if and only if v is not n-adjacent to any 0 of I.*

By Schema 2, $A_{12,12}(v,I)$ can be obtained from $A_{18,12}(v,I)$ by chopping all the pyramids (and gluing 2D cross-polytopes — diamond shape cutting sections) out of $A_{18,12}(v,I)$ at vertices p that satisfy one of the following conditions:

(i) p is a vertex of just one 1 of $I-\{v\}$ or

(ii) p is a vertex of just two 1's of $I-\{v\}$, and those two voxels do not share a face (i.e., they share just the vertex p).

By Schema 3, $(12,12)$-attachment set turns out to be a little easier to use:

Definition 3.3.5. Let v be a 1 of an FCC-binary image I. The $(12,12)^+$-attachment set of v in I, denoted by $A^+_{12,12}(v,I)$, is the subset of $Boundary(v)$ obtained from $A_{18,12}(v,I)$ by chopping tiny pyramids at vertices p that satisfy one of the following conditions:

(a) p is an isolated vertex in $A_{18,12}(v, I)$ (i.e., p is in $A_{18,12}(v, I)$ but none of the faces of v that are incident on p lie in $A_{18,12}(v, I)$).

(b) p is a vertex of just two 1's of $I - \{v\}$, and those two voxels do not share a face (i.e., they share just the vertex p).

Note that $A^+_{12,12}(v, I)$ is a superset of $A_{12,12}(v, I)$, since condition (a) is stronger than condition (i) above, while condition (b) is the same as condition (ii). The following proposition states the properties of $A^+_{12,12}(v, I)$ that we are most interested in. Its proof is straightforward and is left to the reader.

Proposition 3.3.2. Let v be a 1 of an FCC-binary image I. Then:

1. $A^+_{12,12}(v, I)$ is nonempty if and only if $A_{12,12}(v, I)$ is nonempty.
2. $A^+_{12,12}(v, I)$ is connected if and only if $A_{12,12}(v, I)$ is connected.
3. $Boundary(v) - A^+_{12,12}(v, I)$ is nonempty if and only if $Boundary(v) - A_{12,12}(v, I)$ is nonempty.
4. $Boundary(v) - A^+_{12,12}(v, I)$ is connected if and only if $Boundary(v) - A_{12,12}(v, I)$ is connected.

3.4 Topology-preserving deletion of 1's: (m, n)-simple 1's revisited.

Let v be a 1 of an FCC-binary image I. The voxel v is said to be (m, n)-*simple* in I if $F_{m,n}(I)$ can be continuously deformed over itself onto $F_{m,n}(I - \{v\})$; otherwise v is said to be (m, n)-*nonsimple* in I. We need not go into the details of how the continuous deformation process used here is defined, since we will use the characterization of (m, n)-simple 1's given in Theorem 3.4.1 below in all our proofs. If connectedness

of sets of 1's and of 0's of I is defined using m-connectedness for sets of 1's and n-connectedness for sets of 0's, then deletion of $\{v\}$ from I is considered to "preserve topology" if and only if v is (m,n)-simple in I.

Similar to the 3D Cartesian grid, the following theorem gives an easily visualized and essentially discrete characterization of (m,n)-simple 1's in terms of their (m,n)-attachment sets:

Theorem 3.4.1. *Let v be a 1 of an FCC-binary image I. Then, for $(m,n) = (18,12)$, $(12,18)$ or $(12,12)$, v is (m,n)-simple in I if and only if both of the following conditions hold:*

1. *$A_{m,n}(v,I)$ is nonempty and connected.*
2. *$Boundary(v) - A_{m,n}(v,I)$ is nonempty and connected.*

Analogous theorems for a Cartesian grid were given in [13]. Theorem 3.4.1 is proved in much the same way. We omit the details here.

Let the voxels v and w be distinct 1's of an image I. If v and w are disjoint (i.e., $v \cap w = \emptyset$), then $A_{m,n}(v,I) = A_{m,n}(v, I - \{w\})$. Hence Theorem 3.4.1 has the following corollary:

Corollary 3.4.2. *Let v and w be disjoint voxels each of which is a 1 in the FCC-binary image I. Then, for $(m,n) = (18,12)$, $(12,18)$ or $(12,12)$, v is (m,n)-simple in I if and only if v is (m,n)-simple in $I - \{w\}$.*

The following alternative characterizations of (m,n)-simple 1's can be deduced from Theorem 3.4.1 without much difficulty:

Corollary 3.4.3. *Let v be a 1 of an FCC-binary image I. Then:*

1. *v is $(18,12)$-simple in I if and only if both of the following conditions hold:*
   (a) *The set of 1's of I that are 18-adjacent to v is nonempty and 18-connected.*
   (b) *The set of 0's of I that are 12-adjacent to v is nonempty and 12-connected.*
2. *v is $(12,18)$-simple in I if and only if both of the following conditions hold:*
   (a) *The set of 0's of I that are 18-adjacent to v is nonempty and 18-connected.*
   (b) *The set of 1's of I that are 12-adjacent to v is nonempty and 12-connected.*
3. *v is $(12,12)$-simple in I if and only if both of the following conditions hold:*
   (a) *The set of 1's of I that are 12-adjacent to v is nonempty and lies in a single 12-component of the set of 1's of I that are 18-adjacent to v.*
   (b) *The set of 0's of I that are 12-adjacent to v is nonempty and lies in a single 12-component of the set of 0's of I that are 18-adjacent to v.*

Now let S be a set of one or more 1's that is about to be deleted from an image I (e.g., by a parallel thinning algorithm), and suppose connectedness of sets of 1's and 0's of I is defined using m-connectedness for sets of 1's and n-connectedness for sets of 0's. Under what circumstances might we regard the deletion of S from I to "preserve topology"?

As we mentioned above, when S is a singleton set $\{v\}$ we consider the deletion of S to "preserve topology" if v is (m,n)-simple in I. Thus if S is a finite set of 1's of I and the voxels in S can be arranged into a sequence in which each voxel is (m,n)-simple in the image after its predecessors have been deleted, then we must surely consider the deletion of S to "preserve topology". We say that S is (m,n)-simple if it satisfies this condition. Here is a precise definition of this concept:

Definition 3.4.1. A (finite) subset S of the 1's of an image I is said to be (m,n)-simple in I if the elements of S can be arranged into a sequence $< v_1, v_2, ..., v_k >$ such that v_i is (m,n)-simple in $I - \{v_j |\ 1 \leq j < i\}$ for $1 \leq i \leq k$. (In particular, the empty set is (m,n)-simple in I, and a singleton set $\{v\}$ is (m,n)-simple in I if and only if v is (m,n)-simple in I.)

The following proposition states two important properties of (m,n)-simple sets of 1's which can be deduced from Theorem 3.4.1 and Proposition 3.3.1 by induction on the number of elements in S. We leave the details of the proof to the interested reader.

Proposition 3.4.4. *Let Q be an (m,n)-simple set of 1's of an image I, where $(m,n) = (18,12)$, $(12,18)$ or $(12,12)$. Then:*

1. *Each m-component of the 1's of I contains exactly one m-component of the 1's of $I - Q$.*
2. *Each n-component of the 0's of $I - Q$ contains exactly one n-component of the 0's of I.*

The converse of this proposition is not true. (However, the converse of the analogous result for images on a 2D Cartesian grid *is* true, as Ronse showed in [Ronse86].)

3.5 Minimal nonsimple sets and Small sets revisted.

In this chapter we are primarily interested in *minimal* (m,n)-nonsimple sets of 1's of FCC-binary images (i.e., finite sets of 1's that are (m,n)-nonsimple in an FCC-binary image, but which have the property that all of their proper subsets are (m,n)-simple in that image). Such a set will be referred to as an (m,n)-*MNS set* of the image.

Some examples of this concept are shown in Fig. 3.3. The reader is invited to verify the three assertions in the figure's caption.

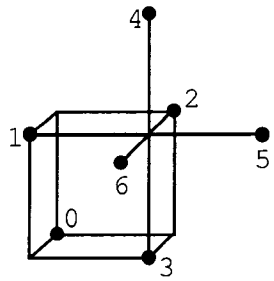

Figure 3.3: Regardless of whether $(m, n) = (18, 12)$, $(12, 18)$ or $(12, 12)$, the voxels centered at the points labeled 1, 2 and 3 form an (m, n)-MNS set in the image whose 1's are the voxels centered at the points labeled 0 through 6. The voxels centered at the points labeled 1, 2, 5 and 6 form a $(12, 12)$-MNS set in the image whose 1's are the voxels centered at the points labeled 0 through 6. The voxels centered at the points labeled 1 and 5 form a $(12, 18)$-MNS set in the same image.

We say that a set of voxels S *can be* (m, n)*-MNS* if there exists an image in which S is an (m, n)-MNS set. We say that a set of voxels S *can be* (m, n)*-MNS without being a component* if there exists an image I such that S is an (m, n)-MNS set of I and S is not an m-component of the 1's of I. Our main goals in this chapter are to identify all the sets of voxels of an FCC grid that can be (m, n)-MNS, and all the sets of voxels that can be (m, n)-MNS without being a component.

We will need the following characterization of (m, n)-MNS sets, whose proof is analogous to the proof of Proposition 4.3 in [13] and will not be given here:

Theorem 3.5.1. *Let S be a finite set of 1's of an FCC-binary image I, and let $(m, n) = (18, 12)$, $(12, 18)$ or $(12, 12)$. Then if S is an (m, n)-MNS set of I, each element v of S satisfies the following two conditions:*

1. *v is (m, n)-nonsimple in $I - (S - \{v\})$.*

2. v is (m,n)-simple in $I - T$ for every proper subset T of $S - \{v\}$.

The converse of this theorem is also true, but we will not need it. Another fact about MNS-sets that we *will* use follows from Theorem 3.5.1:

Corollary 3.5.2. *Let S be an (m,n)-MNS set of an FCC-binary image I, where $(m,n) = (18,12),(12,18)$ or $(12,12)$, and let D be any proper subset of S. Then $S - D$ is an (m,n)-MNS set of $I - D$.*

An immediate and important consequence of Corollary 3.5.2 is:

Proposition 3.5.3. *For $(m,n) = (18,12)$, $(12,18)$ or $(12,12)$, if a set of voxels S can be (m,n)-MNS then every nonempty proper subset of S can be (m,n)-MNS.*

Another important consequence of Theorem 3.5.1 is that every (m,n)-MNS set must be *small* in the sense of the following definition:

Definition 3.5.1. A set of voxels of an FCC grid is said to be small if no two voxels in the set are disjoint (or, equivalently, if every pair of voxels in the set are 18-adjacent).

A small set must evidently be 18-connected. A small set need not be 12-connected since it may consist of two voxels that share just a vertex.

Proposition 3.5.4. *Let S be an (m,n)-MNS set of an FCC-binary image I, where $(m,n) = (18,12)$, $(12,18)$ or $(12,12)$. Then S is small.*

This result is a special case of Theorem 2.4.4. The proof is a reasonably straightforward application of Theorem 3.5.1 and Corollary 3.4.2.

The next proposition identifies all the small sets of voxels of an FCC grid. It is easily proved by inspection and enumeration of cases, and we again omit the details of the proof.

Proposition 3.5.5. *Let S be a set of voxels of an FCC grid G. Then S is small if and only if S satisfies one of the following conditions:*

1. *S is a subset of a set of 6 pairwise 18-adjacent voxels of G.*
2. *S is a set of 4 pairwise 12-adjacent voxels of G.*

Say that two sets of voxels of an FCC grid are *of the same type* if one set is a translate of the other. Then for any FCC grid G there is just one type of set that consists of 6 pairwise 18-adjacent voxels of G (see Fig. 3.4(a)), and just two types of sets that consist of 4 pairwise 12-adjacent voxels of G (the type shown in Fig. 3.4(b), and a mirror image of that type).

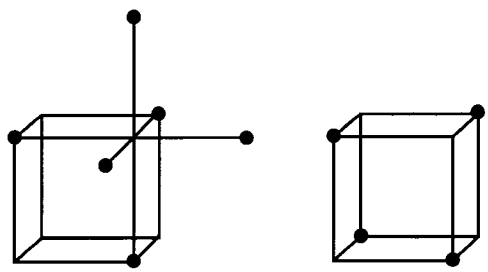

Figure 3.4: The left figure shows centers of 6 pairwise 18-adjacent FCC-xels; the right shows the centers of 4 pairwise 12-adjacent FCC-xels.

Another fundamental restriction on (m, n)-MNS sets is given by the following result:

Proposition 3.5.6. *Let S be an (m, n)-MNS set of an FCC-binary image I, where $(m, n) = (18, 12)$, $(12, 18)$ or $(12, 12)$, and suppose S is not an m-component of the 1's of I. Then every element of S is m-adjacent to a 1 of $I \setminus S$.*

Proof. Let q be any element of S, and let Q be the m-component of the 1's of I that contains q. Then Q is not equal to S (as S is not an m-component of the 1's of I).

Q is also not a proper subset of S, since Q is (m,n)-nonsimple in I (by condition 1 of Proposition 3.4.4) but S is a minimal (m,n)-nonsimple set of I. Hence there is a voxel v in $Q \setminus S$.

$S \setminus \{q\}$ is (m,n)-simple in I, since S is minimal (m,n)-nonsimple in I. So, since q and v lie in the same m-component of the 1's of I (namely Q), q and v must also lie in the same m-component of the 1's of $I \setminus (S \setminus \{q\})$ (by condition 1 of Proposition 3.4.4). So q must be m-adjacent to a 1 of $I \setminus S$ (otherwise the m-component of the 1's of $I \setminus (S \setminus \{q\})$ that contains q would not contain any other voxel). ////

Proposition 3.5.7. *Let S be an (m,n)-MNS set of an FCC-binary image I, where $(m,n) = (18,12)$, $(12,18)$ or $(12,12)$, and suppose S is not an m-component of the 1's of I. Let D be any proper subset of S. Then $S \setminus D$ is not an m-component of the 1's of $I \setminus D$.*

Corollaries 3.5.2 and 3.5.7 together imply the following:

Proposition 3.5.8. *For $(m,n) = (18,12)$, $(12,18)$ or $(12,12)$, if a set of voxels S can be (m,n)-MNS without being a component then every nonempty proper subset of S can be (m,n)-MNS without being a component.*

3.6 (18,12)-MNS sets. Use of a Schlegel diagram of an FCC-voxel.

In view of the fact that only nonempty small sets can be (m,n)-MNS (by Proposition 3.5.4), the following theorem identifies the sets of voxels that can be $(18,12)$-MNS, and the sets of voxels that can be $(18,12)$-MNS without being a component:

Theorem 3.6.1. *Let S be a nonempty small set of voxels of an FCC grid. Then S satisfies exactly one of the following conditions:*

1. *S is a subset of a set of 3 pairwise 12-adjacent voxels.*
2. *S is a set of 4 pairwise 12-adjacent voxels.*
3. *S contains 2 voxels that are not 12-adjacent (i.e., 2 voxels that meet only at a vertex).*

If S satisfies condition 1 then S can be $(18, 12)$-MNS without being a component. If S satisfies condition 2 or condition 3 then S is an $(18, 12)$-MNS set if and only if S is an 18-component of the 1's.

Proof. It is readily confirmed that S must satisfy exactly one of the three conditions. We see from Fig. 3.5 (or Fig. 3.3) and Proposition 3.5.8 that if S satisfies condition 1 then S can be $(18, 12)$-MNS without being a component.

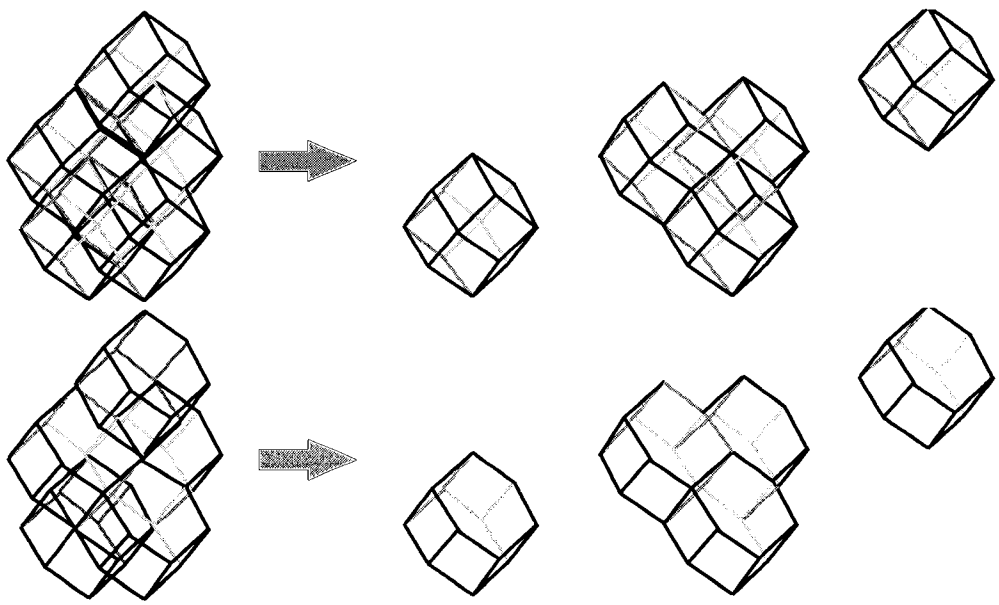

Figure 3.5: The top figure shows a set of three pairwise 12-adjacent FCC voxels in black is a MNS set in its image. Deleting them separates two FCC voxels in blue. An alternative and easier way to observe is given at the bottom, which shows the skewed view of the homotopic image flattening FCC voxels into hexagon prisms.

It is also easily verified that if the small set S is an 18-component of the 1's of an image I then S is an $(18, 12)$-MNS set of I, regardless of whether S satisfies condition

1, condition 2 (see Fig. 3.6) or condition 3 (see Fig. 3.7).

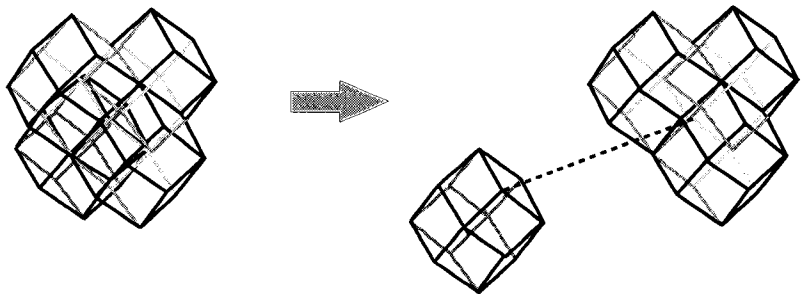

Figure 3.6: The set of four pairwise 12-adjacent FCC voxels is small set in the image on the left. The right figure shows the explosion view.

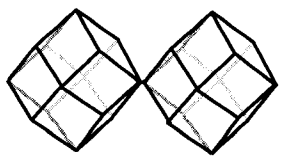

Figure 3.7: It is clear that the 18-component of two FCC voxels sharing only one vertex is MNS in this image.

Suppose S satisfies condition 3. We need to show that S cannot be $(18, 12)$-MNS without being a component. Let v and w be two voxels in S that are not 12-adjacent. By Proposition 3.5.8, it suffices to show that the subset $\{v, w\}$ of S cannot be $(18, 12)$-MNS without being a component. So let us suppose $\{v, w\}$ is an $(18, 12)$-MNS set of an image I. Then it follows from Theorem 3.5.1 that v is $(18, 12)$-nonsimple in $I - \{w\}$ but v is $(18, 12)$-simple in I. Since v is $(18, 12)$-nonsimple in $I - \{w\}$, Theorem 3.4.1 implies that one of the following is true:

(a) $A_{18,12}(v, I - \{w\})$ is empty.

(b) $A_{18,12}(v, I - \{w\})$ is disconnected.

(c) $A_{18,12}(v, I - \{w\}) = Boundary(v)$.

(d) $Boundary(v) - A_{18,12}(v, I - \{w\})$ is disconnected.

Let x be the common vertex of v and w. Then $A_{18,12}(v, I) = A_{18,12}(v, I - \{w\}) \cup \{x\}$. So, since $A_{18,12}(v, I)$ is a closed subset of $Boundary(v)$, if (b), (c) or (d) were true then that same condition would be true with $A_{18,12}(v, I)$ in place of $A_{18,12}(v, I - \{w\})$, and v would be $(18, 12)$-nonsimple in I, a contradiction. Hence (b), (c) and (d) must be false and (a) must be true. Thus (by Proposition 3.3.1) v is not 18-adjacent to any 1 of $I - \{w\}$, and so (by Proposition 3.5.6) $\{v, w\}$ must be an 18-component of the 1's of I, as required.

Now suppose S satisfies condition 2. Again, we need to show that S cannot be $(18, 12)$-MNS without being a component. So let us suppose S is an $(18, 12)$-MNS set of an image I. Let $S = \{v_0, v_1, v_2, v_3\}$. Then it follows from Theorem 3.5.1 that v_0 is $(18, 12)$-nonsimple in $I - \{v_1, v_2, v_3\}$ but v_0 is $(18, 12)$-simple in $I - \{v_1, v_2\}$, $I - \{v_2, v_3\}$ and $I - \{v_1, v_3\}$. Since v_0 is $(18, 12)$-nonsimple in $I - \{v_1, v_2, v_3\}$, Theorem 3.4.1 implies that one of the following is true:

(a1) $A_{18,12}(v_0, I - \{v_1, v_2, v_3\})$ is empty.

(b1) $A_{18,12}(v_0, I - \{v_1, v_2, v_3\})$ is disconnected.

(c1) $A_{18,12}(v_0, I - \{v_1, v_2, v_3\}) = Boundary(v_0)$.

(d1) $(Boundary(v_0)) - A_{18,12}(v_0, I - \{v_1, v_2, v_3\})$ is disconnected.

In fact (c1) is impossible, since the interior of the common face of v_0 and v_1 would not be in $A_{18,12}(v_0, I - \{v_1, v_2, v_3\})$. We will show that (b1) and (d1) are also impossible. In considering (b1) and (d1), it is helpful to look at a Schlegel diagram of the voxel v_0, which is obtained by stereographic projection of $Boundary(v_0)$ onto a plane, as shown in Fig. 3.8.

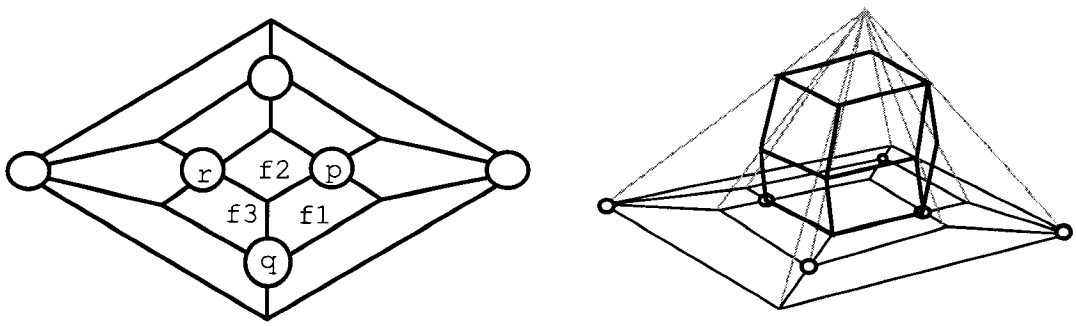

(a) (b)

Figure 3.8: (a) A Schlegel diagram of the voxel v_0 considered in the proofs of Theorem 3.6.1. This is obtained from v_0 by stereographic projection (bird's view perspective projection), as shown in (b). The small disks in the Schlegel diagram (the disks labeled p, q and r, and the three unlabeled small disks) each correspond to a vertex of v_0 that is the center of a void cube of the FCC grid. The unbounded outside region of the Schlegel diagram corresponds to the top face of v_0. Each bounded region of the diagram corresponds to one of the other 11 faces of v_0. For $i = 1, 2, 3$ the region labeled f_i corresponds to the common face of v_0 and the voxel v_i in the proofs of Theorem 3.6.1.

For $i = 1, 2$ and 3, let f_i denote the common face of v_0 and v_i. Then $A_{18,12}(v_0, I - \{v_2, v_3\}) = A_{18,12}(v_0, I - \{v_1, v_2, v_3\}) \cup f_1$. So we see from the Schlegel diagram that if condition (d1) holds then (d1) also holds with $A_{18,12}(v_0, I - \{v_2, v_3\})$ in place of $A_{18,12}(v_0, I - \{v_1, v_2, v_3\})$ [because the interiors of f_2 and f_3 lie in the same component

of $(Boundary(v_0)) - A_{18,12}(v_0, I - \{v_1, v_2, v_3\})$ as the interior of f_1, so that f_1 does not cover an entire component of $(Boundary(v_0)) - A_{18,12}(v_0, I - \{v_1, v_2, v_3\})]$. Hence if condition (d1) holds then v_0 is $(18, 12)$-nonsimple in $I - \{v_2, v_3\}$, a contradiction.

Now suppose condition (b1) holds. Let C_1 and C_2 be two different components of $A_{18,12}(v_0, I - \{v_1, v_2, v_3\})$. We know $A_{18,12}(v_0, I - \{v_1, v_2, v_3\}) \cup f_1 = A_{18,12}(v_0, I - \{v_2, v_3\})$ is connected, since v_0 is $(18, 12)$-simple in $I - \{v_2, v_3\}$. Thus C_1 and C_2 must lie in the same component of $A_{18,12}(v_0, I - \{v_1, v_2, v_3\}) \cup f_1$. In other words, f_1 "joins" the closed sets C_1 and C_2, and so both C_1 and C_2 must meet f_1. Each of C_1 and C_2 either is a union of faces of v_0, or is a vertex where 4 faces meet. The only such vertices that are incident on f_1, are the vertices labeled p and q in Fig. 3.8, and each face of v_0 that meets f_1, contains the vertex p or the vertex q. So, since C_1 meets f_1, C_1 contains one of the vertices labeled p and q in Fig. 3.8. Similarly, C_1 must contain one of the vertices q and r in the diagram, and C_1 must also contain one of the vertices p and r. Thus C_1 contains at least two of the vertices p, q and r. By a symmetrical argument, C_2 also contains at least two of the vertices p, q and r. Hence one of the points p, q and r lies in both of the sets C_1 and C_2. This contradiction shows that (b1) does not hold. It follows that condition (a1) holds, and so (by Propositions 3.3.1 and 3.5.6) S must be an 18-component of the 1's of I, as required. ////

3.7 (12,12)-MNS sets.

The following theorem identifies the sets of voxels that can be $(12, 12)$-MNS, and the sets of voxels that can be $(12, 12)$-MNS without being a component:

Theorem 3.7.1. *Let S be a nonempty small set of voxels of an FCC grid. Then S satisfies exactly one of the following conditions:*

1. *S is a set of 3 pairwise 12-adjacent voxels.*
2. *S is a set of 4 pairwise 12-adjacent voxels.*
3. *S is a subset of a set of 4 voxels $\{v_0, v_1, v_2, v_3\}$ in which v_i is 12-adjacent to v_{i+1} for $i = 0, 1, 2$ but v_i is not 12-adjacent to v_{i+2} for $i = 0$ and 1.*
4. *S contains 4 voxels w_0, w_1, w_2, w_3 such that w_i is 12-adjacent to w_{i+1} for $i = 0, 1, 2$, and w_1 is 12-adjacent to w_3, but w_0 is not 12-adjacent to w_2*

If S satisfies condition 1 or condition 3 then S can be $(12, 12)$-MNS without being a component. If S satisfies condition 2 then S is a $(12, 12)$-MNS set if and only if S is a 12-component of the 1's. If S satisfies condition 4 then S cannot be $(12, 12)$-MNS.

[Note that if in Fig. 3.3 we take v_0, v_1, v_2 and v_3 to be the voxels centered at the points labeled 1, 2, 5 and 6, and take w_0, w_1, w_2 and w_3 to be the voxels centered at the points labeled 1, 2, 5 and 4, then the v's and w's have the properties stated in conditions 3 and 4 (see also Fig. 3.9 and Fig. 3.10).]

Proof. It is readily confirmed by inspection of Figure 3.4 that S must satisfy exactly one of the four conditions. We see from Fig. 3.3 and Proposition 3.5.8 that if S satisfies condition 1 or condition 3 then S can be $(12, 12)$-MNS without being a component. It is also easily verified that if S satisfies condition 2 and is a 12-component of the 1's of an image I then S is a $(12, 12)$-MNS set of I.

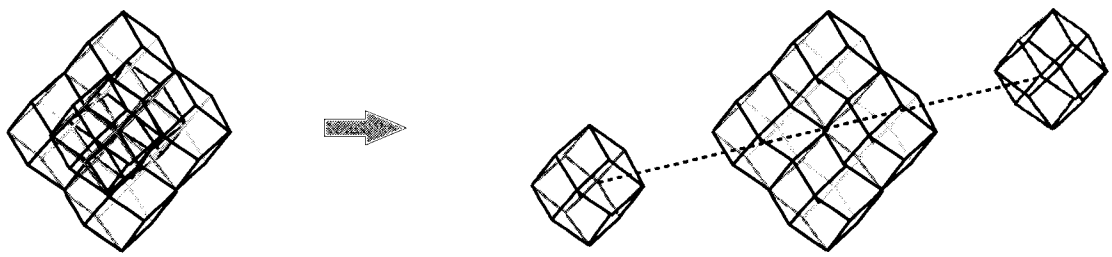

Figure 3.9: The set of four FCC voxels in black satisfying condition 3 is MNS in the image on the left; The red and blue voxels are not connected. The right figure shows the explosion view.

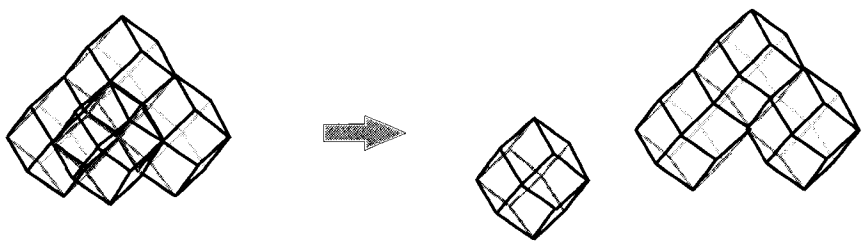

Figure 3.10: The set containing four FCC voxels satisfying condition 4 (as shown on the left) cannot be (12,12)-MNS. The right figure shows its explosion view.

On the other hand, if S satisfies condition 2 and is a $(12, 12)$-MNS set of an image I then we can show that S must be a 12-component of the 1's of I using much the same argument as was used to establish the analogous assertion in the proof of Theorem 3.6.1. (We use the $(12, 12)$-attachment set instead of the $(18, 12)$-attachment set. To show that the analog of condition (b1) is impossible, we let C_1 and C_2 be two different components of $A_{12,12}(v_0, I - \{v_1, v_2, v_3\})$ and argue that, since the closures of C_1 and C_2 must meet f_1, one of the points p, q and r lies in both closures — the argument is essentially the same as the argument in the next-to-last paragraph of the proof of Theorem 3.6.1. We deduce from this that C_1 and C_2 must actually meet, which is a contradiction. The details are left to the reader.)

Now suppose S satisfies condition 4. We need to show that S cannot be $(12,12)$-MNS. By Proposition 3.5.3 it suffices to show that the subset $\{w_0, w_1, w_2, w_3\}$ of S cannot be $(12,12)$-MNS. Let I be an image in which the w's are 1's. Then it is readily confirmed that $A^+_{12,12}(w_0, I-\{w_1, w_2, w_3\}) = A^+_{12,12}(w_0, I-\{w_1, w_3\})$. It follows from this and Proposition 3.3.2 that $A_{12,12}(w_0, I-\{w_1, w_2, w_3\})$ and $Boundary(w_0) - A_{12,12}(w_0, I-\{w_1, w_2, w_3\})$ are nonempty and connected if and only if $A_{12,12}(w_0, I - \{w_1, w_3\})$ and $Boundary(w_0) - A_{12,12}(w_0, I-\{w_1, w_3\})$ are nonempty and connected. Thus w_0 is $(12,12)$-simple in $I - \{w_1, w_2, w_3\}$ if and only if w_0 is $(12,12)$-simple in $I - \{w_1, w_3\}$, by Theorem 3.4.1. So $\{w_0, w_1, w_2, w_3\}$ cannot be a $(12,12)$-MNS set of I, by Theorem 3.5.1 (taking $v = w_0$). ////

3.8 (12,18)-MNS sets.

The following theorem identifies the sets of voxels that can be $(12,18)$-MNS, and the sets of voxels that can be $(12,18)$-MNS without being a component:

Theorem 3.8.1. *Let S be a nonempty small set of voxels of an FCC grid. Then S satisfies exactly one of the following conditions:*

1. *S is a subset of a set of 3 pairwise 12-adjacent voxels.*
2. *S is a set of 4 pairwise 12-adjacent voxels.*
3. *S is a set of 2 voxels that are not 12-adjacent.*
4. *S contains 3 voxels w_0, w_1, w_2 such that w_0 is 12-adjacent to w_1, but not 12-adjacent to w_2.*

If S satisfies condition 1 or condition 3 then S can be $(12,18)$-MNS without being a component. If S satisfies condition 2 then S is a $(12,18)$-MNS set if and only if S is a 12-component of the 1's. If S satisfies condition 4 then S cannot be $(12,18)$-MNS.

[If in Fig. 3.3 we take w_0, w_1, and w_2 to be the voxels centered at the points labelled 1, 2 and 5, then the w's have the properties stated in condition 4 (see also Fig. 3.11).]

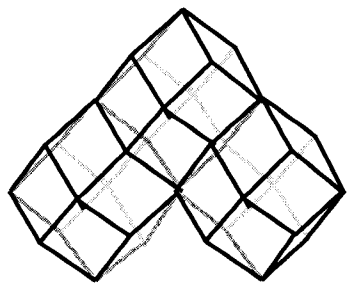

Figure 3.11: This figure shows the configuration of 3 voxels satisfying condition 4.

Proof. It is readily confirmed by inspection of Figures 3.4 that S must satisfy exactly one of the four conditions. We see from Fig. 3.3 and Proposition 3.5.8 that if S satisfies condition 1 (see also Fig. 3.5) or condition 3 (refer to the set of red and blue voxels in Fig. 3.9) then S can be $(12, 18)$-MNS without being a component.

Suppose S satisfies condition 4 (refer to Fig. 3.11). Let I be an image in which the w's are 1's. Then it is readily confirmed that $A_{12,18}(w_0, I - \{w_1, w_2\}) = A_{12,18}(w_0, I - \{w_1\})$. Thus w_0 is simple in $I - \{w_1, w_2\}$ if and only if w_0 is $(12, 18)$-simple in $I - \{w_1\}$, by Theorem 3.4.1. Hence $\{w_0, w_1, w_2\}$ is not a $(12, 18)$-MNS set of I, by Theorem 3.5.1 (taking $v = w_0$). As the subset $\{w_0, w_1, w_2\}$ of S cannot be $(12, 18)$-MNS, it follows from Proposition 3.5.3 that S cannot be $(12, 18)$-MNS.

Now suppose S satisfies condition 2. Let $S = \{v_0, v_1, v_2, v_3\}$. It is readily confirmed that if S is a 12-component of the 1's of an image I, then S is a $(12, 18)$-MNS set

of I. But we still need to show that S cannot be $(12,18)$-MNS without being a component. So let us suppose S is a $(12,18)$-MNS set of an image I. Then it follows from Theorem 3.5.1 that v_0 is $(12,18)$-nonsimple in $I-\{v_1,v_2,v_3\}$, but is $(12,18)$-simple in $I-\{v_1,v_2\}$, $I-\{v_2,v_3\}$ and $I-\{v_1,v_3\}$. Since v_0 is $(12,18)$-nonsimple in the image $I-\{v_1,v_2,v_3\}$, Theorem 3.4.1 implies that one of the following is true:

(a1) $A_{12,18}(v_0, I-\{v_1,v_2,v_3\})$ is empty.

(b1) $A_{12,18}(v_0, I-\{v_1,v_2,v_3\})$ is disconnected.

(c1) $A_{12,18}(v_0, I-\{v_1,v_2,v_3\}) = Boundary(v_0)$.

(d1) $(Boundary(v_0)) - A_{12,18}(v_0, I-\{v_1,v_2,v_3\})$ is disconnected.

Here (c1) is impossible, since the common face of v_0 and v_1 is not in $A_{12,18}(v_0, I-\{v_1,v_2,v_3\})$. Next, we show that (d1) is also impossible. Again, it is helpful to look at the Schlegel diagram of the voxel v_0 in Fig. 3.12. For $i=1$, 2 and 3, let f_i denote the common face of v_0 and v_i. Then $(Boundary(v_0)) - A_{12,18}(v_0, I-\{v_1,v_2,v_3\}) = ((Boundary(v_0)) - A_{12,18}(v_0, I-\{v_2,v_3\})) \cup f_1$. Note that if the set $(Boundary(v_0)) - A_{12,18}(v_0, I-\{v_2,v_3\})$ is connected then, since f_2 lies in $(Boundary(v_0)) - A_{12,18}(v_0, I-\{v_2,v_3\})$ and f_2 meets f_1, the set $((Boundary(v_0)) - A_{12,18}(v_0, I-\{v_2,v_3\})) \cup f_1 = (Boundary(v_0)) - A_{12,18}(v_0, I-\{v_1,v_2,v_3\})$ is also connected.

So if condition (d1) holds then (d1) also holds with $A_{12,18}(v_0, I-\{v_2,v_3\})$ in place of $A_{12,18}(v_0, I-\{v_1,v_2,v_3\})$. Hence if condition (d1) holds then v_0 is $(12,18)$-nonsimple

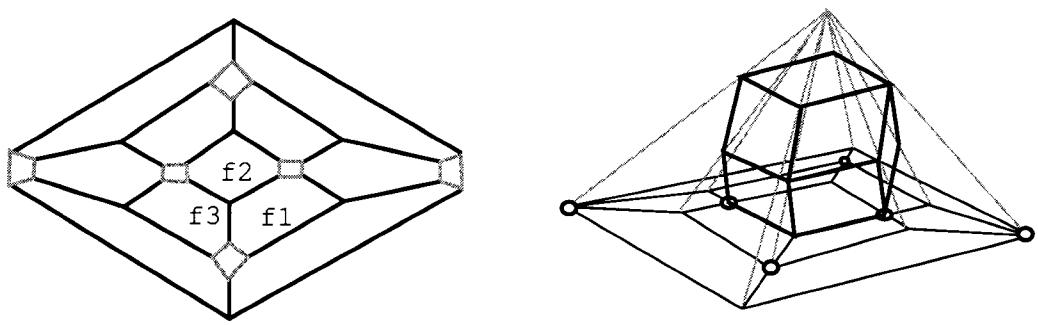

Figure 3.12: (a) A Schlegel diagram of the voxel v_0 is considered in the proofs of Theorem 3.8.1. This is bird's view perspective projection as shown in (b). Instead of small disks, there are six gray quadrilaterals in the Schlegel diagram that are "ready" to be chopped, i.e., the cutting sections of an FCC-xel . The unbounded outside region of the Schlegel diagram corresponds to the top face of v_0. For $i = 1, 2, 3$ the region labeled f_i corresponds to the common face of v_0 and the voxel v_i in the proofs of Theorem 3.8.1.

in $I - \{v_2, v_3\}$, a contradiction.

Now we show (b1) is impossible. Note that the vertices p and q in Fig. 3.12 are not in $A_{12,18}(v_0, I - \{v_2, v_3\})$, because f_2 and f_3 are not in $A_{12,18}(v_0, I - \{v_2, v_3\})$. We also see from Fig. 3.8 that the only faces of v_0 other than f_2 and f_3 that share an edge with f_1 also share an edge with each other (so the interiors of those two faces cannot lie in different components of $A_{12,18}(v_0, I - \{v_1, v_2, v_3\})$. Thus if $A_{12,18}(v_0, I - \{v_2, v_3\})$ is connected then so is $A_{12,18}(v_0, I - \{v_2, v_3\}) - f_1 = A_{12,18}(v_0, I - \{v_1, v_2, v_3\})$. It follows that if condition (b1) holds then (b1) also holds with $A_{12,18}(v_0, I - \{v_2, v_3\})$ in place of $A_{12,18}(v_0, I - \{v_1, v_2, v_3\})$, and that implies v_0 is $(12, 18)$-nonsimple in $I - \{v_2, v_3\}$, a contradiction.

This shows that condition (a1) holds, and so (by Propositions 3.3.1 and 6.7) S must be a 12-component of the 1's of I, as required. ////

3.9 Conclusion of Part III

Theorems 3.6.1, 3.7.1 and 3.8.1 above identify all sets of voxels of a 3D face-centered cubic grid that can be minimal (m, n)-nonsimple, and all sets that can be minimal (m, n)-nonsimple without being an m-component of the 1's, for $(m, n) = (18, 12)$, $(12, 12)$ and $(12, 18)$. We see from these theorems that a minimal (m, n)-nonsimple set that is not an m-component of the 1's can contain at most 3 voxels when $(m, n) = (18, 12)$ or $(12, 18)$, and can contain at most 4 voxels when $(m, n) = (12, 12)$.

Our results were obtained by considering the attachment sets of FCC-xels, using the same general approach as was used in [13] for the Cartesian grid. As our xels are rhombic dodecahedra rather than cubes, xel configurations may be significantly more difficult to visualize and to draw than in the case of the Cartesian grid. However, we have found that in much of our work it is unnecessary to visualize or draw FCC-xel configurations, since the attachment set of a xel is a subset of its boundary and can therefore be represented in a planar Schlegel diagram of a xel, which is easy to draw.

It is interesting to observe that if we slice a set of 3 pairwise 12-adjacent voxels (refer to Fig. 3.5) perpendicular to their shared edge, the cutting section is a 2D maximal small set of hexagons in a triangle grid. This set of 3 pairwise 12-adjacent voxels could be a 3D minimal (18,12)-nonsimple set without being a component according to the theorem 3.7.1. A similar result of a MNS set in 4D Cartesian gird can be obtained by "thickening" a 3D maximal small set in 3D Cartesian gird (please see

next chapter's concluding remark).

We believe that the same methods can be used to solve the analogous problems for binary images on 3D body-centered cubic grids [Kovalevs84] and the 2D and 3D binary images derived from Khalimsky's product topology on $\mathbb{Z}^n$ [11] and [20].

This work also paves the way to study 4D MNS sets in the next chapter.

Chapter 4

MNS set with (80,8)-connectedness

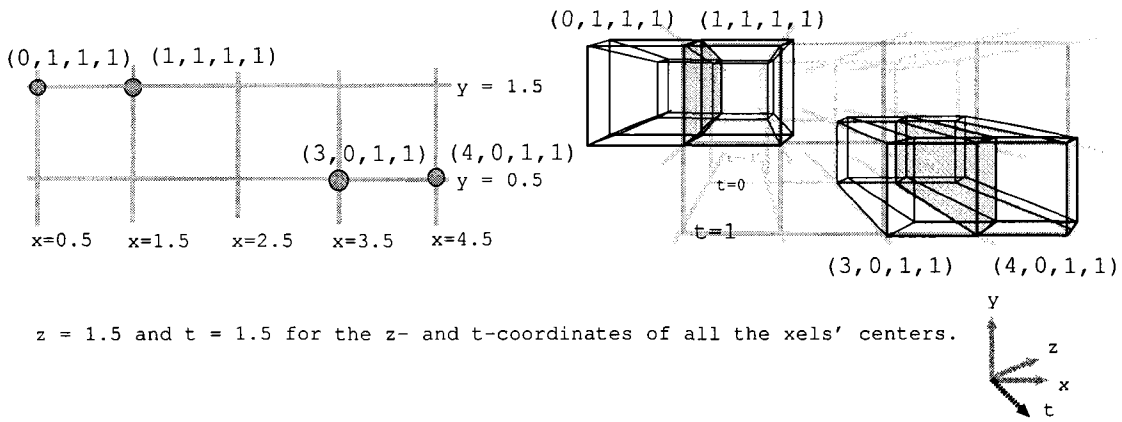

(A) Xels on the orthogonal grid (B) Perspective view

Figure 4.1: This figure shows two 8-adjacent pairs of 4-xels, which are located at (0,1,1,1) and (1,1,1,1), and at (3,0,1,1) and (4,0,1,1) respectively. The intersection of each pair is a 3-xel.

4.1 Preamble

As in previous chapters, we do not work directly with grid points, but prefer to think in terms of their Voronoi neighborhoods. For a 4D Cartesian grid the Voronoi neighborhoods of grid points are "upright" 4-dimensional hypercubes. We will call

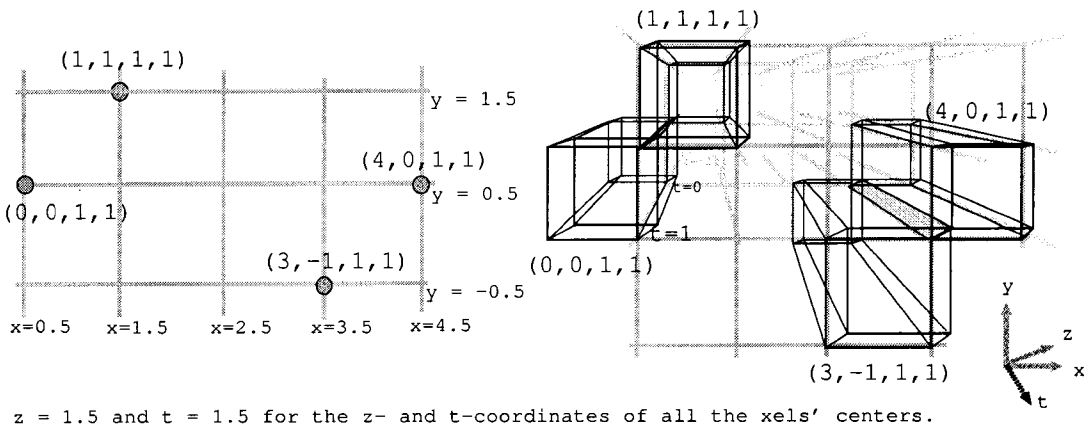

(A) Xels on the orthogonal grid (B) Perspective view

Figure 4.2: This figure shows two pairs of 4-xels, which are located at (0,0,1,1) and (1,1,1,1), and at (3,-1,1,1) and (4,0,1,1) respectively. The intersection of each pair is a 2-xel.

such a hypercube a *4-xel.*

Assuming without loss of generality that the grid points have coordinates of the form $(i_1 + 0.5, i_2 + 0.5, i_3 + 0.5, i_4 + 0.5)$ where the i's are integers, the vertices of a 4-xel have integer coordinates and the edges of a 4-xel have length 1.

We identify each binary image on a 4D Cartesian grid with the set of all 4-xels that are centered at the grid points which have value 1 in the image. This allows us to define a binary image simply as a finite set of 4-xels.

We will sometimes denote a 4-xel $[i_1, i_1+1] \times [i_2, i_2+1] \times [i_3, i_3+1] \times [i_4, i_4+1]$ by the quadruple of integers (i_1, i_2, i_3, i_4). We wish readers will compromise this glitch (as we will show in chapter 6 that this coordinating is easier than center coordinating in some grid system).

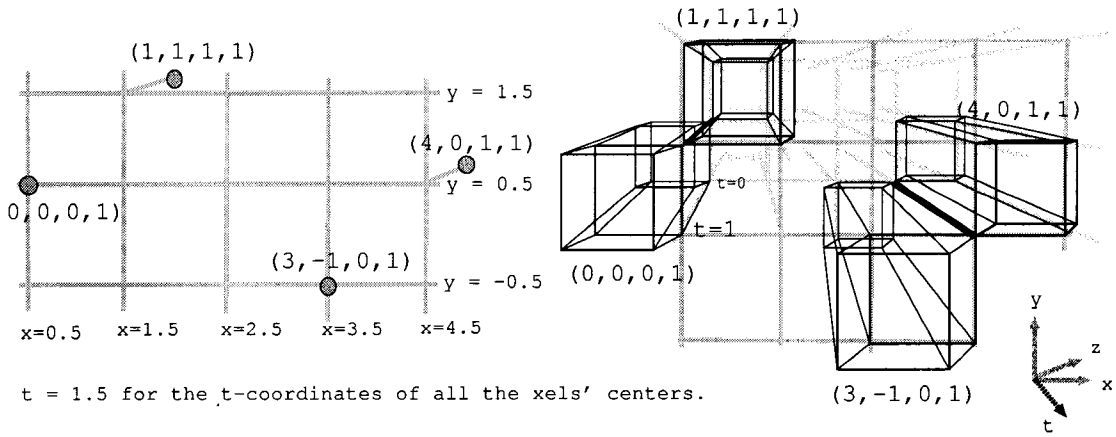

(A) Xels on the orthogonal grid (B) Perspective view

Figure 4.3: This figure shows two pairs of 4-xels, which are located at (0,0,0,1) and (1,1,1,1), and at (3,-1,0,1) and (4,0,1,1) respectively. The intersection of each pair is a 1-xel.

The first three figures in this chapter are for readers, who are interested in reading 4-xels in the 4D perspective view. The figures show the intersection of two pairs of 4-xels respectively presented in the standard orthogonal grid on the left and in the perspective view on the right. They will be used in our proofs.

Each 4-xel intersects just 80 other 4-xels, and shares a 3-face with just 8 other 4-xels. Accordingly, two 4-xels are said to be *80-adjacent* if they are distinct but intersect, and are said to be *8-adjacent* if their intersection is a 3-xel.

The definition of simpleness used in [14] is in fact equivalent to the definition used here, because both definitions are equivalent to the three conditions of Theorem 2.2.1 or 2.2.2. An advantage of the definition we are now using is that it involves only d-xels (and does not involve their attachment sets).

If an n-xel is the trajectory of an $(n-1)$-xel as it moves one unit parallel to a coordinate axis, then the boundary of the n-xel is the trajectory of the $(n-1)$-xel's boundary plus the initial and final locations of the $(n-1)$-xel itself. A useful property of the boundary of an n-xel is that it is topologically equivalent to $\mathbb{R}^{n-1} \cup \{\infty\}$, where ∞ denotes a single point at infinity that is added to $\mathbb{R}^{n-1}$ to compactify it. Moreover, the boundary can be represented by an $(n-1)$-dimensional *Schlegel diagram.* In particular, the boundary of a 4-xel is topologically equivalent to $\mathbb{R}^3 \cup \{\infty\}$, and can be represented by a 3-dimensional Schlegel diagram.

4.2 Main Theorem with (80,8)-connectedness

We now state our Main Theorem, which identifies all sets of 4-xels that can be MNS, and all such sets that can be MNS without being a component:

Theorem 4.2.1 (Main Theorem). *Let D be a set of 4-xels. Then:*

1. *D can be MNS if and only if D is contained in some $2 \times 2 \times 2 \times 2$ block of sixteen 4-xels.*
2. *D can be MNS without being a component if and only if D is a subset of some $2 \times 2 \times 2$ block of eight 4-xels.*

Note that there are four types of $2 \times 2 \times 2$ block: Such a block could be a $1 \times 2 \times 2 \times 2$, a $2 \times 1 \times 2 \times 2$, a $2 \times 2 \times 1 \times 2$, or a $2 \times 2 \times 2 \times 1$ block.

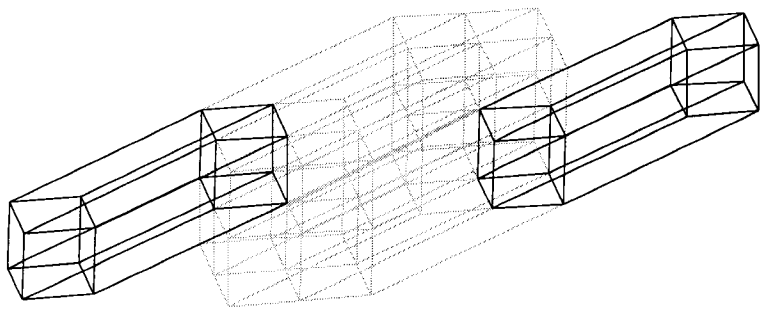

Figure 4.4: The above figure shows a 4d MNS set (2x2x2 block) in gray tone. In order to be easily perceptible on the paper, we elongate the 4d xels. Notice that there exists an edge (highlighted by thick line) that connects two end xels in black and is shared by all the gray xels of this MNS set, so it is easy to see that any subset in this MNS set is simple. And any image consisting of just one gray xel and the end black xels forms a chain. Deleting the gray xel splits the chain.

4.3 Proof of the Main Theorem with (80,8)-connectedness

4.3.1 Useful results

The purpose of this subsection is to present three results that will be used in our proof of the Main Theorem.

The use of the *Inclusion-Exclusion Principle for Euler characteristics* as stated below to establish Case 2 and 3 of the "only if" part of the Main Theorem is due to Dr. Kong.

$$\chi(\bigcup_{i=1}^{n} K_i) = \sum_{T\subseteq\{1,2,\ldots,n\},T\neq\emptyset} (-1)^{|T|-1}\chi(\bigcap_{i\in T} K_i) \tag{4.3.1}$$

Here $K_1, K_2, \ldots, K_n$ are arbitrary xel-complexes. This identity follows from the

Inclusion-Exclusion Principle for finite sets and the definition of $\chi(K)$.

The second result is the next proposition, which is related to the following lemma:

Lemma 4.3.1. *Let $\mathcal{P}$ be a union of xels and let x be an edge or a 2-xel such that $x \not\subseteq \mathcal{P}$ and $\chi(x \cap \mathcal{P}) = 1$. Then one of the following is true:*

1. *$x \cap \mathcal{P}$ consists of a single vertex of x.*
2. *x is a 2-xel and $x \cap \mathcal{P}$ is one of the four edges of x.*
3. *x is a 2-xel and $x \cap \mathcal{P}$ is a union of two edges of x that share a vertex.*
4. *x is a 2-xel and $x \cap \mathcal{P}$ is a union of three of the four edges of x.*

This lemma is easily verified by considering all possible forms of $x \cap \mathcal{P}$. From the lemma it is not hard to deduce Proposition 4.3.2 below, which will be used in section 4.3.3. We omit the proof of the lemma, but expect most readers will find it intuitively clear that all parts of the proposition are valid in each of the four cases of the lemma.

Proposition 4.3.2. *Let q be a 4-xel. Let $\mathcal{P}$ be a union of xels in* Boundary(q) *and let x be an edge or a 2-xel in* Boundary(q) *such that $\chi(x \cap \mathcal{P}) = 1$. Then:*

1. *$\mathcal{P}$ is connected if and only if $\mathcal{P} \cup \{x\}$ is connected.*
2. *$\bigcup$Boundary$(q) \setminus \mathcal{P}$ is connected if and only if $\bigcup$Boundary$(q) \setminus (\mathcal{P} \cup \{x\})$ is connected.*
3. *$\chi(\mathcal{P}) = \chi(\mathcal{P} \cup \{x\})$.*

The following proposition is the third result. This will save us a lot of case-checking in section 4.3.2:

Proposition 4.3.3. *Let q be a 4-xel, and let X be any nonempty set of xels in* Boundary(q) *that satisfies one of the following two conditions:*

A. There is some vertex that belongs to all of the xels in X.

B. $X = Y \cup Z$, where $Y \cap Z \neq \emptyset$, there is some vertex that belongs to all of the xels in Y, there is some vertex that belongs to all of the xels in Z, and no xel in $Y \setminus Z$ intersects a xel in $Z \setminus Y$.

Then X satisfies the following conditions:

1. $\bigcup X$ *is connected.*
2. $\bigcup$Boundary$(q) \setminus \bigcup X$ *is connected.*
3. $\chi(\bigcup X) = 1$.

In fact condition A in this proposition is a special case of condition B (since we may take $Y = Z = X$ in B). The proposition follows from Theorem 4.1 in [29]: Condition B implies that X is SN in the sense of [29], and so the theorem implies $\bigcup X$ is contractible. By standard results of algebraic topology (including the Alexander duality theorem) [24], this implies $\bigcup X$ satisfies conditions 1 – 3.

4.3.2 The "if" parts of the Main Theorem

For any 4-xel q in a 4D binary image I, let $A(q, I) = \{q \cap x \mid x \in I \setminus \{q\}\} \setminus \{\emptyset\}$. Note that $\bigcup A(q, I) = \bigcup$Attach$(q, I)$.

To show that the "if" part of assertion 1 of the Main Theorem is valid, let D be a subset of a $2 \times 2 \times 2 \times 2$ block of 4-xels such that D is an 80-component of a 4D binary image I. We claim D is MNS in I. Evidently, D satisfies condition 1 of Theorem 2.4.1. It remains to show that D also satisfies condition 2 of Theorem 2.4.1. Let $q \in D$ and let I' be obtained from I by deleting any proper subset of the other elements of D. We need to show that q is simple in I'. Let $X = A(q, I')$. As D is contained in a $2 \times 2 \times 2 \times 2$ block of 4-xels, the central vertex of that block belongs to all the 4-xels in D and hence to all the xels in X. So, since $\bigcup X = \bigcup \mathrm{A}ttach(q, I')$, it follows from Proposition 4.3.3 that the three conditions of Theorem 2.2.2 hold with I' in place of I. Thus q is simple in I', as required.

To show that the "if" part of assertion 2 is also valid, let I be a $2 \times 2 \times 2 \times 3$ block of 4-xels and let D be its central $2 \times 2 \times 2 \times 1$ block (which is clearly not an 80-component of I). We claim D is MNS in I. If we can prove this, then, by Theorem 5.4.3, the "if" part of assertion 2 is valid. By symmetry we may assume that $I = \{i_1 \times i_2 \times i_3 \times i_4 \mid i_1, i_2, i_3 \in \{[0,1],[1,2]\}, i_4 \in \{[0,1],[1,2],[2,3]\}\}$ so that $D = \{i_1 \times i_2 \times i_3 \times [1,2] \mid i_1, i_2, i_3 \in \{[0,1],[1,2]\}\}$. Then D clearly satisfies condition 1 of Theorem 2.4.1. To show that D also satisfies condition 2 of Theorem 2.4.1, let $q \in D$ and let I' be obtained from I by deleting any proper subset of the other seven 4-xels in D. We need to show that q is simple in I'.

Let $D^- = \{i_1 \times i_2 \times i_3 \times [0,1] \mid i_1, i_2, i_3 \in \{[0,1],[1,2]\}\}$ and let $D^+ =$

$\{i_1 \times i_2 \times i_3 \times [2,3] \mid i_1, i_2, i_3 \in \{[0,1],[1,2]\}\}$.

Let $X = A(q, I')$. Since $I' \subseteq D^- \cup D \cup D^+$, we have $X = Y \cup Z$, where $Y = A(q, I' \cap (D \cup D^-))$ and $Z = A(q, I' \cap (D \cup D^+))$.

Since $D \cup D^- = \{i_1 \times i_2 \times i_3 \times i_4 \mid i_1, i_2, i_3, i_4 \in \{[0,1],[1,2]\}\}$, the vertex (1,1,1,1) belongs to all the 4-xels in $D \cup D^-$ and hence to all the xels in Y. Similarly, the vertex (1,1,1,2) belongs to all the xels in Z. Moreover, $Y \cap Z = A(q, I' \cap D) \neq \emptyset$ because at least one element of $D \setminus \{q\}$ is in I'. Also, no xel in $Y \setminus Z = A(q, I' \cap D^-)$ intersects a xel in $Z \setminus Y = A(q, I' \cap D^+)$. Since $\bigcup X = \bigcup \mathrm{A}ttach(q, I')$, it follows from Proposition 4.3.3 that the three conditions of Theorem 2.2.2 hold with I' in place of I, which implies q is simple in I', as required.

4.3.3 The "only if" parts of the Main Theorem

The "only if" part of assertion 1 is just Theorem 2.4.4. To prove the "only if" part of assertion 2, let S be any MNS set of a 4D binary image I. By Theorem 2.4.4, S is contained in some $2 \times 2 \times 2 \times 2$ block.

A set T of 4-xels that is contained in some $2 \times 2 \times 2 \times 2$ block will be called a *spanning set* if there is no $2 \times 2 \times 2$ block that contains T.

We now suppose that our MNS set S is a minimal spanning set—i.e., we suppose S is a spanning set but no proper subset of S is a spanning set—and deduce that S must be an 80-component of I. This will show that no minimal spanning set can be

MNS without being a component, which (by Theorem 5.4.3) is enough to establish the "only if" part of assertion 2 of the Main Theorem, since every spanning set contains a minimal spanning set.

For any two 4-xels p and q, let $p - q$ denote the vector from the centroid of q to the centroid of p. We define the l_1-*diameter* of S to be $\max_{p,q \in S} \|p - q\|_1$, where $\|\mathbf{v}\|_1$ is the l_1-norm of the vector $\mathbf{v}$ (i.e., the sum of the absolute values of the four components of $\mathbf{v}$). Since S is a spanning set, the l_1-diameter of S is at least 2, and is therefore equal to 2, 3, or 4.

Case 1: The l_1-diameter of S is 4

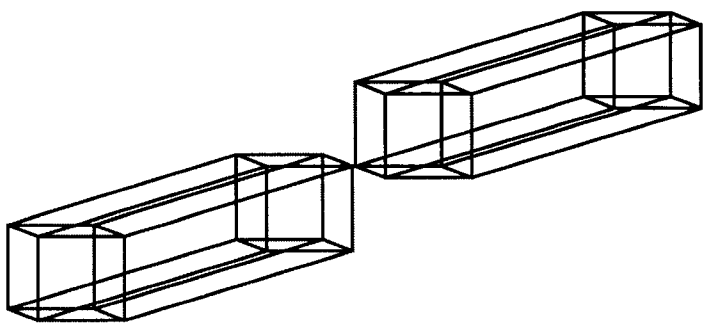

Figure 4.5: This figure shows two 4D xels of Case 1 in an oblique view.

In this case $S = \{q, a\}$ for some 4-xels q and a such that $\|q - a\|_1 = 4$. Note that $q \cap a$ consists of just one vertex, v say. Let $\mathcal{P} = \bigcup \mathrm{A}ttach(q, I \setminus \{a\})$, so that $\bigcup \mathrm{A}ttach(q, I) = \mathcal{P} \cup \{v\}$. Since S is MNS in I, it follows from Theorem 2.4.1 that q is non-simple in $I \setminus \{a\}$ but q is simple in I. The latter and Theorem 2.2.2 imply $\mathcal{P} \cup \{v\} = \bigcup \mathrm{A}ttach(q, I)$ is connected, and so either $v \in \mathcal{P}$ or $\mathcal{P} = \emptyset$. But

$v \in \mathcal{P}$ would imply $\bigcup \mathrm{A}ttach(q, I) = \mathcal{P} \cup \{v\} = \mathcal{P} = \bigcup \mathrm{A}ttach(q, I \setminus \{a\})$, which (by Theorem 2.2.2) would make it impossible for q to be simple in I but non-simple in $I \setminus \{a\}$. Hence $\mathcal{P} = \emptyset$ and so, by Theorem 2.4.2, S is an 80-component of I.

Case 2: The l_1-diameter of S is 3

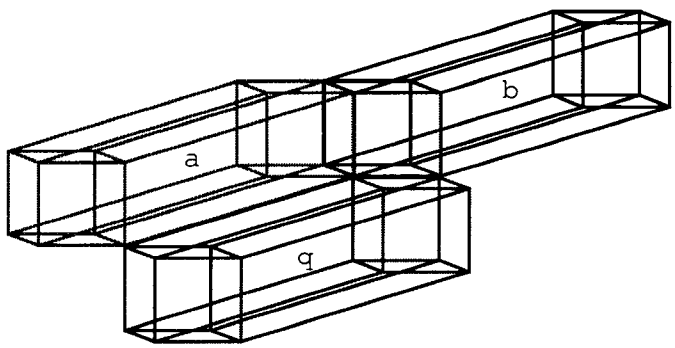

Figure 4.6: This figure shows a configuration of 4D xels of Case 2 in an oblique view.

In this case it is readily confirmed that $S = \{q, a, b\}$ for some 4-xels q, a, and b such that $\|q - a\|_1 = \|q - b\|_1 = 3$ and $\|a - b\|_1 = 2$. Let $q \cap a = e_a$ and $q \cap b = e_b$. Then e_a and e_b are edges and $e_a \cap e_b$ consists of just a vertex.

Let $\mathcal{P} = \bigcup \mathrm{A}ttach(q, I \setminus \{a, b\})$, so $\bigcup \mathrm{A}ttach(q, I) = \mathcal{P} \cup e_a \cup e_b$, $\bigcup \mathrm{A}ttach(q, I \setminus \{a\}) = \mathcal{P} \cup e_b$, and $\bigcup \mathrm{A}ttach(q, I \setminus \{b\}) = \mathcal{P} \cup e_a$. Since S is MNS in I, it follows from Theorem 2.4.1 that q is non-simple in $I \setminus \{a, b\}$ but q is simple in I, in $I \setminus \{a\}$, and in $I \setminus \{b\}$. So it follows from Theorem 2.2.2 and Proposition 4.3.2 that neither $\chi(\mathcal{P} \cap e_a)$ nor $\chi(\mathcal{P} \cap e_b)$ is equal to 1.

As $\bigcup \mathrm{A}ttach(q, I) = \mathcal{P} \cup e_a \cup e_b$, $\bigcup \mathrm{A}ttach(q, I \setminus \{a\}) = \mathcal{P} \cup e_b$, $\bigcup \mathrm{A}ttach(q, I \setminus \{b\}) = \mathcal{P} \cup e_a$, and $\chi(e_a) = \chi(e_b) = \chi(e_a \cap e_b) = 1$, it follows from Theorem 2.2.2 and the

Inclusion-Exclusion Principle for Euler characteristics that

$$1 = \chi(\mathcal{P} \cup e_a) = \chi(\mathcal{P}) + 1 - \chi(\mathcal{P} \cap e_a)$$

$$1 = \chi(\mathcal{P} \cup e_b) = \chi(\mathcal{P}) + 1 - \chi(\mathcal{P} \cap e_b)$$

$$1 = \chi(\mathcal{P} \cup e_a \cup e_b) = \chi(\mathcal{P}) + 1 + 1 - \chi(\mathcal{P} \cap e_a) - \chi(\mathcal{P} \cap e_b) - 1 + \chi(\mathcal{P} \cap e_a \cap e_b)$$

and therefore $\chi(\mathcal{P}) = \chi(\mathcal{P} \cap e_a) = \chi(\mathcal{P} \cap e_b) = \chi(\mathcal{P} \cap e_a \cap e_b)$.

So, since neither $\chi(\mathcal{P} \cap e_a)$ nor $\chi(\mathcal{P} \cap e_b)$ is equal to 1, $\chi(\mathcal{P} \cap e_a \cap e_b) \neq 1$. Thus $\mathcal{P} \cap e_a \cap e_b = \emptyset$ (since $e_a \cap e_b$ consists of just a vertex) and $\chi(\mathcal{P} \cap e_a \cap e_b) = 0$. Therefore $\chi(\mathcal{P}) = \chi(\mathcal{P} \cap e_a) = \chi(\mathcal{P} \cap e_b) = 0$, so $\mathcal{P} \cap e_a = \emptyset$. Now if $\mathcal{P} \neq \emptyset$ then $\mathcal{P} \cup e_a$ is disconnected, which contradicts Theorem 2.2.2 because $\mathcal{P} \cup e_a = \bigcup Attach(q, I \setminus \{b\})$ and q is simple in $I \setminus \{b\}$. Hence $\mathcal{P} = \emptyset$ and so, by Theorem 2.4.2, S is an 80-component of I.

Case 3: The l_1-diameter of S is 2

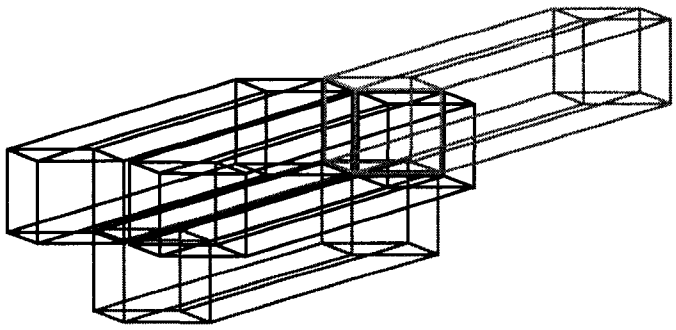

Figure 4.7: This figure shows a configuration of 4D xels of Case 3 in an oblique view.

In this case it is quite easy to verify that $S = \{q, a, b, c\}$, where $\|x - y\|_1 = 2$ for all

distinct x and y in S. Let $q \cap a = f_a$, $q \cap b = f_b$, and $q \cap c = f_c$. Then f_a, f_b, and f_c are 2-xels, every pair of them share an edge, and $f_a \cap f_b \cap f_c$ consists of just a vertex.

Let $\mathcal{P} = \bigcup \mathrm{A}ttach(q, I \setminus \{a,b,c\})$, so that $\bigcup \mathrm{A}ttach(q, I \setminus \{a,b\}) = \mathcal{P} \cup f_c$. Since S is MNS in I, it follows from Theorem 2.4.1 that q is non-simple in $I \setminus \{a,b,c\}$ but q is simple in I, $I \setminus \{c\}$, $I \setminus \{b,c\}$, and $I \setminus \{a,b\}$. So it follows from Theorem 2.2.2 and Proposition 4.3.2 that $\chi(\mathcal{P} \cap f_c) \neq 1$.

Since $\bigcup \mathrm{A}ttach(q, I \setminus \{b,c\}) = \mathcal{P} \cup f_a$, it follows from Theorem 2.2.2, the fact that $\chi(x) = 1$ for any xel x, and the Inclusion-Exclusion Principle for Euler characteristics that $1 = \chi(\mathcal{P} \cup f_a) = \chi(\mathcal{P}) + 1 - \chi(\mathcal{P} \cap f_a)$. Hence $\chi(\mathcal{P}) = \chi(\mathcal{P} \cap f_a)$. By symmetrical arguments we must have

$$\chi(\mathcal{P}) = \chi(\mathcal{P} \cap f_a) = \chi(\mathcal{P} \cap f_b) = \chi(\mathcal{P} \cap f_c) \tag{4.3.2}$$

Similarly, since $\bigcup \mathrm{A}ttach(q, I \setminus \{c\}) = \mathcal{P} \cup f_a \cup f_b$, we have $1 = \chi(\mathcal{P} \cup f_a \cup f_b) = \chi(\mathcal{P}) + 1 + 1 - \chi(\mathcal{P} \cap f_a) - \chi(\mathcal{P} \cap f_b) - 1 + \chi(\mathcal{P} \cap f_a \cap f_b)$ and so by equation (4.3.2) we have $\chi(\mathcal{P}) = \chi(\mathcal{P} \cap f_a \cap f_b)$. By symmetrical arguments we must have

$$\chi(\mathcal{P}) = \chi(\mathcal{P} \cap f_a \cap f_b) = \chi(\mathcal{P} \cap f_b \cap f_c) = \chi(\mathcal{P} \cap f_a \cap f_c) \tag{4.3.3}$$

Again, since $\bigcup \mathrm{A}ttach(q, I) = \mathcal{P} \cup f_a \cup f_b \cup f_c$, we have $1 = \chi(\mathcal{P} \cup f_a \cup f_b \cup f_c) = \chi(\mathcal{P}) + 1 + 1 + 1 - \chi(\mathcal{P} \cap f_a) - \chi(\mathcal{P} \cap f_b) - \chi(\mathcal{P} \cap f_c) - 1 - 1 - 1 + \chi(\mathcal{P} \cap f_a \cap f_b) + \chi(\mathcal{P} \cap f_b \cap f_c) + \chi(\mathcal{P} \cap f_a \cap f_c) + 1 - \chi(\mathcal{P} \cap f_a \cap f_b \cap f_c)$ and so by equations (4.3.2) and (4.3.3) we have:

$$\chi(\mathcal{P}) = \chi(\mathcal{P} \cap f_a \cap f_b \cap f_c) \tag{4.3.4}$$

Recalling that $\chi(\mathcal{P} \cap f_c) \neq 1$, we see that equations (4.3.2) and (4.3.4) imply $\chi(\mathcal{P} \cap f_a \cap f_b \cap f_c) \neq 1$. Thus $\mathcal{P} \cap f_a \cap f_b \cap f_c = \emptyset$ (since $f_a \cap f_b \cap f_c$ consists of just a vertex) and $\chi(\mathcal{P} \cap f_a \cap f_b \cap f_c) = 0$. Therefore, by equations (4.3.2), (4.3.3), and (4.3.4), the 2-xel f_a satisfies $\chi(\mathcal{P} \cap f_a) = \chi(\mathcal{P} \cap f_a \cap f_b) = 0$, since $\chi(\mathcal{P} \cap f_a) = 0$, $\mathcal{P} \cap f_a$ either is empty or is the union of the four edges of f_a. But the latter is impossible because $f_a \cap f_b$ is an edge of f_a that is not contained in $\mathcal{P}$ (since $\chi(\mathcal{P} \cap f_a \cap f_b) = 0$). Hence $\mathcal{P} \cap f_a = \emptyset$. Now if $\mathcal{P} \neq \emptyset$ then $\mathcal{P} \cup f_a$ is disconnected, which contradicts Theorem 2.2.2 because $\mathcal{P} \cup f_a = \bigcup Attach(q, I \setminus \{b, c\})$ and q is simple in $I \setminus \{b, c\}$. So $\mathcal{P} = \emptyset$ and, by Theorem 2.4.2, S is an 80-component of I.

The merit of the simplicity for proving cases 2 and 3 is due to Dr. Kong. The Euler characteristics computation presented here makes a more convincing argument than the lengthy component checking proved by me.

4.4 Conclusion of Part IV

We have identified all types of sets of 4-xels that can be minimal non-simple (MNS) in a 4D binary image, and all types that can be MNS without being an 80-component of the image, when 4D 80-connectedness is used on 4-xels in the image and 4D 8-connectedness is used on 4-xels in its complement. It is interesting to see that the maximal small set in 3D Cartesian grid thickened along the t-axis could be a MNS set in 4D Cartesian grid without being a component. This result is very similar to

that of the maximal small set of a triangle grid mentioned in the concluding remarks relating to the minimal (18,12)-nonsimple sets of a 3D FCC-grid.

This work is based on the characterization of simple 4-xels that was given in [14], and the Inclusion-Exclusion Principle for Euler characteristics.

Chapter 5

MNS set with (8,80)-connectedness

5.1 Preamble

Arguably, the main purpose for preserving topology is to maintain the connectivity of the objects in a 2D input image and the simply-connectedness in a 3D input image. In the previous chapter, we use the widely accepted notion in computer vision that two objects are said to be connected if they share at least a vertex (i.e., 0-*face*). However, here we confine our attention to the images used in engineering, architecture or other fields, and impose a stronger condition[1] — properly connected n-dimensional objects must share a facet (i.e., an $(n-1)$-*face*). For example, if two streets on the map (Fig. 5.1) are connected, then they must share an edge (not just share a vertex) wide enough for vehicles to pass through.

Our main goal in this chapter is to state and prove a theorem that can be used to mathematically verify the topological soundness of parallel thinning algorithms

[1]The term "strong connection" has been used by many authors.

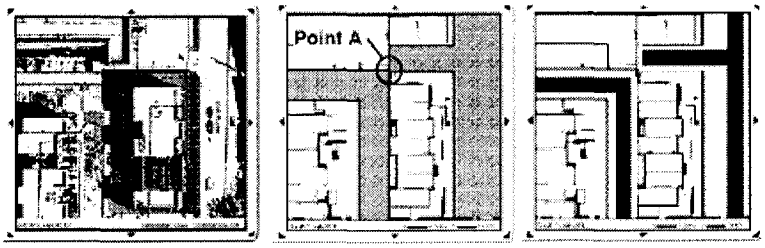

(A) (B) (C)

Figure 5.1: (A) is an aerial view of an urban development section. (B) maps out vehicle accessible area in gray color. The background objects (buildings, landscapes, etc.) are connected at the point A, but the streets are not connected. The street centerline map (C) is a possible result of thinning the gray image in (B).

for 4D images, imposing the strong adjacency condition by using 8-adjacency on 1's. In Section 5.3, we define a simple 4-xel for (8,80)-connectedness in terms of its coattachment set; this concept was originally introduced in [13].

We define the simple xel in (8,80)-image as *cosimple* xel in (80,8)-image, and the topology preservation with (8,80)-connectedness as *cotopology preservation.*

Here we solve the same problem for a 4D Cartesian grid with (8, 80)- connectedness, summarize our result in Theorem 5.5.1, and prove this theorem in Section 5.6.

5.2 n-Xels, 4D Images, Xel-Complexes and Attachment Sets

Suppose that x and y are two xels in a 4D image. $y < x$ denotes that y is a proper subset of x; if y is a k-xel then we say y is a "*k-face*" of x.

Using the notion of polyhedral complex, we define the "*xel-complex*" K as a set of xels such that for every xel x in K, every $y < x$ is also in K. $\bigcup K$ denotes the *polyhedral set* given by the union of all the xels in K.

I^c, the complement of an image I, is the image whose set of 1's is just the set of 0's of I and vice versa.

It is easy to show that a 4-xel has exactly $2^{4-k}C(4,k)$ k-faces where $0 \leq k \leq 3$. Hence, each 4-xel q shares a 3-face with exactly eight other 4-xels, and intersects with exactly eighty other 4-xels. Accordingly, two distinct 4-xels are called *attached* (or *80-adjacent*) if they share a 3-face (or share at least a 0-face) respectively. We name two 4-xels *an antipodean pair*, *a diametric pair*, *a diagonal pair* or *an attached pair* if their intersection is exactly a 0-face, a 1-face, a 2-face or a 3-face respectively.

A sequence of 4-xels $< q_1, q_2, ..., q_j >$, where $j > 1$, is called an 8-*path* if q_i is attached to q_{i+1} for $1 \leq i < j$. Let S be a set of 4-xels. We say two xels p and q are *8-connected in* S if there exists an 8-path in S such that $p = q_1$ and $q = q_j$. We say a set S is 8-connected if every pair of xels in S is 8-connected. If S is a maximal 8-connected set in an image I, then it is called an *8-component* of the image I.

Similarly, we can define an 80-path and an 80-component of a set S with "80-connected" in place of "8-connected".

5.3 Simple 4-Xels with (8,80)-connectedness

Recall the two properties we used the previous chapter: Theorem 2.2.1 and Theorem 2.2.2.

Note that if the complement in the second item is non-empty, then q must be attached to least one xel in the image.

$\chi(K)$ denotes the Euler characteristic of a xel-complex K, which can be computed by $c_0(K) - c_1(K) + c_2(K) - c_3(K) + c_4(K)$ where $c_n(K)$ is the number of n-xels in K. Recall that $\chi(\bigcup K)$ is equal to the value of $\chi(K)$. And it is well known that if S is a polyhedral set in 3-space, then $\chi(S)$ is equal to the number of connected components of S plus the number of cavities in S minus the number of "tunnels" in S [18], so $\chi(S)$ is invariant of the deformation. Thus, for any xel x, $\chi(x) = 1$ because any xel can be deformed into one point.

Recalling the Inclusion-Exclusion principle of the Euler characteristic,

$$\chi(\bigcup_{i=1}^{n} K_i) = \sum_{T \subseteq \{1,2,\ldots,n\}, T \neq \emptyset} (-1)^{|T|-1} \chi(\bigcap_{i \in T} K_i) \tag{5.3.1}$$

Here $K_1, K_2, \ldots, K_n$ are arbitrary xel-complexes. This identity follows from the Inclusion-Exclusion Principle for finite sets and the definition of $\chi(K)$. Again, we are to use the Euler characteristics computation approach suggested by Dr. Kong. Using this principle we can prove the following lemma.

Lemma 5.3.1. *Let x_1, x_2, and x_3 be xels, and P be a union of xels on the boundary of some 4-xel such that $P \cap x_1 \cap x_2 = P \cap x_1 \cap x_2 \cap x_3 \neq \emptyset$ and*

$\chi(P) = \chi(P \cup x_1) = \chi(P \cup x_2) = \chi(P \cup x_3) =$

$\chi(P \cup x_1 \cup x_2) = \chi(P \cup x_2 \cup x_3) = \chi(P \cup x_1 \cup x_3) = 1$

Then $\chi(P \cup x_1 \cup x_2 \cup x_3) = 1$.

Proof:

$\chi(x_i) = 1$ for $i \in \{ 1, 2, 3\}$, because x_i is a xel.

Using the Inclusion-Exclusion principle of the Euler characteristic, expand $\chi(P \cup x_i) = \chi(P) + \chi(x_i) - \chi(P \cap x_i)$. Substituting $\chi(P)$ and $\chi(x_i)$ by value 1, we have $1 = \chi(P \cup x_i) = C(2,1) - \chi(P \cap x_i)$. Therefore,

$$\chi(P \cap x_i) = 1 \quad i \in \{1, 2, 3\} \tag{5.3.2}$$

Note that since $P \cap x_1 \cap x_2 \cap x_3 \neq \emptyset$ so $x_i \cap x_j$ is always a xel for $i, j \in \{1, 2, 3\}$, thus $\chi(x_i \cap x_j) = 1$. The same holds true for $x_1 \cap x_2 \cap x_3$, so $\chi(x_1 \cap x_2 \cap x_3) = 1$. Expanding $\chi(P \cup x_i \cup x_j)$ by the Inclusion-Exclusion principle and substituting all the linear and quadratic terms (w.r.t. $\cap$) by value 1, we have $\chi(P \cup x_i \cup x_j) = C(3,1) - C(3,2) + \chi(P \cap x_i \cap x_j) = 1$ (by the assumptions). Thus,

$$\chi(P \cap x_i \cap x_j) = 1 \quad i, j \in \{1, 2, 3\} \tag{5.3.3}$$

Since $P \cap x_1 \cap x_2 = P \cap x_1 \cap x_2 \cap x_3$ we have $\chi(P \cap x_1 \cap x_2 \cap x_3) = 1$. Again, expanding by the Inclusion-Exclusion principle and substituting all the linear, quadratic and cubic terms by value 1, we have $\chi(P \cup x_1 \cup x_2 \cup x_3) = C(4,1) + C(4,2) + C(4,3) - \chi(P \cap x_1 \cap x_2 \cap x_3) = 4 - 6 + 4 - 1$, which deduces the final result:

$$\chi(P \cup x_1 \cup x_2 \cup x_3) = 1 \tag{5.3.4}$$

5.3.1 (8,80)-simple Xels and Coattachment Sets

We are interested in identifying the 4-xel in (8,80)-images having the property that its deletion "preserves topology". How can one extend the above theorems to characterize simple xels in (8,80)-images?

To answer this question, let us observe that deleting a xel q from the foreground $\mathcal{F}(I)$ is equivalent to adding q to the background, $\mathcal{F}(I^c)$. Let us denote $I^c \cup \{q\}$ by $\mathcal{I}(I,q)$ and refer to it as the *complement image* of q. Then, deleting q augments the background into $\bigcup \mathcal{I}(I,q)$ and vice versa. So, the simple xel in an (8,80)-image can be equivalently defined as follows:

Definition 5.3.1. Let I be an (8,80)-image. A xel q is said to be (8,80)-simple in I if q is simple in the (80,8)-image $\mathcal{I}(I,q)$.

From now on, should there be no ambiguity, we will call this a simple xel instead of a simple xel in an (8,80)-image I. But sometimes we need to distinguish which good pair of connectivity we use. Therefore, we will also call this kind of simple xel a *cosimple* xel in (80,8)-image I. The attachment set of q in $\mathcal{I}(I,q)$ is called the *I-coattachment set* of q or simply the *coattachment set* of q.

Hence, to identify which xel can be (8,80)-simple, we only need to verify the conditions in Theorem 2.2.1 or Theorem 2.2.2 with the coattachment set in place of the attachment set. Since the deformation preserves the properties in Theorem 2.2.1 and 2.2.2, it can be proved that xel q is (8,80)-simple if and only if its coattachment

set can be deformed into a point by elementary collapsing (please refer to Kong's paper [[14]] for details).

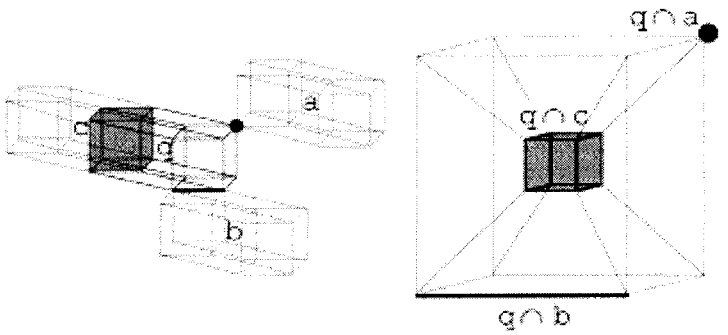

Figure 5.2: The left figure shows an image of four 4-xels. It is helpful to think of 4-xels as trajectories of 3-xels (unit cubes) moving through one unit of time. The centers of xels are labelled by a, b, c and q. The right figure is the Schlegel diagram of xel q, where the inner cube with its proper faces are corresponded with the grid points for $t = -1$, the 3D outer space plus the proper faces of the outer cube are for $t = 1$ and the elements sandwiched in between are for $t = 0$.

5.3.2 Schlegel Diagram

An attachment set or a coattachment set of a 4-xel has many overlapping faces as seen in the previous chapter. Again we use *Schlegel diagram* (see Fig. 5.2), which is a "perspective" view of the boundary set of a 4-xel with its "front 3-face" stretched to the 3D outer space. Therefore, we can infer the connectedness of $\bigcup Boundary(q) \setminus \bigcup Attach(q, \mathcal{I}(I, q))$ in 4-space by studying the 3-dimensional complement of the coattachment of a 4-xel q on a Schlegel diagram (in 3-space).

5.4 Simple sets and MNS sets with (8,80)-connectedness

A set D is simple in a 4D (8,80)-image I if and only if D is simple in the (80,8)-image $I^c \cup D$. Using this definition of simple set we can define the MNS sets the same way as in the previous chapter.

Because an empty set is simple, a singleton set $\{q\}$ in (8,80)-image can be MNS without being a component. Image " 1 q 1 " is an example.

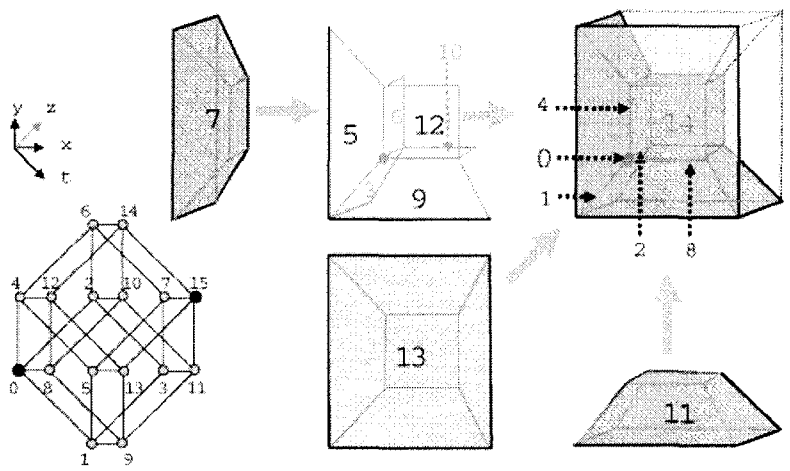

Figure 5.3: The lower left figure shows the centers of xels on a "stretched" 4D grid without showing their hypercubes, and the x, y, z and t-axes are stretched in different scales to avoid the overlapping. The xels are labelled by numbers — $0, 1, \ldots, 15$ — whose binary representations are the 4-tuple coordinates of the xels. The right upper figure shows xel 15's Schlegel diagram. Explosion views of all the attached faces are presented; xel 15's attachment set (in gray) can be assembled by following the thick arrows. The xel 0 is totally encapsulated by other gray faces. Its coattachment set is the closure of the white space (i.e., complement of the gray polyhedra).

Proposition 5.4.1. *Let D be an MNS set in an (8,80)-image I. Suppose that there exist a xel $q \in D$, two xels p and $r \in I$ such that $p \cap q \neq \emptyset$ and $p \cap q < r \cap q$. Then, D cannot contain both p and r.*

The 3D version of this proposition was proved in [13] (see Corollary 5.14); this 4D (8,80) version can be readily confirmed by using much the same argument as was used previously.

A simple consequence of this proposition can be observed in the coattachment set of xel 15 on figure 5.3 as follows:

Corollary 5.4.2. *Let q and r be an antipodean pair in an (8,80)-image I, and D be an MNS set in I such that $q \in D$. Suppose on one of the shortest paths from r to q there exists a xel $p \in D$. Then, any xel $x \in D \setminus \{p, q\}$ cannot be on a shortest 8-path from r to p in $[r, p]$ or on a shortest 8-path from p to q in $[p, q]$.*

For brevity, we will use $[r, p]$ and $[p, q]$ (the notations for lattice) to denote the sets of xels on the (above mentioned) shortest paths, because they are indeed the lattices with the partial ordering relation $x \leq y$ being either $x = y$ or $x < y$ on the boundary of the 4-xel q.

The following theorem is helpful to identify the least upper bound of an MNS chain (to be defined in subsection 5.6.2).

Theorem 5.4.3. *If a set D of 4-xels can be MNS without being a component in an (m,n)-image I, then every subset D' of D can be MNS without being a component.*

5.5 Main Theorem with (8,80)-connectedness

Let us recall that a *spanning set* of 4-xels is a set T, which is contained in some $2 \times 2 \times 2 \times 2$ block and there is no $2 \times 2 \times 2$ block that contains T.

We say a set D is *an* $(\sqrt{2}, \sqrt{3}, \sqrt{3})$ *isosceles set* if D consists of three xels, two of which are a diagonal pair, and both of which are diametric to the other, i.e., corners of a $(\sqrt{2}, \sqrt{3}, \sqrt{3})$ triangle. For brevity, we say it is *an isosceles set*

Theorem 5.5.1 (Main Theorem). *Let D be a set of 4-xels in an (8,80)-image. D can be an MNS set without being a component if and only if D is a subset of one of the following:*

1. *a set of an antipodean pair*
2. *a set of an attached pair*
3. *an $(\sqrt{2}, \sqrt{3}, \sqrt{3})$ isosceles set*
4. *a spanning set of 4 mutually diagonal xels*

Note that the spanning set of 4 mutually diagonal xels is a set of four points in a $2 \times 2 \times 2 \times 2$ block such that there is a fifth point in this block (but not in the set) that is 8-adjacent to each of the four.

5.6 Proof of the Main Theorem with (8,80)-connectedness

5.6.1 The "if" parts of the Main Theorem

Proof:

Without lose of generality, we prove "if" parts of the Main Theorem constructively using the binary image $I = \{0, ..., 15\}$ except Case 2, which is trivial.

From now on we elide the term "xel" prefixing the integers $0, \ldots, 15$, and retain them to denote either xels or the corresponding faces on the boundary of some xel, e.g., a set of an antipodean pair $\{0, 15\}$ means this set is {xel 0, xel 15}. However, in those terms "=0", "=1", "$\neq$ 1", "+1" and "-1", 0 and 1 are still retained their integer values. Also, in this chapter "image" means (8,80)-image unless specified otherwise.

Case 1: A set of an antipodean pair D can be MNS (without being a component).

Sets of this type (refer to the configuration of Fig. 4.5) can never be a component in a (8,80)-image.

It is helpful to look at figure 5.4 by taking $D = \{0, 15\}$. Note that 0's coattachment set can be deformed into a point by some simple sequences such that they delete 3-faces first, 2-faces next, and then 1-face, (15 intersects all the faces; the details are

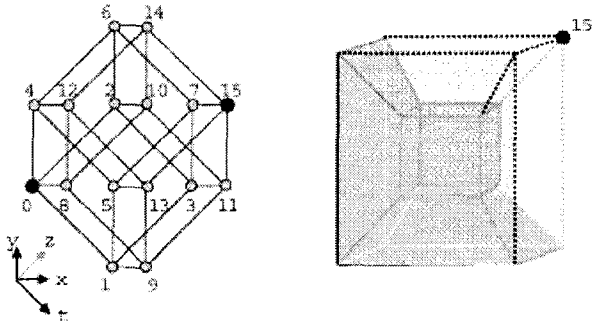

Figure 5.4: The left figure shows the centers of xels on a "stretched" 4D grid. The right figure shows 0's coattachment set in gray, which can be deformed into a point by a simple sequence deleting 3-faces first, 2-faces next, and then 1-faces. Its attachment set is the complement of this gray polyhedra; 15 is totally encapsulated by other faces of the attachment set.

left for the reader).

Thus, the conditions in Theorem 2.2.1 are satisfied, i.e., 0 is simple in the image $\{0,\ldots,15\}$. Since 15 is totally surrounded by other faces, deletion of 0 creates an isolated vertex from the coattachment set. Therefore, 0 is non-simple in image $\{0,\ldots,14\}$. By symmetry of 0 and 15, it follows from Theorem 2.4.1 that {0,15} is MNS.

Case 2: A set D of an attached pair can be MNS (without being a component).

Notice that the sets in Cases 1, 3 and 4 are not 8-connected, and therefore those MNS sets are not 8-components; only in this case do we need to show that the set of an attached pair can be MNS without being an 8-component. The configuration of the set in this case is simple (refer to Fig. 4.1). It suffices to prove this by verifying

that the sequence $< p, q >$ is not simple but q is simple in the following image where z = 0 and t = 0. (The details are left to the reader).

$$\begin{matrix} 1 & p & 1 \\ 1 & q & 1 \end{matrix}$$ ($\{p, q\}$ is MNS and not a component in the image).

Case 3: An $(\sqrt{2}, \sqrt{3}, \sqrt{3})$ isosceles set D can be MNS (without being a component).

Note that sets of this type (refer to the configuration of Fig. 4.6) can never be a component in a (8,80)-image.

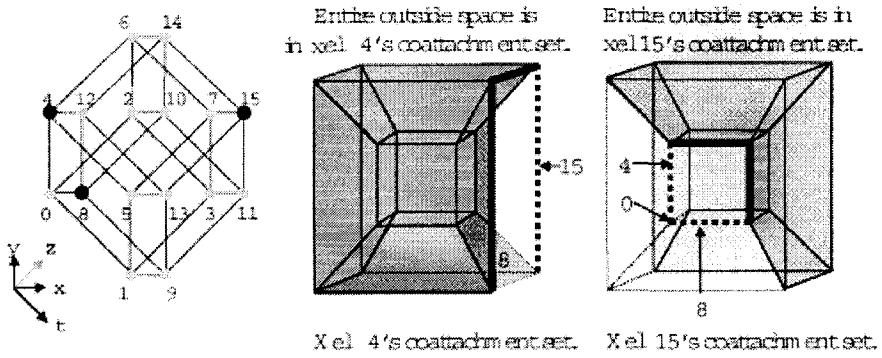

Figure 5.5: The left figure shows an isosceles set $D = \{4, 8, 15\}$ in the (8,80)-image I= {0,...,15} on a stretched 4D grid. The middle figure, 4's coattachment set, can easily be deformed into two thick connected edges by simple sequence (the details are left to the reader). These two connected edges can be further deformed into a point; so can they be deformed after adding either 8 or 15 to them (by deleting one of 8 or 15 from the foreground). But, the deletion of both 8 and 15 dilates the coattachment set to a non-simply connected polyhedra that is homotopic to S^1, a unit circle. The same is true for 15's coattachment set dilating by the deletion of 4 and 8 shown on the right figure. Thus D is MNS.

Let $D = \{d_1, d_2, t\}$. Take d_1 and d_2 to be the diagonal pair 4 and 8, and t to be 15 in figure 5.5. After deletion of d_1 and d_2 t's coattachment set is not simply connected; this implies that t is not simple in $I - \{d_1, d_2\}$. Also, the middle figure demonstrates

that any proper subset of D is simple. Similarly, the deletion of d_2 and t gives the same result for d_1's coattachment set as shown on the right figure. (Should it be difficult to visualize how the outside space deforms, the reader could reverse the time by translate, $-t$, so that the 3D front face of 15 becomes 14, which is then not part of the coattachment set). Furthermore, the d_1 and d_2 are symmetric in an isosceles set, so the same is true for d_2's coattachment set. Thus, D is MNS.

Case 4: A spanning set D of 4 mutually diagonal xels can be MNS (without being a component).

Note that sets of this type can never be a component in a (8,80)-image.

It is helpful to look at figure 5.3 again, taking the spanning set D to be { 3, 9, 10, 15}. On 15's Schlegel diagram, the deletion of 3, 9 and 10 augments its coattachment set and completely encloses a cavity (which looks like a truncated pyramid and is the interior of the 3-xel 15 $\cap$ 11); the complement of the coattachment set is then not connected. So D is not simple. This is not a surprising result judging that the deletion of D removes all the 8-adjacencies from 11 in this (8,80)-image. Removing proper subsets of D cannot make the coattachment set completely enclose 11; they look like an open box augmenting from the coattachment set and wrapping the truncated pyramid (face 11). Polyhedral set of D's proper subset are simply connected, therefore the open box can be deformed onto 15's coattachment set by simple sequence. (The details are trivial.)

Since on the 4D grid, 3, 9, 10 and 15 are symmetric with respect to 11, the argument here applied to 15 on its Schlegel diagram suffices to deduce that D is MNS.

We see from Theorem 5.4.3 that subsets of an MNS set are MNS, hence all the sets specified in the main theorem can be MNS sets. Only the singleton MNS set and the MNS set of an attached pair could be components in an (8,80)-image, so they are the only types of sets that can be MNS either being or not being a component. ////

$$\textit{Singleton} \subset \begin{cases} \textit{Antipodean pair} \quad (I) \\ \textit{8-Adjacent pair} \ (II) \\ \textit{Diagonal pair} \quad \subset \\ \textit{Diametric pair} \subset \end{cases} \begin{cases} \ldots \subset \textit{Spanning set of 4 mutually} \\ \qquad \textit{diagonal xels} \qquad (III-a) \\ \textit{Isosceles set} \qquad\qquad (III-b) \end{cases}$$

Figure 5.6: 4D MNS chains in (8,80)-images. Note that the set of Diametric pair only links to the Isosceles set, and "..." indicates the link, which is a set of 3 mutually diagonal xels.

5.6.2 The "only if" parts of the Main Theorem

Proof:

Let $B = \{0, ..., 15\}$. In this section we are to find the least upper bounds (*lub*) of all the *MNS chains* in (8,80)-images. An "MNS chain" is a non-decreasing sequence of subsets of B that can be MNS with the total ordering of relation $\subset$. Figure 5.6 shows the framework of all the chains that are to be built in this proof.

On an MNS chain we say that a set D is a *child* of a set S if D is an MNS set

contains exactly one more xel than S. We divide the proof into four cases, and start each case with a set S of a pair of xels and trace all possible branches of S. There are four cases in total for four different pairs, allowing us to proceed with *tree pruning.*

Case I: A set S of an antipodean pair in B is a lub.

Take {0,15} to be S on figure 5.3. Suppose S has a child D. Then Theorem 2.4.4 implies $D \subsetneqq \{0,\ldots 15\}$. On the other hand, Corollary 5.4.2 implies that if $x \in D \setminus \{0, 15\}$ then $x \notin$ [0,15]. Thus, S has no child; S is a lub of the MNS chain:

a singleton set $\subset$ *a set of antipodean pair.*

We name proper supersets containing an antipodean pair *type I sets*; this type of set cannot be MNS.

Case II: A set S of an attached pair in B is a lub.

Suppose $S \subsetneqq D \subsetneqq B$ and D can be MNS. WLOG, let S be $\{14, 15\}$. It follows from Corollary 5.4.2 that if $x \in D \setminus \{14, 15\}$ then $x \notin$ [0,14] (otherwise, $14 \in [x, 15]$). Similarly, $x \notin$ [1,15]. But $B = [1, 15] \cup [0, 14]$. Hence $D \setminus [14, 15] = \emptyset$

Thus, S has no child. S is a lub of the MNS chain:

a singleton set $\subset$ *a set of an* 8*-adjacent pair.*

We name proper supersets containing an attached pair *type II sets*; this type of set cannot be MNS.

Case III: S is a set of a diagonal pair in B.

We are to show that there are only two MNS chains containing S. WLOG, let us take $\{0, 12\}$ to be S (see figure 5.7), and show that the lubs containing $\{0, 12\}$ are exactly $\{0, 5, 6, 12\}$ and $\{0, 11, 12\}$ and sets symetrical with these, i.e., the isosceles and the spanning sets specified in the main theorem.

$$\{0,\ 12\} \subset \begin{cases} \{0,\ 6,\ 12\} \subset \begin{cases} \{0,\ 5,\ 6,\ 12\} \subset \{0,\ 5,\ 6,\ 11,\ 12\}\checkmark \\ \{0,\ 6,\ 10,\ 12\}\checkmark \\ \{0,\ 6,\ 11,\ 12\}\checkmark = \end{cases} \\ \{0,\ 11,\ 12\} \subset \begin{cases} \{0,\ 7,\ 11,\ 12\}\checkmark \\ \{0,\ 5,\ 11,\ 12\}\checkmark = \\ \{0,\ 6,\ 11,\ 12\}\checkmark = \end{cases} \end{cases}$$

Figure 5.7: This graph is a tree consisting of all the MNS sets, and its root is $\{0, 12\}$ — a diagonal pair. Sets checked by "$\checkmark$" are not MNS. Sets postfixed with "=" are the same up to symmetry.

It is helpful to look at figure 5.8.A. Again, applying Corollary 5.4.2, we see on figure 5.8.A that none of the xels marked "X" can be elements of S's descendants.

Among all the child candidates of S, $\{0, 6, 12\}$, $\{0, 5, 12\}$, $\{0, 9, 12\}$, $\{0, 10, 12\}$ are the same up to symmetry; $\{0, 7, 12\}$ and $\{0, 11, 12\}$ also are the same up to symmetry. There are only two possible candidates: $\{0, 6, 12\}$ and $\{0, 11, 12\}$.

They are indeed S's children because the isosceles set $\{0, 11, 12\}$ and the spanning set $\{0, 5, 6, 12\}$ can be MNS (as shown in the "if" part of the proof) and it follows from Theorem 5.4.3 that

$\{0, 12\} \subset \{0, 6, 12\} \subset \{0, 5, 6, 12\}$ is an MNS chain.

Subcase III-a: A spanning set of four mutually diagonal xels in B is a lub.

Because 5 and 10, and 9 and 6 are antipodean pairs and a child cannot cannot

contain any antipodean pair, therefore no child of {0, 5, 6, 12} contains 9 or 10. Since 6 and 7 constitute an attached pair, no child of {0,5,6,12} contains 7 either (see figure 5.8). This leads to nothing else but the question: could {0, 5, 6, 11, 12} be a child?

The answer is "no" if we can show that {0, 6, 11, 12} cannot be MNS (for {0, 5, 6, 11, 12} is a superset of {0, 6, 11, 12}).

With the aim of getting a contradiction, assume that {0, 6, 11, 12} can be MNS (in some image I). Let P be the I-coattachment set of xel 0, i.e., $\bigcup Attach(0, \mathcal{I}(I, 0))$, $x_1 = 11 \cap 0$, $x_2 = 12 \cap 0$ and $x_3 = 6 \cap 0$. Observe that $x_1 \cap x_2 = x_1 \cap x_2 \cap x_3 =$ vertex 15. It is clear that P, x_1, x_2 and x_3 satisfy the conditions of Lemma 5.3.1. Therefore,

$$\chi(P \cup x_1 \cup x_2 \cup x_3) = 1 \tag{5.6.1}$$

By Theorem 2.4.1, xel 0 is simple in $I \setminus \{6, 12\}$. Then, Theorem 2.2.2 tells us that both the coattachment set $P \cup x_2 \cup x_3$ and its complement are connected, and $\chi(P \cup x_2 \cup x_3) = 1$.

Since $P \cup x_2 \cup x_3$ is connected, and $x_1 \cup x_2 \cup x_3 \neq \emptyset$, $P \cup x_1 \cup x_2 \cup x_3$ is also connected. Since the complement of $P \cup x_2 \cup x_3$ in the $Boundary(0)$ is connected, and x_1 is a 1−xel, the complement of $P \cup x_1 \cup x_2 \cup x_3$ in $Boundary(0)$ is also connected. These facts, (5.6.1), and Theorem 2.2.2 implies that 0 is simple in $I \setminus \{6, 12, 11\}$ (since the coattachment set of 0 in $I \setminus \{6, 12, 11\}$ is just $P \cup x_1 \cup x_2 \cup x_3$). This contradicts

Theorem 2.4.1 and the fact that $\{0, 6, 11, 12\}$ is MNS.

We conclude that {0, 5, 6, 11, 12} cannot be a child.[2]

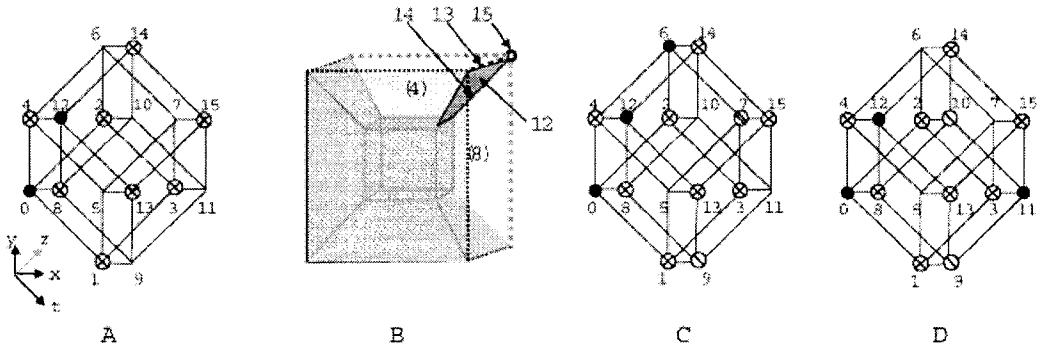

Figure 5.8: Figure A shows that if $D \subseteq \{0,\ldots,15\}$ is a child of $\{0, 12\}$ then by Corollary 5.4.2 all the xels marked "X" shall not be in D, for they are either in [12,15] or [0,12] of 0's coattachment set (see figure B), or in [0,3] of 12's coattachment set on its Schlegel diagram (not shown). Moreover, figure C shows that child D of $\{0, 6, 12\}$ cannot contain 7 and 9, (because D cannot contain attached nor antipodean pairs). Similarly, figure D shows that child D of {0, 11, 12} cannot contain 9 and 10.

Besides {0, 5, 6, 12}, does {0, 6, 12} have other children?

The answer is negative. Assume by contradiction that it has a child $D \subseteq B$. (Caution that the same block B can be used; suppose that the child $D = \{0, 6, 12, x\}$, and x is in time slice $t = -1$, we can flip it back to {0, ..., 15} by a simple transformation $-t$ due to the symmetry of B and the fact $\{0, 6, 12\} \subseteq B$). Thus, slashing out xels in figure 5.8.C by Cases I and II, and the fact that $\{0, 6, 11, 12\}$ is not MNS, we observe that {0, 6, 10, 12} is the only candidate left. But, can it be MNS?

[2]The merit of using Euler characteristics computation to simplify the proof of this subcase is again due to Dr. Kong.

Let $P = \bigcup Attach(0, \mathcal{I}(I, 0))$, the coattachment set of xel 0 in some image I, and let $x_1 = 6 \cap 0$, $x_2 = 10 \cap 0$ and $x_3 = 12 \cap 0$. Observe that $x_1 \cap x_2 = x_1 \cap x_2 \cap x_3$ = edge 14, (they look like a three-leaf propeller with central axis 14 on figure 5.8.B; 6 and 10 are behind 4 and 8 respectively). P, x_1, x_2 and x_3 satisfy the conditions of Lemma 5.3.1, and we have

$$\chi(P \cup x_1 \cup x_2 \cup x_3) = 1 \tag{5.6.2}$$

By Theorem 2.4.1, 0 is simple in $I \setminus \{6, 12\}$. Then, Theorem 2.2.2 tells us that both the coattachment set $P \cup x_2 \cup x_3$ and its complement are connected, and $\chi(P \cup x_2 \cup x_3) = 1$.

Since $P \cup x_2 \cup x_3$ is connected, and $x_1 \cup x_2 \cup x_3 \neq \emptyset$, $P \cup x_1 \cup x_2 \cup x_3$ is also connected. We know that the complement of $P \cup x_2 \cup x_3$ in the $Boundary(0)$ is connected, and x_1 is a 2−xel. If $x_1 \cap (P \cup x_2 \cup x_3)$ is anything other than the union of all 4 edges of x_1 then the complement of $P \cup x_1 \cup x_2 \cup x_3$ in $Boundary(0)$ is also connected. These facts, (5.6.2), and Theorem 2.2.2 implies that 0 is simple in $I \setminus \{6, 10, 12\}$, a contradiction.

But, if $x_1 \cap (P \cup x_2 \cup x_3)$ is the union of all 4 edges of x_1, then $\chi(x_1 \cap (P \cup x_2 \cup x_3)) = 0$. So $\chi(P \cup x_1 \cup x_2 \cup x_3) = \chi(x_1) - \chi(x_1 \cap (P \cup x_2 \cup x_3)) + \chi(P \cup x_2 \cup x_3) = 1 + \chi(P \cup x_2 \cup x_3)$. But $\chi(P \cup x_2 \cup x_3) = 1$ as 0 is simple in $I \setminus \{10, 12\}$, we have a contradiction of (5.6.2).

Thus, we conclude that {0, 5, 6, 12} is the unique lub for the MNS chain containing {0, 6, 12} that follows.

a singleton set $\subset$ *a set of diagonal pair*

$\subset$ *a set of* 3 *mutually diagonal xels*

$\subset$ *a spanning set of* 4 *mutually diagonal xels*

This is the end of Subcase III-a.

Subcase III-b: An isosceles set in B is a lub

WLOG, we are to show that {0, 11, 12} has no child.

Assume by contradiction that {0, 11, 12} has a child $D \subseteq B$ Since a child cannot strictly contain a Case I or Case II set, it follows from figure 5.8.D that there are only three possible candidates: {0, 5, 11, 12}, {0, 6, 11, 12} and {0, 7, 11, 12}.

Here, we claim that {0, 7, 11, 12} cannot be MNS (with 7 in place of 6, using a similar argument as in the case III-a's proof of {0, 6, 11, 12} cannot be MNS). Also note that {0, 5, 11, 12} and {0, 6, 11, 12} are the same up to reflection, which deduces that {0, 11, 12} has no child.

We have completely traced the subgraph in figure 5.6, where the root of this subtree is a set of a diagonal pair.

Case IV: S is a set of a diametric pair.

Let S be {0, 11}. In Case III, we proved that {0, 11, 12} is a lub. So, the following is a trivial consequence of Theorem 5.4.3.

Singleton set $\subset$ *Set of diametric pair* $\subset$ *Isosceles set*

Besides the isosceles set, does S have children on another MNS chain?

The answer is "no". Since if $x \in B \setminus \{0, 11\}$ then $\{0, 11, x\}$ either contains an attached pair (in which case it cannot be MNS) or is an isosceles set.

We have finished the search and discovered all the lubs of the 4D MNS chains and completed the "only if" part of the proof. ////

5.7 Concluding Remarks

We have identified all possible types of sets of 4-xels that can be minimal non-simple (MNS) in 4D binary images with (8,80)-connectedness, and all types that can be MNS without being a component of the image in this thesis. This work is based on one of the characterizations of simple 4-xels that was given in [14], the tree pruning, the study of the complement image and the 4D projection of a coattachment set on the Schlegel diagram.

4D image analysis has been engaged in "solid" robot path planning and many other field applications, which require thinning algorithms for strong connection between components of images. We believe this work is the first result of 4D MNS sets, which provides a tool to verify algorithms of these kind of applications.

Chapter 6

A Good Tiling System for Studying Thinning

6.1 Bricks and Mortar revisited

Too much with the digital paradox....

At the end, I would like to propose a simple tiling system in Euclidean d-space, whose tiles are hypercubes but not Voronoi neighborhoods. This tiling uses the same technique as masons use for many thousand years, i.e., staggering the bricks so mortar can be applied in between bricks to form a strong bond. The result is a cubical tiling system with no digital paradox and requiring no schema.

6.2 The Staggering Procedure

The procedure to create this tiling is simple and straightforward.

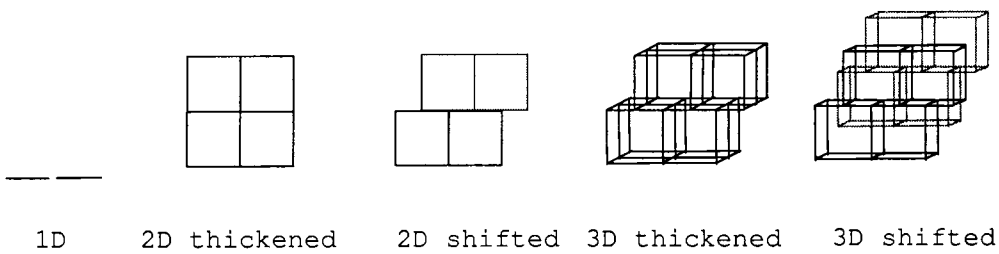

Figure 6.1: This figure shows the staggering procedure to create a simple tiling system, which is the best for verifying thinning algorithm.

1. (Level 1) Starting with 1-space, tile (or slice) it into unit intervals.

2. (Level 2) Thickening this 1D tiling into 2-space along x_2-axis, and slice it perpendicular to x_2-axis into strips with unit width.

3. Staggering each thickened layer (i.e., strip) by shifting $1/2$ along x_1-axis.

4. (Level 3) Thickening the current 2D tiling into 3-space along x_3-axis, and slice it perpendicular to x_3-axis into layers with unit width.

5. Staggering each thickened layer of 2D tiling by shifting $1/4$ along x_1-axis and $1/2$ along x_2-axis.

6. (Level i) One can continue this inductive process until d-space is tiled.

The key step in this inductive staggering is shifting each layer 2^{k-d} along x_k-axis for $k < i$ at each level.

6.3 Simple Features

We list herewith many simple features without rigorous proofs; they are almost readily confirmed by the procedure.

Just like the 2D tile created by this procedure is equivalent to the hexagon tile, its d-tile always shares a facet with any of its neighbors. Therefore, only single adjacency needs to be applied to both foreground and background.

The d-tile has $\sum_{k=1...d} 2^k = 2^{(d+1)} - 1$ neighbors, i.e., 4-tile has 30 neighbors against 80 in 4-space; 62 neighbors against 242 in 5-space!

Each 3-tile of this staggered tiling has 14 adjacent neighbors; only 2 more than an FCC-tile has. This tiling can simulate FCC-grid (at Step 3, Level 2) by deforming 2D tiles into hexagons and thickening them into hexagonal prisms (and wobbling them closer to rhombic dodecahedra, if necessary).

One may argue: because of the staggering, the coordinates of each tile is not easy to be identified. However, if the dimension d is given at the beginning, an even staggering can be obtained by shifting $1/(d-k+1)$ along x_k-axis at each step. Nowadays computing power is getting stronger and we are facing more digital format than analog format. Most electronic devices have step motors for applications. To calculate the location of tile by the aid of the current computing power would be an easy job.

6.4 No Digital Paradox

Defy the gravity and learn from the bees.

This staggered tiling system in Euclidean d-space does use natural d-tiles (not natural here but cubical shape that we are familiar with so we can still analyze the

boundary condition of a xel with ease). More importantly, the maximal small set in this tiling consists of only $d+1$ tiles (against 2^d tiles in Cartesian grid) therefore, the computation efforts to avoid the small sets are almost the same as that to avoid the MNS sets during scanning phase. (The MNS sets are readily identified; having d tiles as l.u.b.) Also, this tiling system has only one configuration of the maximal small set (not like the FCC-grid has two different configurations).

Only single adjacency is required for both foreground and background of any image in this tiling system; there is no more digital paradox. Thus, this tiling system of the Euclidean d-space very well suits studying thinning.

Appendix

.1 Some Application Considerations for Staggered Tiling

In Chapter 6, we just introduced the staggered tiling system, in which d-tile can be considered as a d-dimensional counterpart of 2D hexagon. This system has many good features for analyzing thinning algorithms.

FCC-grid is a good grid system as well, so we suggested using staggered tiling (at Step 3, Level 2) by deforming 2D tiles into hexagons and thickening them into hexagonal prisms to simulate FCC-grid.

This tiling system can not benefit research application unless static graphics reconstruction (or moving object reconstruction with relatively fixed lighting source) is developed. I would suggest the following setting with the even (not the inductive bisecting) staggering procedure:

1. Align the image object's major axial line on the x_3-axis. (The x_3-axis can be

tilted.)

2. Set the view point from which the projection line is perpendicular to the major axial line. The base of the projection shall be the center of the image to be focused for audience.

3. Locate the lighting source such that the ray of light to the same base point shall be perpendicular to the axial line. (i.e., make the major axial line perpendicular to the plane shared by the view point, lighting source and the base.)

This system builds tiles layer by layer, therefore it may be handled recursively. This system is a byproduct of my thesis research; we leave the programming development of thinning algorithms to readers who interested in exploring this tiling system.

Bibliography

[1] K. W. Auvil, *Perspective drawing*, Mayfield Publishing Company, 1998.

[2] D. C. Dubosque, *Draw 3-d: A step by step guide to perspective drawing*, North Light Books, 2002.

[3] R. O. Duda, P. E. Hart, and J. H. Munson, *Graphical data processing research study and experimental investigation*, AD **650926** (1967), 28–30.

[4] S. Fourey and R. Malgouyres, *A concise characterization of 3d simple points*, Discrete Applied Mathematics **125** (2003), 59–80.

[5] N. Gagvani and D. Silver, *Parameter controlled skeletonization of three dimensional objects*, Technical Report, Rutgers University CAIP-TR **216** (1997).

[6] C. J. Gau and T. Y. Kong, *Minimal nonsimple sets of voxels in binary images on a face-centered cubic grid*, International Journal of Pattern Recognition and Artificial Intelligence **13** (1999), 485–502.

[7] ———, *4d minimal non-simple sets*, Discrete Geometry for Computer Imagery **2301** (2002), 81–91.

[8] G. Gimel'farb, *Finite lattice topology and image segmentation*, CITR-TR-5 **0** (1997), 1–5.

[9] R. W. Hall, *Tests for connectivity preservation for parallel reduction operators*, Topology and Its Applications **46** (1992), 199–217.

[10] G. T. Herman, *Geometry of digital spaces*, Birkhäuser, 1998.

[11] E. D. Khalimsky, *Pattern analysis of n-dimensional digital images*, Proceedings of the IEEE International Conference on Systems, Man and Cybernetics, 1986, pp. 1559–1562.

[12] T. Y. Kong, *A digital fundamental group*, Computers and Graphics **13** (1989), 159–166.

[13] ———, *On topology preservation in 2D and 3D thinning*, International Journal of Pattern Recognition and Artificial Intelligence **9** (1995), 813–844.

[14] T. Y. Kong, *Topology preserving deletion of 1's from 2-, 3- and 4-dimensional binary images*, Discrete Geometry for Computer Imagery: 7th International Workshop (DGCI '97, Montpellier, France, December 1997), Proceedings (E. Ahronovitz and C. Fiorio, eds.), Springer, 1997, pp. 3–18.

[15] T. Y. Kong, R. Kopperman, and P. R. Meyer, *A topological approach to digital topology*, American Mathematical Monthly **98** (1991), 901–917.

[16] T. Y. Kong and A. W. Roscoe, *Characterizations of simply-connected finite polyhedra in 3-space*, Bulletin of the London Mathematical Society **17** (1985), 575–578.

[17] T. Y. Kong, A. W. Roscoe, and A. Rosenfeld, *Concepts of digital topology*, Topology and Its Applications **46** (1992), 219–262.

[18] ———, *Concepts of digital topology*, Topology and Its Applications **46** (1992), 219–262.

[19] T. Y. Kong and A. Rosenfeld, *Digital topology: Introduction and survey*, Computer Visioin, Graphics, and Image Processing **48** (1989), 357–393.

[20] R. D. Kopperman, P. R. Meyer, and R. G. Wilson, *A Jordan surface theorem for three-dimensional digital spaces*, Discrete and Computational Geometry **6** (1991), 155–161.

[21] Christophe Lohou and Gilles Bertrand, *A new 3d 12-subiteration thinning algorithm based on p-simple points*, Electronic Notes in Theoretical Computer Science (Sébastien Fourey, Gabor T. Herman, and T. Yung Kong, eds.), vol. 46, Elsevier, 2001.

[22] C. M. Ma, *On topology preservation in 3D thinning*, CVGIP: Image Understanding **59** (1994), 328–339.

[23] R. Malgouyres and Sébastien Fourey, *Strong surfaces, surface skeletons, and image superimposition*, Vision Geometry VII **3454** (1998), 16–27.

[24] C. R. F. Maunder, *Algebraic topology*, Dover, 1996.

[25] J. Pach and P. K. Agarwal, *Combinatorial geometry*, Wiley-Interscience Series in Discrete Mathematics and Optimization, 1995.

[26] G. M. Reed, A. W. Roscoe, and R. F. Wachter, *Topology and category theory in computer science*, Clarendon Press, Oxford. Chapter 11 authors: T. Y. Kong and A. Rosenfeld, 1991.

[27] C. Ronse, *Minimal test patterns for connectivity preservation in parallel thinning algorithms for binary digital images*, Discrete Applied Mathematics **21** (1988), 67–79.

[28] A. Rosenfeld and J. L. Pfaltz, *Sequential operations in digital processing*, J. Assoc. Comput. **13** (1966), 471–494.

[29] P. K. Saha, T. Y. Kong, and A. Rosenfeld, *Strongly normal sets of tiles in* N *dimensions*, Electronic Notes in Theoretical Computer Science **46** (2001), URL: http://www.elsevier.nl/locate/entcs/volume46.html.

[30] E. H. Spanier, *Algebraic topology*, Springer, 1989.

[31] S. Willard, *General topology*, Addison-Wesley Publishing Company, Inc, 1970.

[32] G. M. Ziegler, *Lectures on polytopes*, Springer-Verlag, 1994.

Index

$<$ (proper face), 7

I^c, 26

$[p, q]$, 100

A*ttach*(q, I), 40

B*oundary*(q), 40

$\mathcal{F}(I)$, 30

$\delta(I)$, 30

$\delta(q, I)$, 23

dD(m,n) image, 29

l_1-diameter, 86

m-components, 38

antipodean, 18

attached, 18

attachment set, 38

coattachment set, 97

complement of image, 26

core cube, 51

cosimple, 97

dD(m,n) digital space, 29

diagonal, 18

diametric, 18

digital space, 7, 29

Euler characteristic, 40

face, 6

facet, 7

foreground, 30

good pair, 26

graph approach, 10

grid point, 7

hereditarily simple, 44

lattice, 100

minimal non-simple set, 44

MNS chains, 106

MNS set, 44

nearest-neighbor adjacency, 17

polyhedral complex, 7

polytope, 6

Schlegel diagram, 32

simple set, 42

simple xel, 39

small set, 46

spanning set, 101
staggered tiling, 116
staggering procedure, 114

tesseract, 34
Theorem with (12,12)-connectedness, 69
Theorem with (12,18)-connectedness, 71
Theorem with (18,12)-connectedness, 63
Theorem with (8,80)-connectedness, 101
Theorem with (80,8)-connectedness, 80
tile assembly, 23
tile-adjacency, 17
tiles, 7
topological approach, 11
truncated tile, 20

Voronoi neighborhood on an FCC-grid, 50

X -to-tetrahedron, 35
xel q, 23

Y-to-$\triangle$, 35